ADVANCING TEMPERATURE DEVELOPMENT AND SUSTAINABILITY OF ANIMAL MORTALITY COMPOSTING SYSTEMS USING BIOCHAR AMENDMENT AND UTILIZING THE END-PRODUCT TO IMPROVE CROP RESILIENCE

BY

YUCHUAN WANG

DISSERTATION

Submitted in partial fulfillment of the requirements

for the degree of Doctor of Philosophy in Agricultural and Biological Engineering

in the Graduate College of the

University of Illinois Urbana-Champaign, 2022

Urbana, Illinois

Doctoral Committee:

Clinical Assistant Professor Neslihan Akdeniz, Chair

Associate Professor Paul Curtis Davidson

Research Assistant Professor Mei Tessum

Professor Thanh Huong Nguyen

ABSTRACT

Livestock and poultry disease outbreaks threaten animal and human health, national food security, and the environment. For example, African swine fever is a highly contagious animal disease affecting more than 20 countries worldwide. The only way to stop the outbreak is to depopulate all affected animals because, currently, there is no treatment or vaccine. Once animals are depopulated, proper disposal of the mortalities is critical in preventing the spread of the disease. During the 2014-2015 highly pathogenic avian influenza outbreak in the U.S., which remains the largest animal health emergency in the U.S., about 85% of 50 million poultry mortalities were disposed of by composting. Biosecurity agencies recognize composting as the preferred disposal method for routine and emergency management. However, composting has its limitations, such as the case of low surrounding temperature, ammonia emission, and leaching. This study aimed to test the impact of biochar amendment on temperature development and sustainability of animal mortality composting systems and the end-product.

First, we completed a quantitative literature review on the role of co-composted biochar (COMBI) in plant growth using meta-analysis. A total of 794 studies were scanned, with 233 observations. Results indicated that COMBI generally yielded a 22.8% improvement in plant productivity. COMBI's application rates of less than 20 t/ha (n=42) and more than 30 t/ha (n=82) significantly increased plant productivity by 48.3 and 15.7%, respectively. The greatest increase in plant productivity (48.9%, n=36) was observed when soil pH was 4 and 5. Regarding plant species, grain yields of cereal grasses significantly increased (39.7%, n=133) when grown with COMBI. COMBIs made from wood-based biochar (29.4%, n=155) and animal manure (44.1%, n=94) were the most popular types and yielded significant increases in plant productivity.

Second, using pilot-scale composting bins, wood-based biochar at 0, 2.6, 13, 36, and 39% (v/v) was co-composted with chicken mortalities and woodchips. Results indicated that biochar amendment significantly increased (3.4–7 °C) the maximum temperatures reached during the process compared to control test units without biochar. Biochar amendments at 13, 26, and 39% resulted in prolonged periods of temperature over 67 °C to inactivate the highly pathogenic Avian influenza (H7N1) and a reduced cumulative chemical oxygen demand of the leachate by 80.4 ± 3.07% on average. At 26 and 39%, biochar amendment significantly reduced the

cumulative ammonia emissions by 40.4% and 56.8%, respectively. Biochar amendment at 39% increased the total nitrogen content of the final compost by 34.7%.

Third, three commercially available biochars (wood-based, distillers grains, and cow manure biochar) were added to the composting process of chicken mortalities at 13% (v/v), respectively. Results showed that the BET surface area of wood-based biochar was 2.4 and 29 times greater than those of cow manure and distillers grain biochar, respectively. Poultry mortalities with wood-based and cow manure biochar increased compost temperatures by 2.0 to 3.3 °C. Compared to no biochar addition, wood-based biochar resulted in significantly higher compost temperatures (p=0.02), lower leachate COD (p=0.02), higher total nitrogen (p=0.01), and manganese (p=0.0006) contents, and there was no increase in sodium (p=0.94) content of the finished compost. It also lowered the cumulative chemical oxygen demand of the leachate samples by 87% (p=0.02).

Fourth, we developed a mathematical model to understand the impact of biochar on the heat profile of the composting process. This study investigated whether biochar increases compost temperatures by improving insulation or enhancing microbial activity. The model partially relied on some measurements of the previous two pilot-scale studies. Results indicated that the model could achieve an R^2 value of 0.85 during the 2nd heating cycle. Biochar additions increased the overall heat loss because of the decreased thermal resistance. At the biochar addition rate of 13% (v/v), the predicted longitudinal conductive resistance of the compost pile was reduced by 12.6%. However, as the cumulative heat unit generation increased by 11.8%, this finding may indicate that biochar may increase the compost temperature by improving the microbial activity rather than providing insulation.

The last chapter focuses on crop growth utilizing the end product of the composting. Finished animal mortality compost with no biochar addition, wood-based biochar, distillers grains biochar, and cow manure biochar at 13% (v/v) were mixed with the topsoil at 30% (v/v) as soil amendments. Buttercrunch lettuce (Lactuca sativa var. capitata) was grown on different soil amendments in a controlled environment using T5 grow lights (200 µmol m^{-2} s^{-1}). Results indicated that adding all composts to the soil increased its water holding capacity (WHC) by 29% to 34%. There was no inhibition found in lettuces' growth among treatments. However,

composts with wood-based biochar and distillers grain biochar significantly reduced the nitrate content in lettuce leaves by 26.8% and 34.1%, respectively.

In conclusion, wood-based biochar addition at a minimum of 13% (v/v) is recommended to improve the composting process (e.g., temperature, leachate COD, final N content). The temperature improvement by adding biochar, which is critical in eliminating foreign animal diseases such as avian influenza, was more likely the result of enhanced microbial activity. COMBI did not have an adverse effect on crop growth under the controlled conditions studied. Future research can focus on 1) investigating biochar's influence on the temperature profile using different compost materials and 2) growing plants using different COMBIs and under conditions such as drought.

ACKNOWLEDGMENTS

The four years' experience at U of I has been not only training for my technical background but also a life lesson to stabilize my personality. I got a chance to know myself and think about myself, and I sincerely thank those who helped and inspired me.

I shall be no more thankful to my advisor Dr. Akdeniz. She is a very hard-working person. With great patience, Dr. Akdeniz has worked with me on all the experiments and manuscript writings. With so many skills and ideas I have learned from her, I truly feel that I am becoming a more knowledgeable person. I greatly thank my committee members: Dr. Davidson, Dr. Nguyen, and Dr. Tessum. Thank you so much for reviewing my manuscript and giving me advice. Thank you for the time you kindly spent on me to improve the experiment quality. I also thank those university staff and faculty who have helped me with my experiment, including Dr. Maria Bonita Villamil, Timothy Lecher (ABE farm manager), Wayne M Bugaj (who provided us with woodchips from Ground Storage Barn), Dr. Ronaldo G Maghirang, and all department advisors. Meanwhile, I thank all my colleagues for their help and company. Doing the experiment was tough; however, your help gave me the mental power that buffed me to pick up the confidence and fight again.

At last, I have to thank my parents and grandparents. They have been supporting me all the time. We met some difficulties during the covid period. Although none of us was infected, things that happened turned us upside down. During the toughest period, they showed no fear. Their positive attitude to encounter problems encouraged me.

TABLE OF CONTENTS

CHAPTER 1

INTRODUCTION AND OBJECTIVES

Livestock and poultry disease outbreaks threaten animal and human health, national food security, and the environment. For example, African swine fever is a highly contagious animal disease affecting more than 20 countries worldwide. The only way to stop the outbreak is to depopulate all affected animals because there is no treatment or vaccine currently (USDA, 2021)(EFSA). Once animals are depopulated, proper disposal of the mortalities is critical to prevent the spread of the disease. During the 2014-2015 highly pathogenic avian influenza outbreak in the U.S., which remains the largest animal health emergency in the U.S., about 85% of 50 million poultry mortalities were disposed of by composting (Costa and Akdeniz, 2019).

Biosecurity agencies recognize composting as the preferred disposal method for routine and emergency management. However, composting has its limitations. For example, composting can be limited by the temperature of the surrounding environment and materials, resulting in a low compost temperature (Akratos et al., 2017; Brust, 2019; H. Liu et al., 2019). During the composting process, ammonia emission and leachate generation can cause air quality issues, soil and groundwater contaminations, and decreased value of the end compost (Roy et al., 2018; Shan et al., 2021).

Biochar is a porous, stable, and carbon-rich material that can be made from heating biogenic materials, including plant waste, animal manure, food waste, industrial bio-waste, and bio-solids, with minimal oxygen (Elkhalifa et al., 2019; Pariyar et al., 2020; Weber and Quicker, 2018). Biochar can have large surface areas, high water-holding capacities, strong adsorption capacities, and suitable environments for microbial growth (Neslihan Akdeniz, 2019). The addition of biochar to the composting process has shown promising results in improving the composting performance. So far, biochar has been tested to co-compost with different organic wastes, including animal manure, green waste, sewage sludge, and food waste (Agyarko-Mintah et al., 2017; Neslihan Akdeniz, 2019; Du, Zhang, Qu, et al., 2019; Qiu et al., 2019; Waqas et al., 2018). However, composting animal mortalities with biochar has not been studied yet. If biochar enhances compost temperatures, as reported in previous studies (Akdeniz, 2019), the biochar amendment would help to prevent the spread of animal diseases. Besides, biochar's benefits in retaining essential nutrients such as nitrogen and other organic compounds would reduce the

environmental impact during the animal mortality composting while producing a more fertile final compost.

The overall goal of this research project was to test the impact of biochar amendment on temperature development and sustainability of animal mortality composting systems and the end-product.

Objectives in this project are:

1. A quantitative literature review on the role of co-composted biochar (COMBI) in plant growth using meta-analysis.
2. A pilot-scale co-composting test by adding wood-based biochar at 0, 2.6, 13, 26, and 39% (v/v) to chicken mortalities and woodchips.
3. A pilot-scale co-composting test by adding three commercially available biochars (wood-based, distillers grains, and cow manure biochar) at 13% (v/v) to chicken mortalities and woodchips.
4. Development of a mathematical model to understand the impact of biochar on the heat profile of the composting process.
5. A lab-scale test to utilize the mature composts to grow Buttercrunch lettuce (Lactuca sativa var. capitata).

CHAPTER 2

A QUANTITATIVE UNDERSTANDING OF THE ROLE OF CO-COMPOSTED BIOCHAR IN PLANT GROWTH USING META-ANALYSIS

2.1. Introduction

Biochar is a carbon-rich material produced by heating biomass such as wood, manure, or crop residues in an oxygen-limited environment. Biochar is applied to soils to improve soil structure or sequester carbon (Lehmann and Joseph, 2015). Interest in biochar and its effects on crop productivity has been increasing rapidly. In many recently published sources, biochar applications to soils, along with fertilizers, have been shown to improve plant growth and yield (Jeffery et al., 2011, 2015; Yu et al., 2019). Jeffery et al. (2011) evaluated the relationship between biochar additions and productivity (yield and above-ground biomass) for several crops and found that biochar increased crop productivity by 10% on average. The authors reported two main mechanisms of biochar explaining the improved productivity: the liming effect (increased pH) and the improved water holding capacity of the soil. Jeffery et al. (2015) showed that when grown with biochar, the crop yield of rice (*Oriza sativa* L.), wheat (*Triticum aestivum* L.), maize (*Zea mays* L.), and soybean (*Glycine max* L. Merr.) increased by 16, 17, 19, and 22%, respectively. Liu et al. (2013) reported that biochar amendment rates lower than 30 t/ha increased crop yield by 11% on average, yet the responses varied with the experimental conditions. Biederman and Harpole (2013) performed a comprehensive meta-analysis of published studies that tested the effects of biochar on crop productivity and reported that biochar addition to soils resulted in an increased above-ground biomass and crop yield by 26% and 17%, respectively. Although all these studies are very promising, the concern with soil application of fresh or pure biochar is that the high carbon content of biochar may eventually cause immobilization of soil nitrogen (N), which would adversely affect plant growth and decrease crop yield (Bengtsson et al., 2003; Clough et al., 2013; DeLuca et al., 2015; Johannes Lehmann et al., 2003). However, this is more likely to happen if biochar is made from biomass with a high carbon to nitrogen (C/N) ratio, such as softwood (Mukome and Parikh, 2016). Therefore, the impact of biochar on crop productivity mainly depends on the soil's physical and chemical properties and presence of a nitrogen source (e.g., manure, compost, synthetic fertilizer) during biochar application to the soil. The use of biochar may be beneficial to soils with

relatively low C/N ratios (optimum soil C/N ratio is 24:1). Presence of an additional N source like animal manure will be needed along with biochar in soil with high C/N ratios. The combined use of biochar and finished compost (biochar-compost mix) as a soil amendment has been shown to improve nitrogen use efficiency and prevent nitrogen immobilization (Steiner et al., 2008, 2015). A more effective way is to co-compost biochar with an organic matter source, such as animal manure, which would lead to an accelerated composting process as well as the production of an end-product with enhanced fertility and carbon sequestration potential (Fischer and Glaser, 2012; Jia et al., 2016; Sánchez-García et al., 2015; L. Zhang and Sun, 2014). Recent literature reviews on the effects of biochar (Jeffery et al., 2011) and biochar-compost mixtures (Jones et al., 2016; Lee et al., 2018; Schulz and Glaser, 2012) on plant productivity have been published. Our goal is to conduct a meta-analysis to understand the co-composted biochar's (COMBI) role in plant productivity, which has not previously been published. Fig. 2.1 explains the characteristics of COMBI applications. The objective of this review is to analyze how variations in COMBI application rates, soil pH, plant type, biochar feedstock, and compost material affect plant yields.

2.1.1. The effect of biochar on composting

Biochar has been utilized as a soil amendment for hundreds of years (Glaser et al., 2001; Ogawa and Okimori, 2010). Biochar has been successfully used as a compost amendment over a wide range of application rates (Awasthi et al., 2017; Keiji Jindo et al., 2012; Sánchez-García et al., 2015; L. Zhang and Sun, 2014). The distinct properties of biochar, such as high internal surface area and its ability to sorb soluble organic matters, gases, and inorganic nutrients, lead to complex interactions between the biochar and soil components (Thies et al., 2015). These interactions are also expected to occur within a compost mix when biochar is used as a compost amendment (Steiner, Sanchez, et al., 2015). Compost microorganisms colonize on the surface of biochar, which is attributed to the increased surface available for the microorganisms, the favorable moisture levels resulting from the increased water-holding capacity, enhanced micro-aeration, and the sorption of available carbon compounds that can be readily used by the microorganisms (Steiner, Sanchez, et al., 2015; Sun et al., 2016). Potential benefits of using biochar as a compost amendment can be summarized as i) increasing microbial activity by enhancing aeration, ii) reducing soil bulk density, iii) increasing compost temperature, iv) decreasing ammonia volatilization, v) enhancing water holding capacity, vi) reducing nutrient

losses by leaching, vii) reducing greenhouse gas (GHG) and odor emissions, and viii) increasing the degree of humification (Fig. 2.1) (Neslihan Akdeniz, 2019; El-Naggar et al., 2019; Godlewska et al., 2017).

2.1.2. The effect of composting on biochar

While biochar affects the composting process, composting also benefits the biochar properties in the formation of COMBI. Although biochars prepared at low temperatures (<550 °C) may contain some organic matter that can be degraded, in general, biochars with low H/C ratios are not expected to degrade during the composting process. However, biochar particles can still undergo surface oxidation that alters their physicochemical properties, a process that is known as biochar "aging" or "weathering." Biochar aging or weathering is an abiotic process consisting of the oxidation of exposed carbon rings with high-density π-electrons and free radicals (Joseph et al., 2010; Steiner et al., 2015). Without oxidation, biochar's ability to improve soil fertility by increasing the soil's cation exchange capacity (CEC) and nutrient retention is limited. However, oxidation is a slow process (C. H. Cheng et al., 2008). Composting biochar with an organic material has been proven to facilitate natural oxidation. Composting increases surface oxidation both abiotically by the elevated temperatures and biotically by high microbial activity (Dias, Silva, Higashikawa, Roig, Sánchez-Monedero, et al., 2010; Sanchez-Monedero et al., 2017). Additionally, sorption of organic compounds on the surface of biochars leads to an increase in the number of functional groups that can be oxidized (Prost et al., 2013). Cheng et al. (2006) incubated wood-based biochar at 30°C and 70°C for four months. Rather than biotic processes, abiotic processes were found to be causing oxidation of the biochar during this short-term incubation. Biochar incubated at 30°C and 70°C without microbial activity showed an increase in cation exchange capacity (CEC) by 53% and 538% and in oxygen (O) content by 4% and 38%, respectively (C.-H. Cheng et al., 2006). In another study, the aging of biochar was simulated in the laboratory by continuous heating at 110°C for eight weeks. This artificial aging increased the CEC of biochar by 50%, but the heating process inhibited the microbial activity and excluded the interaction between the biochar and the organic material (Hale et al., 2011). In other studies, Prost et al. (2013) and Khan et al. (2016) tested co-composting wood-based biochar with manure, and they reported that composting can lead to up to a six-fold increase in the CEC of biochar.

2.1.3. The effect of compost and biochar application on soil

Field application of finished compost has been shown to increase the organic matter content of the soil, promote the formation of soil aggregates, enhance the availability of soil nutrients, and alter the soil microbial content and the enzymes involved in nutrient mobilization (Bedada et al., 2014). Using biochar as an amendment during composting has the potential to improve these benefits even further. The physicochemical properties of biochar responsible for changes in soil include nutrient content, pH, water retention, and microbial activity (Y. Yuan et al., 2017; Zhu et al., 2017).

2.1.3.1. Nutrients

Compost and COMBI contain essential macro and micro-nutrients for plants depending on the feedstock, pyrolysis, and composting conditions. Nitrogen is an essential plant nutrient, and it is also the most sensitive of all macronutrients to heating. Biochar contains a considerable amount of nitrogen (0.04-2.4%) (Al-Wabel et al., 2018), but this nitrogen is heterocyclic, and only a small portion of it can be directly released into soils. Biochar can reduce compost and soil nitrogen losses by decreasing ammonia volatilization, nitrous oxide emission, and nitrogen leaching (Jeffery et al., 2015). The carboxylic and phenolic groups attached to the surface of the biochar as a result of the aging process have a negative charge. Therefore, they can adsorb ammonium (NH_4^+) by electrostatic attraction (Montes-Morán et al., 2004; Nguyen et al., 2017). Nitrate (NO_3^-), which is an unstable form of nitrogen, cannot be adsorbed on the surface of biochar by electrostatic attraction since the biochar surface is negatively charged. However, base functional groups such as chromenes, ketones, and pyrones and unconventional hydrogen bonding can facilitate NO_3^- adsorption on the surface of biochar (Mukherjee and Lal, 2013; Nguyen et al., 2017). Pyrolysis temperature impacts the adsorption of NO_3^- (Alsewaileh et al., 2019). If any, plant growth improvement is primarily mediated by nitrate capture and its subsequent slow release (Kammann et al., 2015).

Most agricultural systems are limited in their ability to supply phosphate (P) to crops because crops primarily take up phosphate in orthophosphate anion (PO_4^{-3}) form, which requires mineralization of organic phosphate or solubilization of inorganic phosphate (Gao et al., 2019). It has been reported that biochar enhances plant-available phosphate by 1) increasing pH of acidic

soil, which reduces fixation of phosphate by Fe and Al so that previously bound phosphate becomes available (soils with pH values between 6 and 7.5 are ideal for P-availability), 2) stimulating the formation of organo-mineral complexes, and 3) altering phosphate solubility by influencing microbial enzyme activities (Gao et al., 2019; G. Xu et al., 2014; Zheng et al., 2019). Biochar also improves the retention of potassium (K^+), which is another essential macronutrient for crops, by enhancing the cation exchange capacity of the soils.

In addition, by changing soil pH, biochar can increase the availability of micro-nutrients such as calcium (Ca) and magnesium (Mg), or boron (B) and molybdenum (Mo), which play an important role in biological nitrogen fixation (Jeffery et al., 2015; Rondon et al., 2007). Biochar can also reduce phytotoxic organic compounds in the soil, which helps enhance crop yields (Oleszczuk et al., 2012). On the other hand, reduction in crop yields has been associated with 1) high sulfur content, salinity, and high pH of biochar, 2) Al and Mn toxicity, and 3) restricting nutrient availabilities due to immobilization (Jeffery et al., 2015).

2.1.3.2. Water holding capacity

Besides nutrients, water is the most limiting factor in crop production. NO_3^- and PO_4^- are poorly adsorbed by negatively charged soil particles and can be easily lost following rainfall or irrigation events. Runoff and leaching of N and P can lead to water quality problems. Soil K becomes available to plants mainly when dissolved in water. However, K is absorbed in the soil colloids, which can be carried away and lost from the soil by surface runoff (Wang et al., 2018a). Biochar has the potential to reduce surface runoff. Changing water holding capacity depends on the changes in volume, size, and connectivity of the spaces between or within the soil particles. This can happen because biochar has a different shape, size and/or internal porosity compared to the soil particles (Masiello et al., 2015). Bulk density is one of the most important soil characteristics affecting rainfall infiltration. Depending on biochar's feedstock and production conditions, the bulk density of biochar ranges from 0.08 g cm^{-3} to 1.7 g cm^{-3}. Considering the bulk density of the mineral soil ranges from 1.16 to 2.0 g cm^{-3}, a decrease in bulk density is expected after biochar applications (Khanmohammadi et al., 2015; Rakshit, 2018). This would lead to an increase in soil porosity. Changes in the interparticle porosity (space between the particles) vary with both soil type and biochar porosity. When biochar is added to soil, if soil particles are smaller than interparticle pores, interparticle pores are rapidly filled with soil particles. Changes in the intraparticle porosity (space

within the particles), on the other hand, would depend on the characteristics of biochar. Intraparticle pores are filled slowly depending on soil particle size, biochar porosity, soil microbial processes, and hydrologic conditions (Masiello et al., 2015). Fresh biochar tends to be hydrophobic; however, as the biochar surface is oxidized (aging), it becomes more hydrophilic due to the increased number of carboxylic groups attached to its surface (Basso et al., 2013).

Research often focuses on the water holding capacity of biochar. However, the addition of biochar to the soil does not necessarily increase the water holding capacity of the soil. After mixing soil with biochar, the interparticle pore space can be lost. The most meaningful measurements are made when biochar-soil mixtures are used instead of pure biochar. The application depth of biochar is important. The preferred depth is 4 to 6 cm (Ibrahim et al., 2017). Biochar application rate is also critical. Its effect mainly depends on the soil type. Devereux et al. (2012) reported that the pore size of sandy loam soils decreased at biochar applications rates higher than 5% (w/w), which affected the hydraulic conductivity of the soil. Biochar would be of significant agronomic benefit when it increases not the water stored in the soil but the plant-available moisture content of the soil (Masiello et al., 2015).

2.1.3.3. Soil pH

One of the main mechanisms behind the reported positive effects of biochar application on acidic soils is biochar's liming effect. Liming improves phosphate availability and other nutrients (N, Ca, Mg, Mo). While soils with pH values between 6 and 7.5 are ideal for the formation of orthophosphate ions ($H_2PO_4^-$ and HPO_4^{2-}), pH values below 5.5 limit P-availability (Cerozi and Fitzsimmons, 2016). Other benefits of liming include 1) increasing N_2 fixation in legumes, 2) limiting the availability of some toxic elements such as Al^{3+} and Mn^{2+}, and 3) improving microbial degradation of the organic matter (Jeffery et al., 2015).

Although biochar application to acidic soils is effective in increasing crop yield, it may not be economically feasible to apply biochar solely for pH adjustment. About 42.5 t/ha of biochar is required to increase the pH of sandy soil by one unit (Jeffery et al., 2015). Galinato et al. (2011) reported that applying biochar to soils can be profitable when all benefits (compost and soil amendment and carbon sequestration) are considered.

2.1.3.4. Soil biological processes

Changes in soil biota directly impact plant growth (Kavitha et al., 2018). The porous structure of biochar provides a good shelter for soil microorganisms, protecting them from predation or desiccation (K. Jindo et al., 2014; Shaaban et al., 2018).

2.1.3.4.1. Mycorrhizal fungi growth

Biochar has been reported to have positive effects on mycorrhizal fungi growth. Mycorrhizal fungi contribute to plants' nutrient and water uptake and play a role in soil aggregation and structural stability. Although the relationship between biochar and mycorrhizal colonization is not yet entirely clear, one of the reasons for the beneficial effects is the porous structure of biochar, which physically protects hyphae from fungal grazers (Ortas, 2016). Warnock et al. (2007) reported that biochar might indirectly affect mycorrhizal fungi by altering other soil microorganisms. Biochar may also affect plant-fungus signaling interference and detoxification of allelochemicals on biochar (Warnock et al., 2007).

2.1.3.4.2. Bacteria abundance

Bacteria may sorb to the surface of biochar, which makes them less susceptible to leaching. The processes leading to attachment include 1) flocculation, 2) adsorption on surfaces, 3) covalent bonding to carriers, 4) cross-linking of cells, and 5) encapsulation or entrapment in a matrix (Johannes Lehmann et al., 2011a). This would not affect mycorrhizal fungi abundance, as fungi are less mobile owing to their hyphal networks (Johannes Lehmann et al., 2011a). Li et al. (2016) showed that adding biochar to paddy soil increased bacterial abundance by 161%, where biochar influenced gram-positive bacteria more than gram-negative bacteria.

2.1.3.4.3. Biological nitrogen fixation

Ishizuka (1992) reported that biological nitrogen fixation contributes about 17.2×10^7 t of nitrogen to soils globally every year. Biochar application affects N_2-fixing bacteria that convert atmospheric N_2 to ammonia (NH_3) (Thies et al., 2015). Different mechanisms for the observed effect of biochar on biological nitrogen fixation have been proposed: 1) immobilization of inorganic N, which is known to stimulate biological nitrogen fixation, 2) increased nodulation, 3)

increased P availability, 4) adsorption of flavonoids and nod-factors by biochar, which increases signaling for nodulation, 5) increased pH, and 6) introduction of macro and micro-nutrients (Mia et al., 2014). Increasing biochar application rates may increase biological nitrogen fixation (Rondon et al., 2007; Tagoe et al., 2008). However, Quilliam et al. (2013) reported that elevated application rates caused a reduction in nodulation, although nitrogenase activity remained unchanged.

2.1.3.4.4. Plant pathogens

Another effect of biochar application is suppressing pathogens that cause plant diseases by 1) immediate release of inhibitors to plant pathogens, 2) promotion of microorganisms that act antagonistically to plant pathogens (compete for nutrients or produce antibiotics), 3) improving plant nutrient uptake, which leads to enhanced disease resistance, 4) activating plant defense mechanisms by enhancing the abundance of certain microorganisms, 5) sorption of organic compounds on the surface of biochar that alters the signaling between plant and pathogens, and 6) affect the mobility of the pathogens (Johannes Lehmann et al., 2011b).

It has been shown that co-composting biochar with organic waste benefits both the composting and biochar aging processes. Although a considerable amount of research on biochar and biochar-compost mixtures has been conducted, limited information exists on COMBI applications. Thus, this review paper focuses on summarizing the impact of COMBI on plant productivity.

2.2. Material and methods

2.2.1. Literature search

A systematic literature search was conducted on the Web of Science, Elsevier Science Direct, Google Scholar, and Scopus databases using the keywords “biochar and compost” in the title, abstract, and keywords, which identified a total of 1,417 sources. The search was not limited to a certain timespan. The oldest paper was published in 2007, while the newest one was published in 2018. After the removal of duplicates, there remained 794 studies. For our meta-analysis, two criteria were used to exclude sources not relevant to the present review: 1) studies that only discussed the impact of biochar use on the composting process were not included because they did not provide any information about the soil application of their end-product, 2) publications that

focused on the compost-biochar mixtures were not included either since the scope of this paper is COMBI. Fourteen papers were utilized in the meta-analysis, while a number of research, review papers and books were used to explain how biochar affects plant productivity. Both data points were extracted when a paper presented both COMBI and compost data. Meta-analyses of COMBI data were done as explained below, and the results are presented in Fig. 2.2 to Fig. 2.6. Meta-analyses of compost data were completed following the same method, and the results are presented in Appendix Fig. 2.8 to Fig. 2.11. The reason for not including compost graphs in the paper is that they were prepared based on a limited number of studies only for comparison purposes to certain COMBIs instead of scanning the entire compost literature (it is not the scope of this paper).

2.2.2. Data extraction

The following data were extracted from the identified studies to assess the effect of COMBI on plant productivity: 1) COMBI application rate, 2) soil pH, 3) plant type, 4) biochar feedstock, 5) compost material. Depending on the plant type, plant productivity was measured as dry plant biomass, shoot dry biomass, grain yield, seed yield, flowers per shoot, fruit to flower ratio, fruit per plant, or fruit volume. If more than one productivity data was reported (e.g., both shoot and root biomass) in a study, the data point related to the edible part of the plant (e.g., grain yield for corn, shoot biomass for lettuce) was used in the meta-analysis. Data were extracted from the graphs using the WebPlotDigitizer online tool (version 4.1). Corresponding authors were contacted if data could not be extracted using the WebPlotDigitizer (corresponding authors contacted are stated in Acknowledgment).

In this study, control refers to soil or soil+fertilizer. Treatment means control+COMBI. Besides the 14 included studies, the following studies were not included in the meta-analysis for the stated reasons: 1) Glaser et al. (2015) and Kaudal and Weatherley (2018) compared compost to COMBI, and there was no control that we could use in our meta-analysis and 2) Lashari et al. (2013, 2015) added a byproduct of the pyrolysis process (pyroligneous solution) to only treatments but did not add to the control, which might have affected the results. Although these studies did not fit our meta-analysis model, they still provide valuable information and were included in the summary table (Table 2.1). Agegnehu et al. (2015 and 2016a) and Bass et al. (2016) measured soil pH using two methods. The average of the two measurements was used in the meta-analysis (Table 2.1).

2.2.3. Meta-analyses

Univariate meta-analysis models were applied, in which the response ratio was modeled as a function of a study-level random effect and one explanatory factor variable (Jeffery et al., 2011; Jian et al., 2016). The advantage of using the response ratio is that it allows normalization of the experimental results on the same scale, which allows making comparisons between different experimental results. The limitation is that the interpretation of the results should be undertaken with care because the wide range of co-variables is not represented in all instances (Jeffery et al., 2015). The response ratio was calculated in OpenMEE statistical software (Wallace, 2017), which is considered as a graphical user interface to the metafor R package (Viechtbauer, 2010), using equation Eq. 2.1 (Hedges et al., 1999):

$$ln\ (RR) = ln\ (\frac{\overline{x}_t}{\overline{x}_c}) \qquad \text{Eq. 2.1}$$

where $\overline{x}_t$ and $\overline{x}_c$ are the mean plant productivity values of the treatment and control groups, respectively. A response ratio greater than 1 suggests that COMBI has a stronger effect on plant productivity than control. To normalize the data set, we used a natural logarithmic transformation (Zuber and Villamil, 2016). A Funnel plot was plotted to test the effect of publication bias. The X-axis shows the effect size (ln RR), and Y-axis presents the inverse standard error of the effect size as an index of precision (Egger et al., 1997).

2.2.4. Presentation of graphs

Forest plots showing the effect size (ln RR) calculated from each group are presented in Fig. 2.2a to Fig. 2.6a. Each point shows the mean effect size for each grouping, with the lines representing 95% confidence intervals (CIs). To improve visual quality of the graphs, forest plots were prepared in Microsoft® Office 365® Excel using the results obtained with OpenMEE software.

The percent changes in plant productivity are presented in Fig. 2.2b to Fig. 2.6b. The effect size (ln RR) and confidence intervals (CI) were exponentially transformed, and equation Eq. 2.2 was used to calculate the percentage change in crop productivity. The numbers shown in parenthesis on the graphs are the total number of replicates (n) and the total number of studies (#)included in each grouping.

$$\text{Percentage change} = [\exp(\ln \text{RR or } 95\%\ \text{CI}) - 1] \times 100\% \qquad \text{Eq. 2.2}$$

2.3. Results and discussion

Table 2.1 summarizes the key findings of the studies found during the systematic review. The results of the COMBI meta-analysis are shown in Fig. 2.2 to Fig. 2.6. The results of the compost meta-analysis are presented in Appendix Fig. 2.8 to Fig. 2.11. The results are significant at $P \leq 0.05$ if the bar does not cross the 0% change in crop productivity, represented by the vertical line. Using univariate meta-analysis allows for a clearer picture than looking at individual studies (Jeffery et al., 2015). However, it should be noted that interpretation of the range of results is affected by a number of differences among studies, such as soil type, biochar feedstock, plant type, as well as being a field or greenhouse study (Table 2.1). The funnel plot of the data Fig. 2.7 and Fig. 2.12 shows that the studies were reasonably symmetrically distributed around the mean effect size, presenting a random sampling error.

2.3.1. Application rate

Fig. 2.2 shows the effects of application rates on plant productivity. COMBI was applied to fields at a wide range of application rates in different studies, ranging from 10 t/ha to 150 t/ha. When the application rate was <20 t/ha, COMBI significantly increased plant productivity by an average of 48.3% ($P<0.001$). This result is promising since it is unlikely that field-scale application of large amounts of COMBI would be economical. No significant yield increases were found for the application rates between 20 to 30 t/ha. The benefits of applying COMBI might have been canceled out due to increased salt contents at these application rates (Spokas et al., 2012). Similar results were found for compost application (Fig. 2.8). Some studies reported that the excess amount of biochar or compost applied to the soil might increase soil salinity, especially in arid and semiarid regions, and inhibit plant growth (Cai et al., 2010; Reddy and Crohn, 2012). Livestock manure and municipal solid waste were composted in most of the studies reported in this review. These compost materials are known to increase soil salinity (Cai et al., 2010; Li-Xian et al., 2007). High salinity causes poor plant growth and low soil microbial activity due to osmotic stress and toxic ions (Yan et al., 2015). At higher application rates (>30 t/ha), the increase in plant productivity was significant again ($P<0.001$) but lower (67% lower) than that measured at <20 t/ha

application rates. At these application rates (>30 t/ha), the benefits provided by compost and biochar might have overcome the salinity problem. The longevity of these results is not known yet because all the studies included in this review took place in less than a year. As more data becomes available, the meta-analysis can be updated to distinguish the different application rates.

2.3.2. Soil pH

Fig. 2.3 presents the effects of COMBI application on plants grown on soils with different pH values. The lowest and highest soil pH values were 4.2 and 8.29, respectively. Depending on the feedstock, biochar and compost generally have a neutral or basic pH. During the initial stage of the composting process, the pH of compost decreases due to the release of organic acids. Following the initial stage, organic acids are decomposed, and NH_3 is generated due to the breakdown of proteins, which increases pH. In the final stage, pH again decreases due to NH_3 volatilization and nitrification and eventually stabilizes at values between 7 and 8.5 (Akdeniz, 2019; Wang et al., 2018b). The addition of biochar may help reduce ammonia volatilization, which would cause an elevation in final pH (Hagemann et al., 2017; Kammann et al., 2015). Besides, it is also possible that compost material may contain carbonate compounds due to the reaction between carbon dioxide (CO_2) and mineral metals, leading to an increase in alkalinity (Castán et al., 2016).

The liming effect of biochar or compost is often reported as one of the main mechanisms behind the increased crop yields (Butnan et al., 2015; Kätterer et al., 2019; Qiao-Hong et al., 2014). Fig. 2.3 and Fig. 2.9 illustrates further evidence for this hypothesis as the most significant plant productivity was observed at soil pH values between 4 and 5. At this pH range, COMBI showed a significant increase (48.9%, $P<0.001$) in crop productivity. The impact was positive and significant at soil pH values between 5-6 (23.9%, $P=0.003$) and 6-7 (13%, $P<0.001$). No significant response was observed at neutral (7-8) and basic (8-9) pH values. Jeffery et al. (2015) reported similar results. Although these results are promising, no data shows how COMBI or compost applications changed the soil pH. Interpretation of pH data should be undertaken with care.

The grand means reported in Fig. 2.2 and Fig. 2.3 were different since the number of studies (n) that were included in the meta-analysis was different. There were studies that did not report application rates but provided information about soil pH. These studies were not included in Fig. 2.2, but they were included in Fig. 2.3.

2.3.3. Plant type

Fig. 2.4 shows the effect of COMBI on plant productivity relative to the plant type. Plant types are (1) cereal grass: barley (*Hordeum vulgare* L.), maize (*Zea mays* L.), oat (*Avena sativa* L.), quinoa (*Chenopodium quinoa*), wheat (*Triticum aestivum* L.), (2) grass: halophyte (not reported), ryegrass (*Lolium multiflorum*), (3) oilseed: peanut (*Arachis hypogaea* L.), rapeseed (*Brassica napus* L.), (4) vegetable: bok choy (*Brassica rapa*), lettuce (*Lactuca sativa* L.), (5) fruit: banana (*Musa acuminata*), braeburn (*Malus domestica* Braeburn) papaya (*Carica papaya* L.), and (6) tree: alder (*Alnus glutinosa* L. Gaertn), poplar (*Populus tremula* L.), and willow (binomial name not reported).

When grown with COMBI, cereal grasses (barley, maize, oat, quinoa, and wheat) showed a statistically significant increase in grain yield (39.7%, $P<0.001$). Other plants did not show any significant change. But some results were based on only one or two studies. The forest plot should be updated when more data becomes available. Unlike COMBI data, compost data showed significant increases in the productivity of grasses (53.3%) and oilseeds (18.1%) (Fig. 2.10), but again, these results were based on only one or two studies. This analysis contained the full number of observations (n=233). The grand mean indicates that COMBI overall significantly increased the plant productivity by 22.8%.

Besides the type of the plant, soil fertility also has an impact on the effect size. The plants that are grown on poor soils may benefit more from COMBI. On the other hand, the plants that are grown on more fertile soils may not benefit much from COMBI. A negative response could be due to the dilution effect of the amendment on soil nutrients (Jeffery et al., 2011; Steiner et al., 2010b; L. Zhang and Sun, 2014). Fig. 2.4 provides valuable information for future research, but the yields shown in Fig. 2.4 should not be taken as absolute values.

2.3.4. Biochar feedstock

Fig. 2.5 shows the effects of biochar produced from a range of feedstocks following composting and application to soil. Wood-based biochars include different feedstocks such as wood chips, green cuttings, garden waste, and forest wood residues, which showed a statistically significant increase in productivity (29.4%, $P<0.001$). Rice husk biochar also increased plant

productivity (54%, P=0.005), but this result was based on only one study. Peanut shell biochar or garden peat did not significantly affect plant growth.

Although the type of feedstock used to produce biochars has a big impact on biochars' physical and chemical properties, pyrolysis conditions (e.g., temperature, time) also affect biochar properties. Brunauer-Emmett-Teller (BET) surface area, porosity, bulk density, and pH are often used as measures of biochars' properties (Neslihan Akdeniz, 2019; Weber and Quicker, 2018). Whenever information about biochar properties was available, it was added to Table 2.1. As seen in Table 2.1, currently, there is not enough data, but in future studies, having forest plots that show the changes in plant productivities relative to the BET surface area or other characteristics of biochars would be very helpful.

2.3.5. Compost material

Fig. 2.6 shows the effects of COMBI on plant productivity relative to the compost type (animal manure, green waste, sewage sludge, and seafood/peanut shell). Animal manure compost (e.g., dairy, horse, poultry, farm manure) showed the largest percent change in crop productivity (44.1%, $P<0.001$), while the sewage sludge had the second-largest impact (26%, $P<0.001$). Animal manure and sewage sludge composts are rich in nitrogen (Bernal et al., 2009; Joern and Brichford, 1993; Sommers, 1977), and the increase in crop productivity might be due to their high nitrogen contents. No significant difference was found for green waste compost or seafood/peanut shell compost materials. Similar results were found for compost applications (Fig. 2.11).

2.4. Conclusions

Although results varied, COMBI and compost amendments had some benefits at low (<20 t/ha) and high (>30 t/ha) application rates. While the interpretation of meta-analysis results is affected by the differences among studies, the advantage of conducting a meta-analysis is that the results point out future research needs. For instance, Fig. 2.3 indicates that more studies are needed at low (4-5) and high (8-9) pH values. Fig. 2.4 shows that grain yields of cereal grasses (maize, wheat, oat, barley) increased with COMBI application (39.7%). This result is promising, but it was based on six studies (one or two studies per group). Based on Fig. 2.5, it can be concluded that other than wood-based biochar, different biochar types should be studied. Fig. 2.6 points out that the immediate research needs are sewage sludge composting.

Although more studies are needed to make solid conclusions, our meta-analyses showed that COMBI and compost applications showed similar results. Any increase in plant productivity was most likely due to compost addition, not due to biochar addition. However, Table 2.1 points out that the plants that are grown on sandy soils or during a drought benefit from COMBI addition. For example, Mekuria et al. (2014) reported that during a drought, plots amended with COMBI showed a lower reduction in grain yield (35-36%) compared to the plots amended with compost (40-64%). Glaser et al. (2015b) showed that COMBI increased maize yield by 26% compared to compost when grown on sandy soil. Future research should focus on poor soil or drought conditions. Biochar is the name of a wide range of carbon-rich materials. Reporting biochar characteristics and production conditions is very important to make robust comparisons in future studies. In some studies, binomial names of the plants were not reported. As much as biochar characteristics, it is also essential to state binomial names of the plants.

2.5. Acknowledgment

This project was supported by a HATCH Grant (no. ILLU-741-328) from the USDA National Institute of Food and Agriculture. We thank Dr. Getachew Agegnehu and Dr. Hardy Schulz for kindly providing information for the meta-analysis.

2.6. Figures and Tables

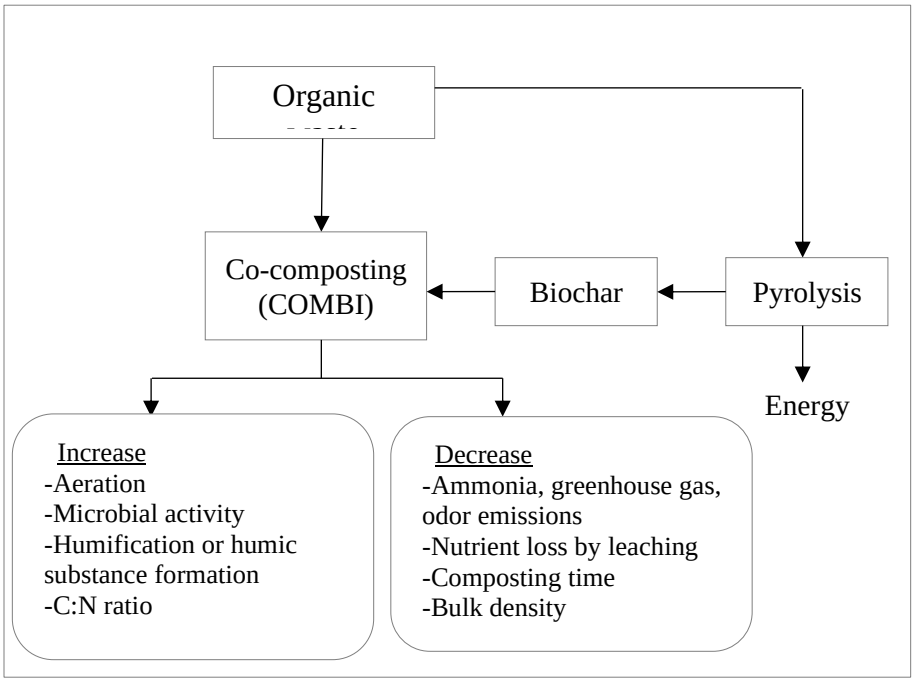

Fig. 2.1. Potential benefits of co-composting organic wastes with biochar (COMBI) on the composting process

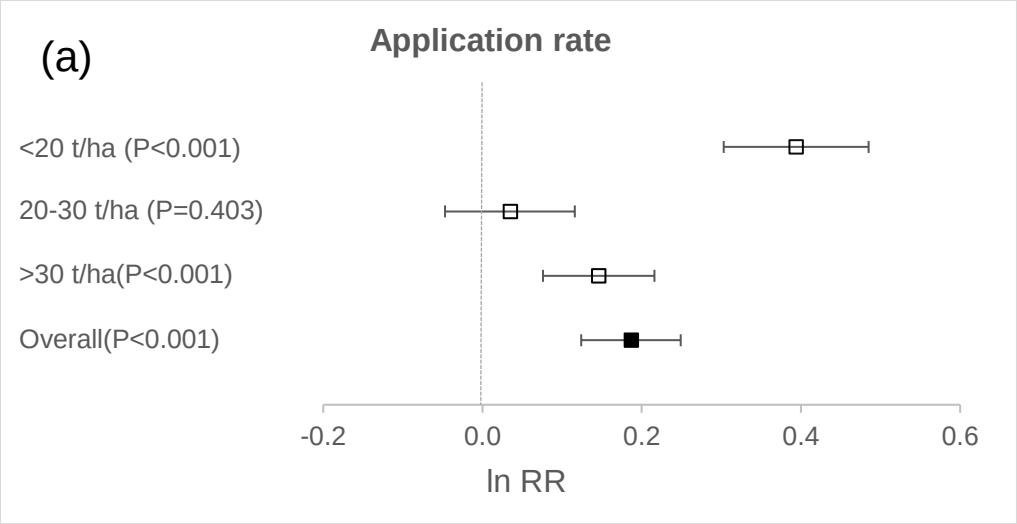

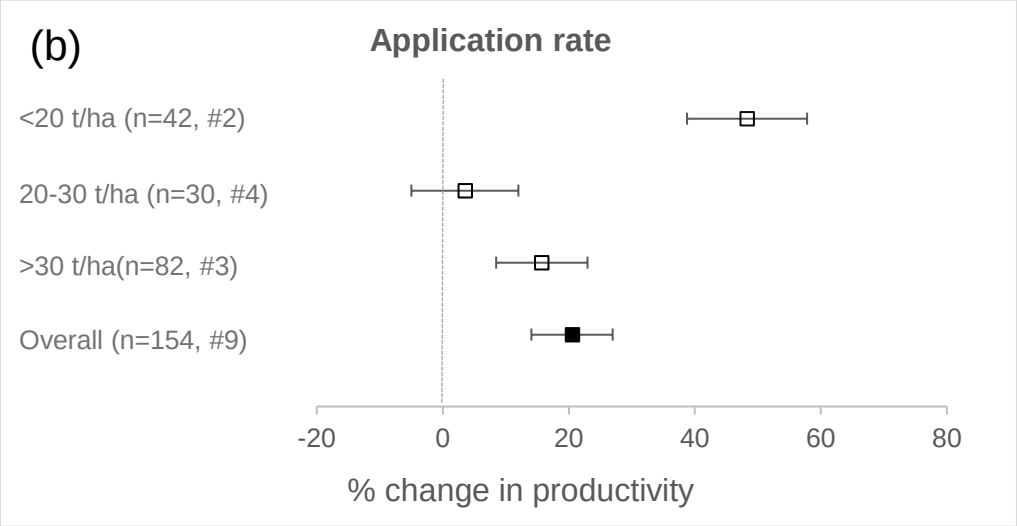

Fig. 2.2. Forest plots showing the effects of different COMBI application rates: a) A forest plot showing the effect size (ln RR) calculated from each group presented. Each point shows the mean effect size for each grouping, with the lines representing 95% confidence intervals (CIs). b) A forest plot presenting percent changes in plant productivity. The total number of replicates (n) and the total number of studies (#) included in each grouping are shown in parenthesis.

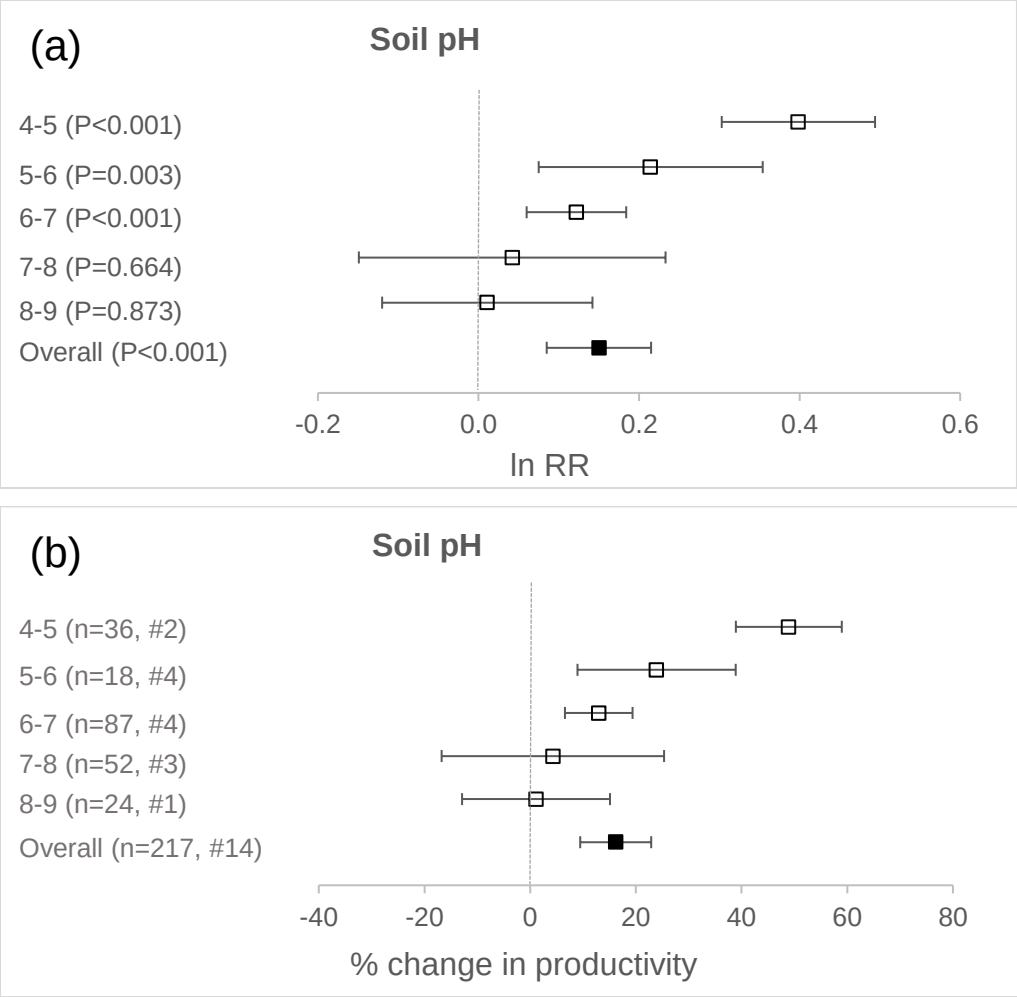

Fig. 2.3. Forest plots showing the effects of COMBI applications to soils with a range of pH values: a) A forest plot showing the effect size (ln RR) calculated from each group presented. Each point shows the mean effect size for each grouping, with the lines representing 95% confidence intervals (CIs). b) A forest plot presenting percent changes in plant productivity. The total number of replicates (n) and the total number of studies (#) included in each grouping are shown in parenthesis.

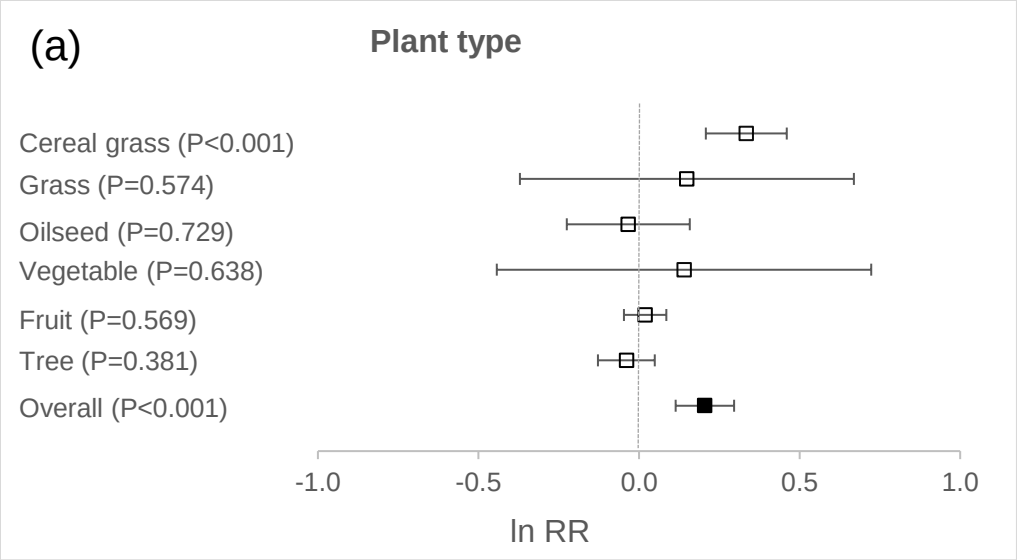

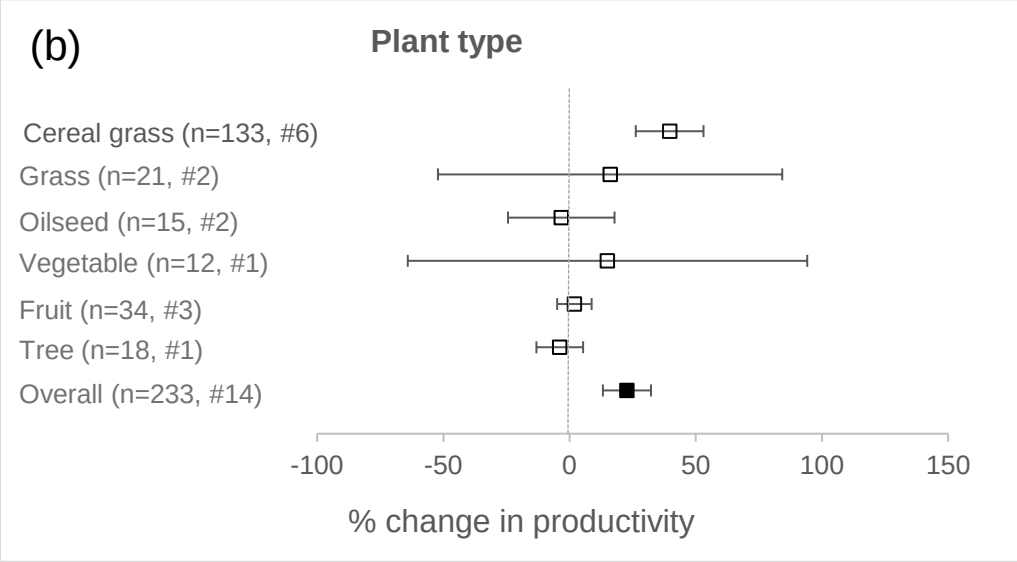

Fig. 2.4. Forest plots showing the effects of COMBI on different plant types: a) A forest plot showing the effect size (ln RR) calculated from each group presented. Each point shows the mean effect size for each grouping, with the lines representing 95% confidence intervals (CIs). b) A forest plot presenting percent changes in plant productivity. The total number of replicates (n) and the number of studies (#) included in each grouping are shown in parenthesis.

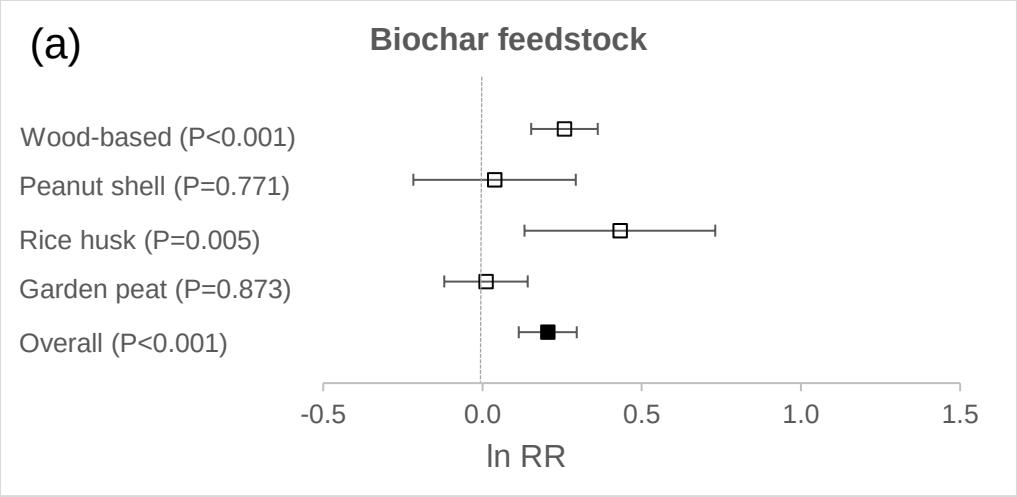

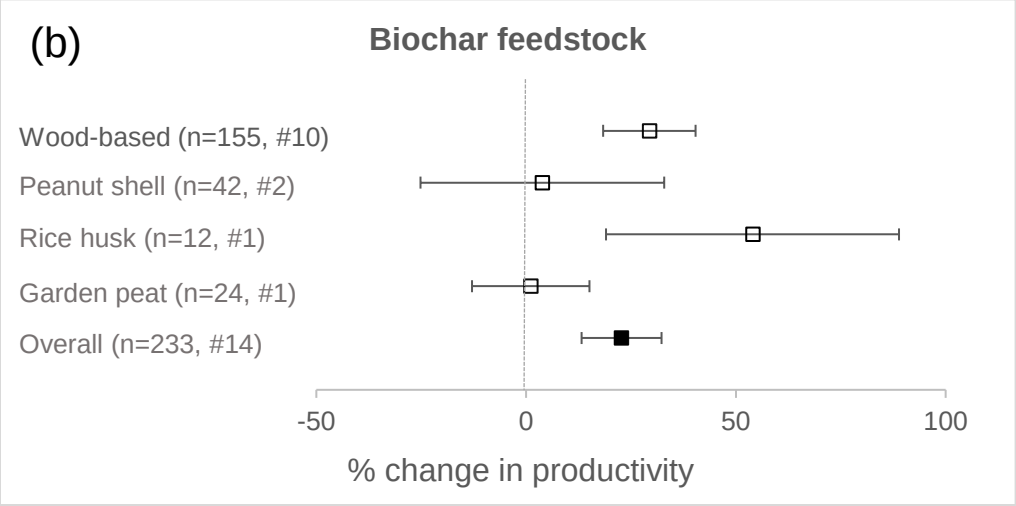

Fig. 2.5. Forest plots showing the effects of biochar produced from a range of feedstocks: a) A forest plot showing the effect size (ln RR) calculated from each group presented. Each point shows the mean effect size for each grouping, with the lines representing 95% confidence intervals (CIs). b) A forest plot presenting percent changes in plant productivity. The total number of replicates (n) and the total number of studies (#) included in each grouping are shown in parenthesis.

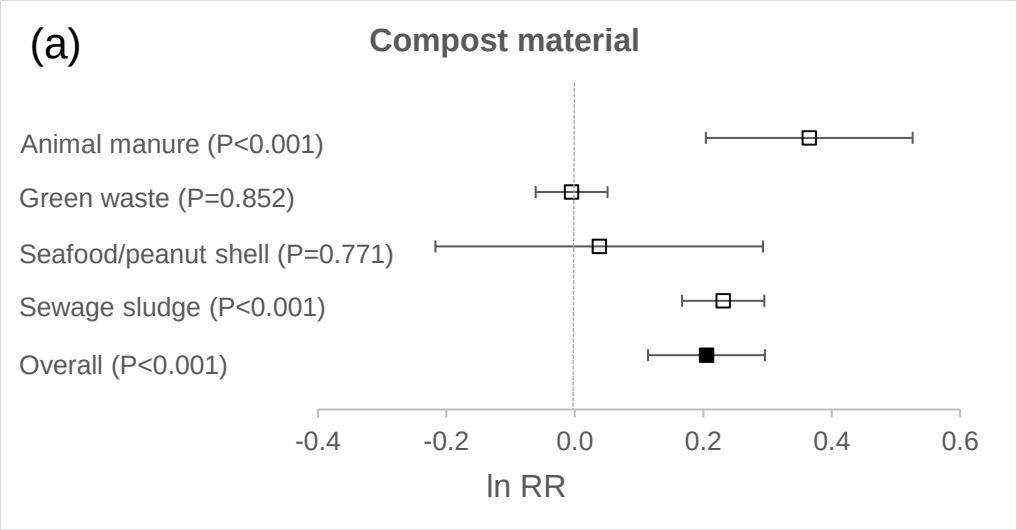

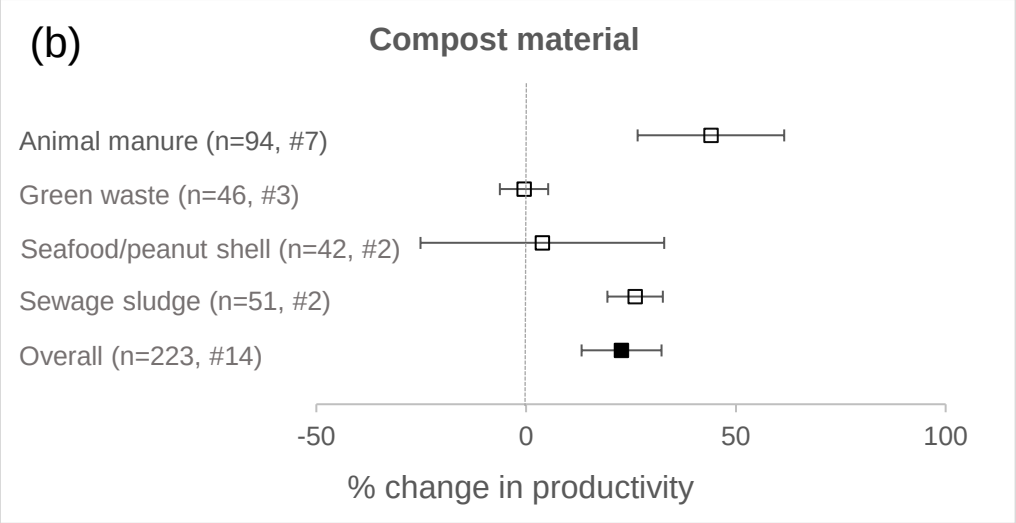

Fig. 2.6. Forest plots showing the effects of biochar composted with a range of compost material: a) A forest plot showing the effect size (ln RR) calculated from each group presented. Each point shows the mean effect size for each grouping, with the lines representing 95% confidence intervals (CIs). b) A forest plot presenting percent changes in plant productivity. The total number of replicates (n) and the total number of studies (#) included in each grouping are shown in parenthesis.

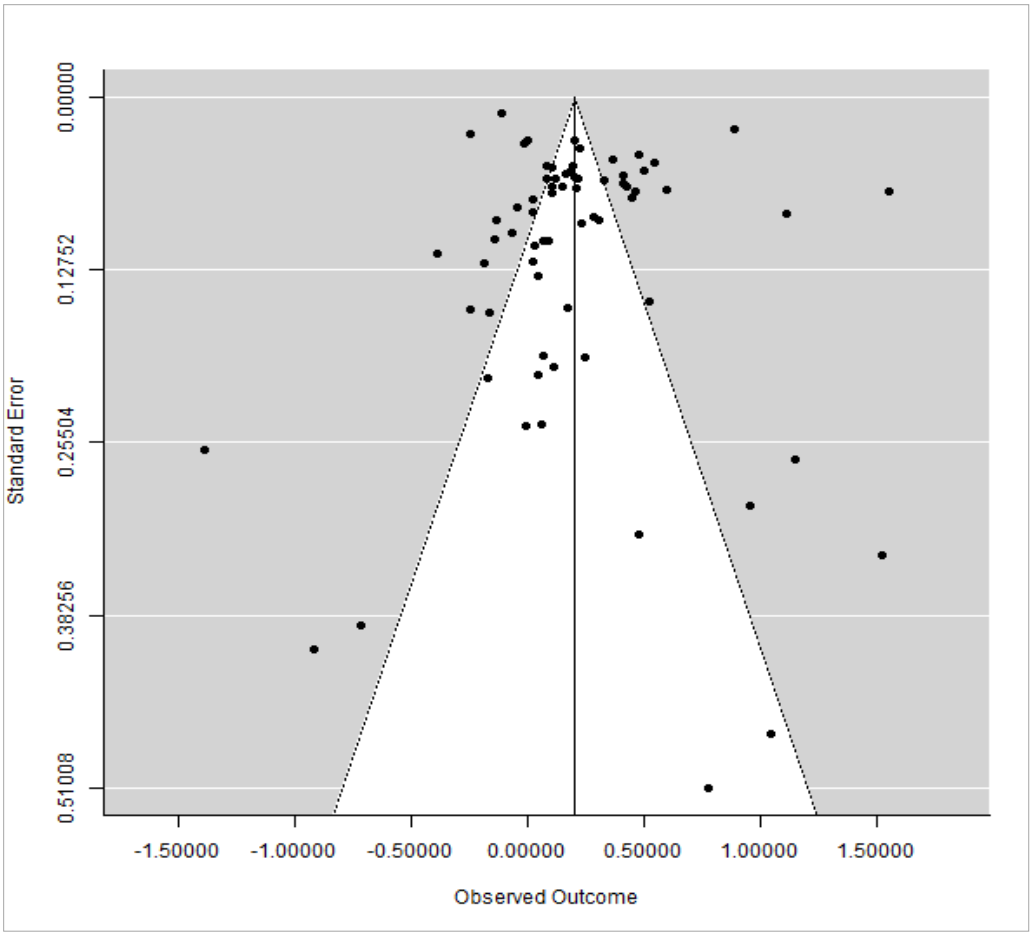

Fig. 2.7. A Funnel plot: The x-axis shows the effect size (ln RR), and y-axis presents the standard error of the effect size as an index of precision.

Table 2.1. The summary of the systematic review on the effects of co-composted biochar amendment on plant productivity

#	Biochar feedstock, pyrolysis T, BET surface area	Compost feedstock, composting time	Plant type	COMBI application rate	Scale *	Soil type	Soil pH	Impact on plant growth	Reference **
1	Willow wood (550 °C for 5-7 h, BET: 332 m^2/g)	Green waste, Bagasse, Chicken manure	Peanut	25 t ha^{-1} (9% biochar v/v)	Field	Red Ferrosol	5.9	Applications of compost and COMBI increased pod yield by 17 and 24%, respectively, compared to control conditions.	(Agegnehu et al., 2015) [a]
2	Willow wood (550 °C for 5-7 h)	Green waste, bagasse, chicken manure	Maize	25 t ha^{-1} (9% biochar v/v)	Field	Red Ferrosol	5.35	Applications of compost and COMBI increased grain yield by 10 and 13%, compared to control conditions.	(Agegnehu, Bass, et al., 2016) [a]
3	Acacia (350-450 °C for 6 days)	Manure, dairy cattle feed leftovers, bedding (15 weeks)	Barley	10 t ha^{-1} (1:5 biochar: compost d.w.)	Field	Eutric Nitisol (acidic)	4.97 4.83	Barley yields were 30, 41, 49, and 42% higher at Holetta location and 67, 78, 70, and 51% higher at Robgebeya location, respectively for biochar, compost, compost-biochar mix, and COMBI soil amendments compared to control conditions.	(Agegnehu et al., 2016b)
4	Willow wood >550°C for 5-7 h)	Green waste, Bagasse, chicken manure (98 days)	Banana, papaya	25 t ha^{-1} (9% biochar v/v)	Field	Red clay	5.89	Counter to the expectations, compost, and COMBI applications reduced banana crop yield by 12 and 24%, respectively, while no significant effect was found on papaya yield.	(Bass et al., 2016) [a]
5	Green cuttings (650 °C)	Straw, draff, horse manure, maize silage, loam, stone powder (45 days)	Maize	200 kg N ha^{-1} (3.7% biochar w/w, or 10 t ha^{-1} biochar)	Field	Sandy	7.5	Application of COMBI increased maize yield by 26% compared to compost only.	(Glaser et al., 2015) [b]

Table 2.1. (cont.)

#	Biochar feedstock, pyrolysis T, BET surface area	Compost feedstock, composting time	Plant type	COMBI application rate	Scale *	Soil type	Soil pH	Impact on plant growth	Reference **
6	Wood chips (~700 °C for 36 h)	Cow, horse, poultry manure (~60 days)	Quinoa	2% w/w. (20% biochar v/v)	Lab	Sandy loam, sand, gravel	-	COMBI application increased the quinoa yield up to 305%, while the addition of untreated biochar decreased the yield by 60% compared to control conditions. Electron microscope images showed that composting increased the dissolved organic carbon content of the biochar.	(Kammann et al., 2015)
7	Sludge biosolids and green waste (mainly garden waste) (650°C for 40 min, BET: 396 m^2/g)	Food waste (coffee grounds, fruit peel, vegetables) and sawdust (11 weeks)	Sorghum	10% v/v	Green house	Brown Chromosol	5.2	COMBI treatment had a significantly higher (21%) crop yield compared to compost treatment. The composting process reduced the surface area of the biochar from 396 to 12 m^2/g.	(Kaudal and Weatherley, 2018) [b]
8	Wheat straw (350-550 °C)	Poultry manure (6 weeks)	Wheat	12 t ha^{-1} (75% biochar v/v)	Field	Moderately salt-stressed Antisol	8.25	Application of COMBI, pyroligneous solution (a byproduct of the pyrolysis process), and fertilizer increased wheat yield by 36.5% during the second year of the study compared to control conditions (only fertilizer).	(Lashari et al., 2013) [b]
9	Wheat straw (480 °C)	Poultry manure (6 weeks)	Maize	12 t ha^{-1} (75% biochar v/v)	Field	Moderately salt stressed Antisol	8.25	Application of COMBI, pyroligneous solution (a byproduct of the pyrolysis process), and fertilizer increased maize yield by 140% during the second year of the study compared to control conditions (only fertilizer).	(Lashari et al., 2015) [b]
10	Peanut shell (350°C for 2 h)	Seafood shell powder, peanut shell humate, inorganic nutrients (30 days)	Halophyte (sesbania, seashore mallow)	1.5% w/w, 5% w/w 10% w/w. (50% biochar w/w)	Lab	Coastal	7.98	COMBI applications at low rates (1.5%) increased sesbania and seashore mallow growth by 309 and 70.8%, respectively. High rates of COMBI (10%) significantly inhibited the growth of both halophytes.	(Luo et al., 2017)

Table 2.1. (cont.)

#	Biochar feedstock, pyrolysis T, BET surface area	Compost feedstock, composting time	Plant type	COMBI application rate	Scale *	Soil type	Soil pH	Impact on plant growth	Reference **
11	Rice husk	Cow manure, Clay (3 weeks)	Maize	10 t ha^{-1} (50% biochar w/w)	Field	Gleyic Acrisol	4.2 5.4	Experiments continued for two years. The second year's yields were lower than the first year's yields due to a late-season drought. Plots amended with biochar and COMBI showed a lower reduction in grain yield (35-36%) compared to the plots amended with bentonite clay and clay manure compost (40-64%).	(Mekuria et al., 2014)
12	Garden peat (450°C)	Farm manure (2.5 months)	Wheat	2% w/w (0%, 25%, 50%, 75%, 100% biochar)	Lab	Alkaline	8.29	A significant interaction between the fertilizer levels and COMBI rates was found. The increase in plant height and grain yield at lower fertilizer levels was attributed to increased nutrient retention by COMBI.	(Qayyum et al., 2017)
13	Woodchips (750 °C for 36 h, BET: 144 m^2/g)	Green waste (8 weeks)	Grape	63 t ha^{-1} (20% biochar v/v, or 8 t ha^{-1})	Field	Haplic regosol	7.9	Application of biochar or COMBI had no economically significant effect on vine health and grape quality over three years.	(Schmidt et al., 2014)
14	Beechwood (350-450 °C for 6 days)	Sewage sludge, freshly chaffed lop, soil (8 weeks)	Oat	50, 100, and 200 t ha^{-1} (5-50 % biochar w.b.)	Lab	Washed sand, loamy soil	6.3, 6.4	Application of COMBI increased the oat height by 24%. Plant growth was generally higher on loamy soil. There was no significant correlation between the plant height and compost amount in sandy soil.	(Schulz et al., 2013)
15	Holm oak (650 °C for 12-18 h)	Green waste, municipal solid waste (3 months)	Ryegrass	39 kg P ha^{-1} (10% biochar d.w.)	Lab	Silt loam (40 mg P/kg)	5.33	Application of COMBI increased the ryegrass yield by 34.7% compared to control conditions, but it did not significantly increase the yield compared to compost and compost-biochar mix applications.	(Vandecasteele et al., 2016)

Table 2.1. (cont.)

#	Biochar feedstock, pyrolysis T, BET surface area	Compost feedstock, composting time	Plant type	COMBI application rate	Scale *	Soil type	Soil pH	Impact on plant growth	Reference **
16	Forest wood residues (up to 700 °C)	Green cuttings, garden debris	Poplar, willow, alder	30 t ha^{-1} (15% and 30% biochar v/v)	Field	Luvic Stagnosol	6.5	The fruit yield and quality were not affected by the application of COMBI. The authors did not recommend using the COMBI amendment for apple orchards with fertile soils.	(von Glisczynski et al., 2016a)
17	Forest wood residues (up to 700 °C)	Green cuttings, garden debris	Braeburn tree	3 kg per tree (15% and 30% biochar v/v)	Field	Luvic Stagnosol	6.5	Application of COMBI did not improve plant yield under temperate soil and climate conditions.	(von Glisczynski et al., 2016b)
18	Peanut shell (350 °C for 3 h)	Seafood shell powder, peanut shell humate, inorganic nutrients (30 days)	Rapeseed Lettuce, bok choi	31.5 t ha^{-1}	Lab	Sandy Loam	7.61	COMBI application without a fertilizer significantly increased root (153%), shoot (219%), and total biomass (186%) compared to control conditions (only soil). COMBI application with an N fertilizer reduced root (39.3%), shoot (31.3%), and total biomass (31.6%) compared to control with fertilizer.	(H. Wang et al., 2017)

*Lab-scale refers to greenhouse studies or pot studies **[a] average soil pH from multiple measurement methods (ex. KCl and H_2O), [b] excluded from the meta-analysis (please see the methodology section for an explanation)

2.7. Appendix

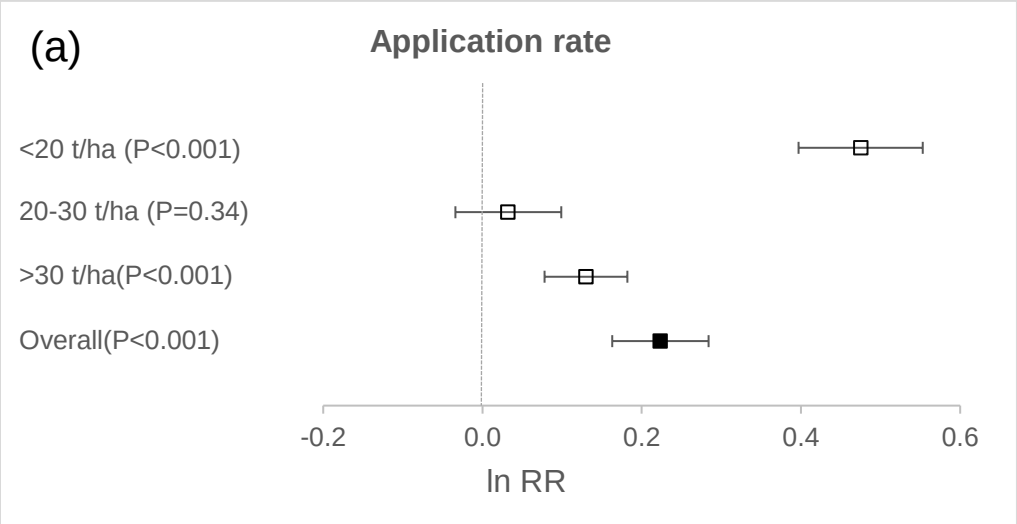

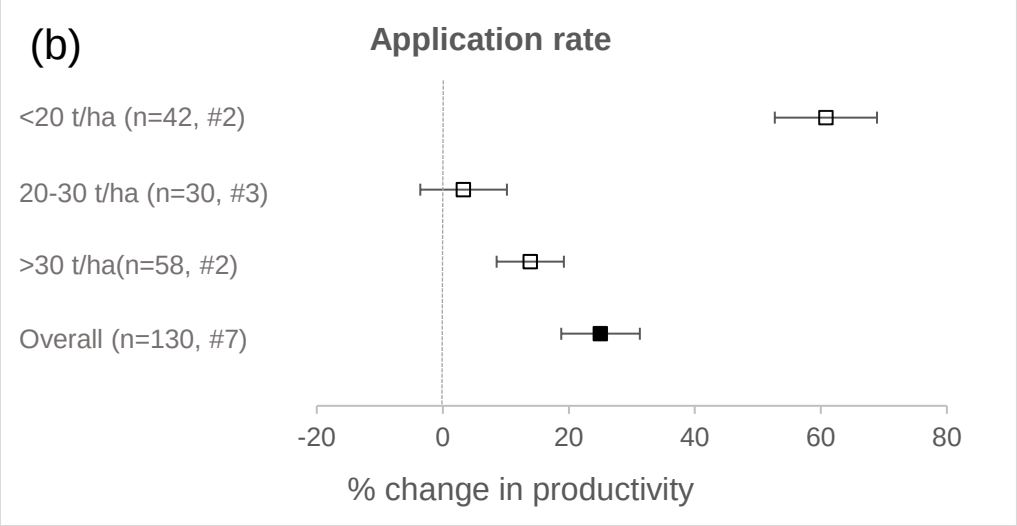

Fig. 2.8. Forest plots showing the effects of different compost application rates: a) A forest plot showing the effect size (ln RR) calculated from each group presented. Each point shows the mean effect size for each grouping, with the lines representing 95% confidence intervals (CIs). b) A forest plot presenting percent changes in plant productivity. The total number of replicates (n) and the total number of studies (#)included in each grouping are shown in parenthesis.

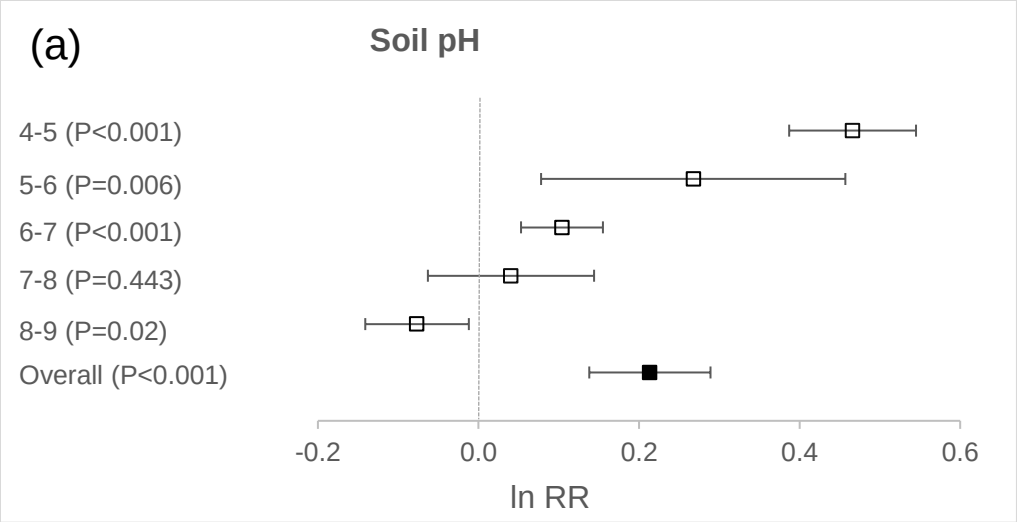

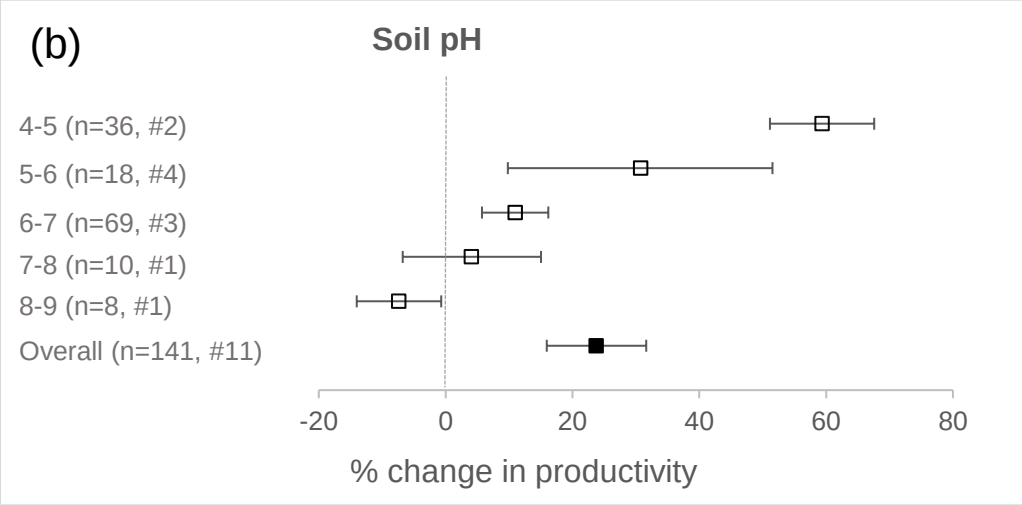

Fig. 2.9. Forest plots showing the effects of compost applications to soils with a range of pH values: a) A forest plot showing the effect size (ln RR) calculated from each group presented. Each point shows the mean effect size for each grouping, with the lines representing 95% confidence intervals (CIs). b) A forest plot presenting percent changes in plant productivity. The total number of replicates (n) and the total number of studies (#)included in each grouping are shown in parenthesis.

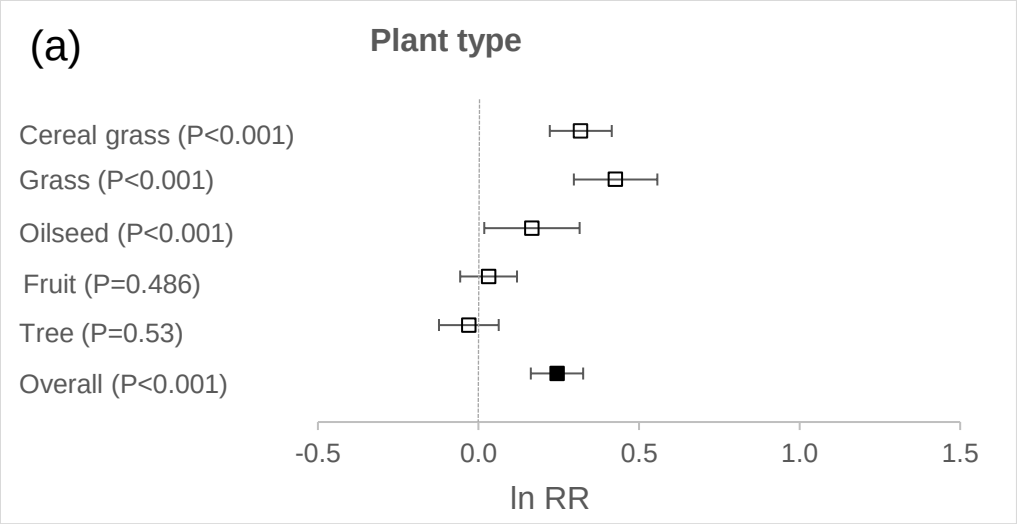

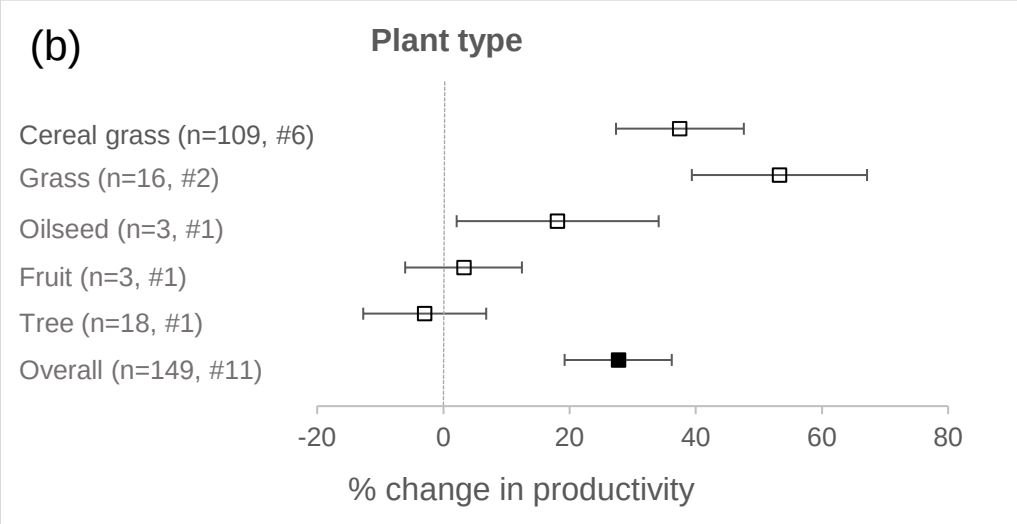

Fig. 2.10. Forest plots showing the effects of compost on different plant types: a) A forest plot showing the effect size (ln RR) calculated from each group presented. Each point shows the mean effect size for each grouping, with the lines representing 95% confidence intervals (CIs). b) A forest plot presenting percent changes in plant productivity. The total number of replicates (n) and the total number of studies (#) included in each grouping are shown in parenthesis.

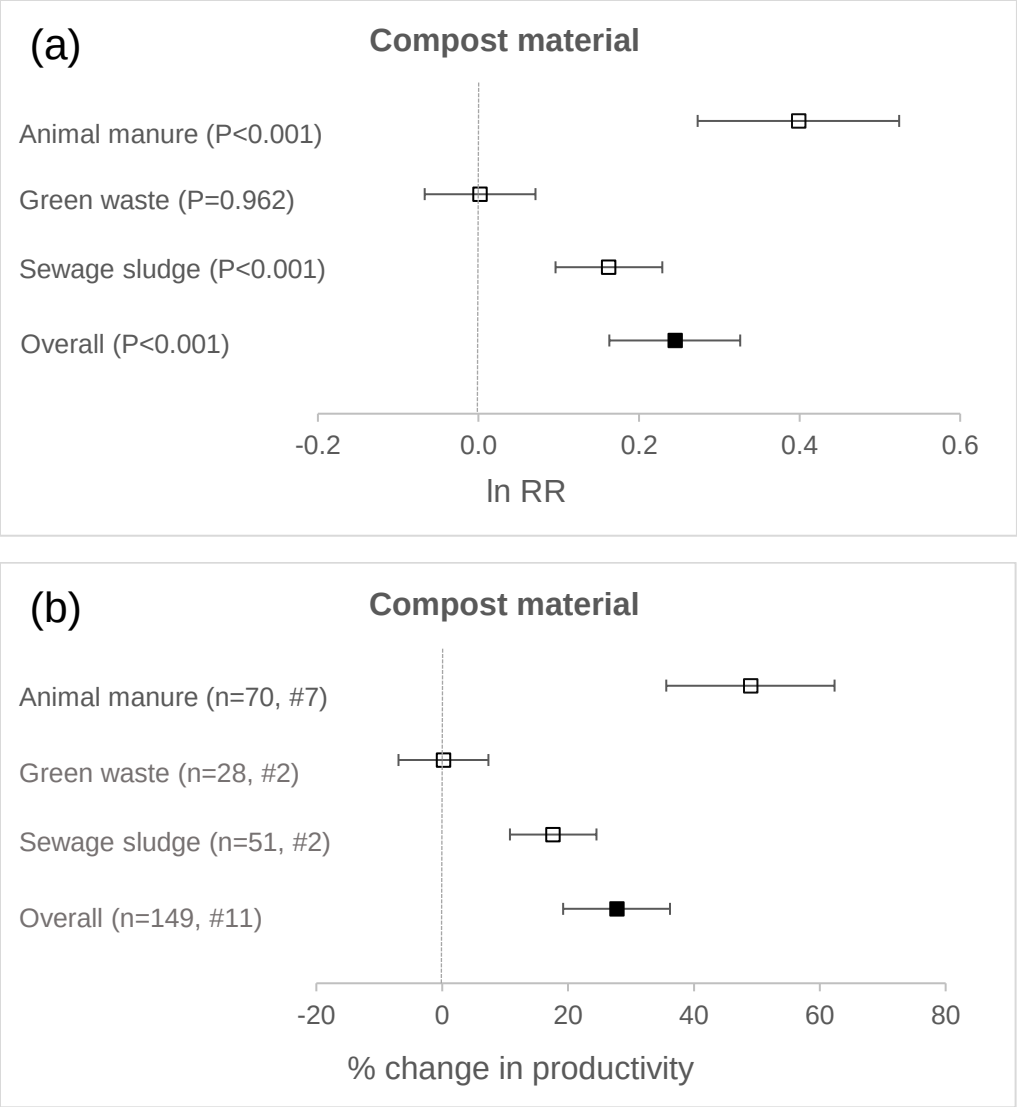

Fig. 2.11. Forest plots showing the compost treatment data corresponding to COMBI treatments with different compost materials: a) A forest plot showing the effect size (ln RR) calculated from each group presented. Each point shows the mean effect size for each grouping, with the lines representing 95% confidence intervals (CIs). b) A forest plot presenting percent changes in plant productivity. The total number of replicates (n) and the total number of studies (#) included in each grouping are shown in parenthesis.

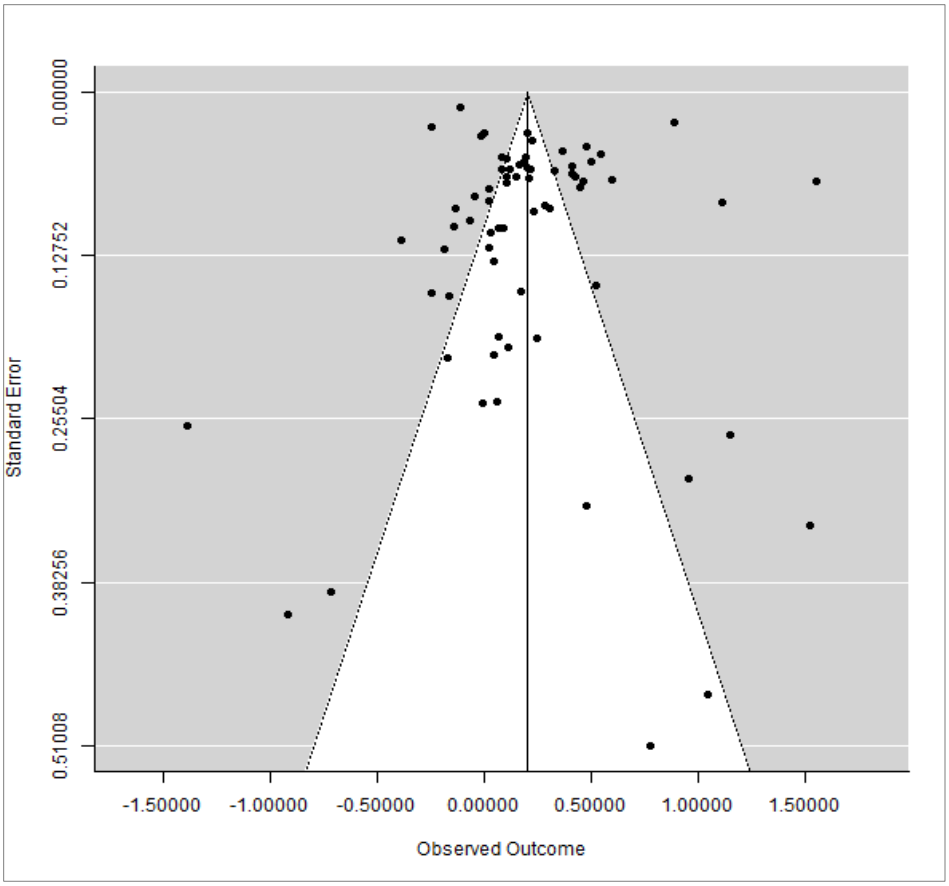

Fig. 2.12. A Funnel plot: The x-axis shows the effect size (ln RR), and y-axis presents the standard error of the effect size as an index of precision.

CHAPTER 3

BIOCHAR-AMENDED POULTRY MORTALITY COMPOSTING TO INCREASE COMPOST TEMPERATURES, REDUCE AMMONIA EMISSIONS, AND DECREASE LEACHATE'S CHEMICAL OXYGEN DEMAND

3.1. Introduction

Livestock mortalities are caused by many reasons, including birth defects, infectious animal diseases, or injuries. As an example, an animal feeding operation with one million laying hens (which is typical in the Midwest U.S.) would have 100 to 250 mortalities every day (assuming 4 to 10% mortality rate over 60 weeks) (USDA-APHIS, 2014). This means producers need to handle about 1,000 to 2,500 kg of mortalities per week (assuming 1.5 kg/hen). For a larger-size facility with five million laying hens (a handful of them exist in the Midwest U.S.), the mortality rate would be about 5 to 12.5 tons per week. This can represent a significant challenge. A mortality disposal method that processes mortalities into valuable products eliminates risks of spreading infectious animal diseases and reduces environmental impacts of the mortality management is critical for the sustainability of the poultry industry. Despite the widely appreciated magnitude of this problem, unfortunately, little progress has been made in this area (G. Flory and Peer, 2017).

In Illinois (U.S.), where the research was conducted, poultry mortalities are managed according to the Dead Animal Disposal Act. The Act allows poultry producers to dispose of their mortalities using one of the four disposal methods-burial, composting, incineration, and rendering (IL Dept. of Agriculture, 1990). The number of rendering facilities that accept animal mortalities is decreasing rapidly, and most of the existing rendering facilities do not accept animal mortalities due to Bovine Spongiform Encephalopathy (BSE) concerns. Incineration is energy intense, and burial has the risk of contaminating ground and underground water sources. Composting, if done properly, is the preferred on-farm animal mortality disposal method (Costa and Akdeniz, 2019).

Composting is a natural and aerobic process involving the biological degradation of organic wastes into a humus-like product (Imbeah, 1998). The high temperature generated during the mesophilic and thermophilic stages can effectively eliminate the pathogens, ensuring final

product safety (Neslihan Akdeniz, 2019; Costa and Akdeniz, 2019). The temperature increase results from the heat generated from microbial and enzymatic activity, resulting in the rapid decomposition of organic matter (Godlewska et al., 2017). During the composting process, moisture content of around 40-50% is required to ensure microbial activity (MAFES, 2016). Maintaining proper moisture content in the composting pile can be challenging. The high temperatures can increase water evaporation and result in the over-drying of the pile (Neslihan Akdeniz, 2019). Reduced moisture content in the composting pile can lower microbial activity (Godlewska et al., 2017).

The decomposition of protein and amino acids during the degradation process leads to ammonia formation during the composting process (Martins and Dewes, 1992). Ammonia volatilization can be increased by higher temperatures, pH, aeration rate, and organic matter mineralization (Guo et al., 2020) and is the major cause of nitrogen losses during the composting process. Previous studies reported that the nitrogen losses by ammonia volatilization counted for 16% to 77.4% of the initial nitrogen content (Barrington et al., 2002; Martins and Dewes, 1992; Steiner et al., 2010b). The loss of nitrogen causes odor and health concerns during the composting process and decreases the final compost quality as a soil amendment (Wang et al., 2017).

Biochar is a carbon-rich material produced by heating biomass in an oxygen-limited environment (Johannes Lehmann and Joseph, 2015). It has been tested as a soil amendment in many studies (Abbott et al., 2018; Cooper et al., 2020; Gul et al., 2015; L. Xiao et al., 2020). Biochar has also been used as a compost amendment because it is expected to have the following benefits: 1) increase aeration and microbial activity, 2) reduce nitrogen loss and ammonia emission, 3) enhance water holding capacity and reduce the amount of leachate, and 4) increase the degree of humification (Neslihan Akdeniz, 2019; Godlewska et al., 2017; Guo et al., 2020; Oldfield et al., 2018; Yuchuan Wang et al., 2019; R. Xiao et al., 2017). The effects of biochar amendment on various compost materials have been researched so far. These compost materials include poultry litter/manure (W. Chen et al., 2017a; Sánchez-Monedero et al., 2019), dairy/beef manure (Awasthi et al., 2019; Duan et al., 2019), swine manure (Ravindran et al., 2019; Yang et al., 2019; J. Zhang et al., 2016), sewage sludge (Du, Zhang, Hu, et al., 2019), and food waste (Waqas et al., 2017). Animal mortalities are another solid waste that animal producers need to manage daily. To date, composting animal mortalities with biochar has not been studied yet. If

biochar enhances compost temperatures, as reported in previous studies (Neslihan Akdeniz, 2019), the biochar amendment would help to prevent the spread of animal diseases. Besides, biochar's benefits in retaining essential nutrients such as nitrogen and other organic compounds would reduce the environmental impact during the animal mortality composting while producing a more fertile final compost.

The present study demonstrates the co-composting process of poultry mortality amended with the biochar. Previously, a wide range of biochar application rates (from 3 to 50% by weight) during composting have been investigated (Dias, Silva, Higashikawa, Roig, and Sánchez-Monedero, 2010; N. Liu et al., 2017). Some researchers discouraged using biochar at high rates (e.g., 50%) because, at high rates, biochar may cause water losses (N. Liu et al., 2017), adversely affecting the degradation process. The cost of biochar is another limiting factor. In this pilot-scale composting study, we tested five biochar application rates (0, 2.6, 13, 26, and 39% by volume). The objectives of the study were to test if biochar amendment could 1) increase compost temperatures, 2) reduce ammonia emissions, 3) decrease leachate's organic content, and 4) enhance the nutrient content of finished compost.

3.2. Materials and Methods

3.2.1. Composting chicken mortalities

Chicken mortalities were provided by the Poultry Research Farm (PRF), located about six miles south of the campus. Chickens were euthanized at the farm, and the mortalities were immediately transferred to the experimental site. They were stored in a freezer until being used for the experiments. One day was allowed to thaw the frozen chicken mortalities before loading them into the composting pile. Woodchips were collected from the Ground Storage Barn on campus. Biochar selected for the composting experiments was produced by Chip Energy (Goodfield, Illinois) by the gasification process (520°C) using waste wood pallets as feedstock. The pilot-scale composting test units were made of 32-gallon bins. A steel mesh was placed about 10 cm above the bottom of the bin to create an air plenum. About 15 cm of wood chips were placed on the steel mesh. Four to five chicken mortalities (8.8 ± 0.4 kg) were placed on the woodchips. Mortalities were capped with 15 cm of woodchips. A thin layer of biochar (up to 6 cm in total) was placed evenly both under and above the mortalities. The calculated initial carbon

(C) to nitrogen (N) ratio of the bins was around 22, which was within the recommendation of 20-40 (NRAES, 1999). The total fresh weight of the woodchips was 12 ± 0.9 kg. Biochar was added at 0% (control), 2.6, 13, 26 and 39% (by volume). These rates were equivalent to 0%, 1%, 5%, 10%, and 15% by fresh weight (dry biochar by fresh mortalities and woodchips). There were three replicates for each treatment. Physico-chemical characteristics of biochar and woodchips are shown in Table 3.1.

Each bin was aerated at a rate of 1.5 L/min using a vacuum pump (Thomas Pump, Slidell, LA) equipped with a flowmeter (Cole-Parmer, IL). This airflow rate was chosen based on previously published studies (Janczak, Malińska, et al., 2017; J. Yuan et al., 2016). A small hole was made on the sidewalls of the bins (near the bottom) to collect leachate. The hole was plugged with a rubber stopper when not used. The outer surfaces of the bins were wrapped with glass wool to improve insulation.

Composting experiments were run for 11 weeks, from July 16, 2019, to October 8, 2019, on the Agricultural and Biological Engineering Research and Training Farm at the University of Illinois. The compost material (chicken mortality, woodchips, and biochar) went through three heating cycles. At the end of each heating cycle (at the 4^{th}, 8^{th}, and 11^{th} weeks), the compost material was turned to distribute moisture uniformly. During the first and second turns, the overall moisture content of the materials was adjusted to 50.4±2.69 %, and about 3 kg of fresh woodchips were added on top of the bins to cover the remaining chicken tissues completely.

3.2.2. Measuring physicochemical characteristics of biochar and woodchips

On the same day as the beginning of composting, the moisture content, bulk density, and water holding capacity of biochar and woodchips were measured according to the Test Method for the Examination of Composting and Compost TMECC (Thompson et al., 2002). Considering chicken mortalities have a moisture content of 75% (NRAES, 1999), the compost mix's estimated overall initial moisture content (chicken mortalities, woodchips, and biochar) was around 50.3±1.4%. pH and conductivity were measured with a regularly calibrated Oakton PC2700 meter (Cole-Parmer, IL). The carbon (C) and nitrogen (N) ratios and Brunauer-Emmett-Teller (BET) surface area were measured by the Microanalysis Laboratory at the University of Illinois using a CE 440 CHN analyzer (Exeter Analytical Inc., U.K) and a 3Flex analyzer coupled with a SmartVac degasser (Micrometrics Instrument Corp., Norcross, GA), respectively.

The color of the biochar and woodchips was measured with a handheld color meter (TES-135A, TES, Taiwan).

3.2.3. Temperature and gas measurements

Temperatures of the mortality layers (1st heating cycle) or the pile centers (2nd and 3rd heating cycles) were recorded every 10 minutes using pre-calibrated K-type thermocouples and 4-channel data loggers (Tekcoplus Ltd, Hong Kong). To ensure consistent positioning, thermocouples were placed inside vertical PVC pipes. The oxygen concentrations at the mortality layer were measured once a week using a portable gas monitor (RKI - Eagle II®, Union City, CA). The instrument was regularly calibrated/checked using calibration gases (3, 6, 9, 12, 18, 20.9% O_2 by volume). The calibration gases were prepared by diluting 20.9% O_2 with N_2 using an Environics Gas Dilution System (Environics 4040, Tolland, CT) (A. J. Heber et al., 2008; Albert J. Heber et al., 2006)(Fig. 3.4).

Ammonia emissions from the bins were measured by the titration method (Meeker and Wagner, 1933). A stainless steel funnel was buried about 5 cm below the surface of the compost material. Two small weights (about 2 kg each) were placed on top of the funnel to prevent tipping (Neslihan Akdeniz and Janni, 2012). An SKC pump (Eighty-Four, PA) connected to the funnel drew air samples at a rate of 1L per minute for 3 to 15 minutes. NH_3 was captured into 2% boric acid and measured by titrating with H_2SO_4 (Meeker and Wagner, 1933). 0.005 M H_2SO_4 was used for ammonia titration. The boric acid and sulfuric acid were purchased from ThermoFisher Scientific Inc. The method was validated by testing known concentrations of ammonia (10.53, 21.06, 52.65, and 105.3 ppm in the air)(Fig. 3.5). The accuracy of the method was 96.1±2.01%. The calibration gases were prepared by diluting 105.3 ppm NH_3 with N_2 using an Environics Gas Dilution System (Environics 4040, Tolland, CT). The gas cylinders were purchased from Airgas (Denver, IL). Daily NH_3 emission rates m_{NH3} (mg NH_3 day^{-1} kg^{-1}) were calculated using Eq. 3.1.

$$m_{NH3} = \left(\frac{C_{NH_3}}{10^6}\right)\left(\frac{P}{R}\cdot\frac{MW_{NH_3}}{T}\right)\cdot 1000\frac{mg}{g}\cdot 60\frac{min}{h}\cdot 24\frac{h}{day}\cdot\frac{1}{W_{mortality}}\cdot Q_{air} \qquad \text{Eq. 3.1}$$

where C_{NH3} is ammonia concentrations in ppm; P is the standard air pressure; R is the ideal gas constant; MW_{NH3} is the molecular weight of ammonia; T is the ambient temperature, $W_{mortality}$ is the initial mortality weight in kg, and Q_{air} is the airflow rate in L min^{-1}.

3.2.4. Assessment of temperature data

The U.S. Environmental Protection Agency's (USEPA) Class A and Class B time-temperature criteria were used to assess the reduction of bacteria and viral pathogens during the composting process. Class A criteria require composting temperatures of 55 ºC or higher for at least three consecutive days. On the other hand, Class B criteria require a composting temperature of at least 40 ºC for five or more consecutive days, with the temperature exceeding 55 ºC for at least 4 hours during this period (USEPA, 2003). Previous studies have shown that both criteria can eliminate bacterial pathogens such as Salmonella and Campylobacter and viral pathogens, including bovine viral diarrhea virus (BVDV) (Elving et al., 2012; Guan et al., 2009). Other than class A and B criteria, it was reported that a compost temperature of 67 °C or higher for at least one day could inactivate avian influenza A H7N1 virus (Elving et al., 2012).

3.2.5. Leachate measurements

Rubber stoppers were removed, and leachate (if any) was collected every other day. Leachate samples were stored in a refrigerator at 4°C. All leachate samples collected in a heating cycle were combined and analyzed for their physicochemical characteristics. The volumes of the samples were measured using a graduated cylinder. pH and conductivity of the leachate samples were measured, as explained in section 2.2. Total solids (TS) and volatile solids (VS) were measured according to EPA method #1684 (2001). The chemical oxygen demand (COD) was measured using COD test kits (Hach, Loveland, CO) following EPA approved reactor digestion method for wastewater (EPA method# 5220D, 1980; Jirka and Carter, 1975). Cumulative COD values were calculated by dividing the average COD of three heating cycles by the initial weight of the mortalities. The purpose of calculating the cumulative COD was to compare the overall COD values of the treatments.

3.2.6. Measuring physicochemical characteristics of the finished compost samples

At the end of week 11, the compost materials were mixed one more time, and five to six compost sub-samples were collected from each test unit. Those sub-samples were combined and sent to the Midwest Laboratories (Omaha, NE, USA) for analysis. Briefly, pH, conductivity, total nitrogen, ammonium nitrogen, and other macro/micro-nutrients were analyzed according to

the NEMI-SM 4500 H+B (2011), NEMI-SM 2510B (1997), PAI-DK01 (1994), NEMI-SM 4500 NH3 (1997), and EPA 200.7 (1994), respectively. The color of the finished compost material was also measured.

3.2.7. Statistical analysis

All experiments were conducted in triplicate. Data were analyzed by one-way analysis of variance. Significance was indicated by the Analysis of Variance (ANOVA) and Tukey HSD test. All analyses were performed by JMP (SAS Institute, Cary, NC, USA) at the 5% significance level. Standard error bars were not shown on the figures because they lowered the legibility of the figures, but relative standard deviations (%RSD= standard deviation/mean ×100) were calculated and reported in the figure captions.

3.3. Results and Discussion

3.3.1. Mortality layer temperatures

Compost and ambient temperatures are shown in Fig. 3.1. Compost heating cycles and temperatures of the mortality layers. The compost material went through three heating cycles, separated by “turning 1” and “turning 2” vertical lines. Each heating cycle is characterized by a temperature increase to a peak value followed by a drop. The first and second heating cycles lasted for four weeks (each), while the last heating cycle lasted for three weeks. As expected, during each cycle, mesophilic and thermophilic phases were followed by the cooling phase (Neslihan Akdeniz, 2019; Janczak, Malińska, et al., 2017). At the beginning of the first cycle, the chicken mortalities were intact (based on our visual inspection). However, the second cycle started with relatively decomposed mortalities. Soft tissues were degraded and mixed with woodchips and biochar, while the remainings could be easily broken apart. Turning compost material accelerated the degradation process and resulted in higher temperatures. The ambient temperature ranged from 16.7 to 27.7°C. The maximum temperatures reached during the process are presented in Table 3.2. With a minimum of 2.6% biochar addition, statistically higher (3.4-7 °C) peak temperatures were found compared to control units (P<0.0015). There was no statistically significant difference among the maximum temperatures reached with 13, 26, and 39% biochar addition. All the test units met both Class A and Class B temperature-time criteria,

which indicates that composting was done properly. However, only the ones with 13, 26, and 39% biochar met Elving et al.'s (2012) AI H7N1 criteria. These findings indicated that adding biochar at a minimum rate of 13% would have benefits on temperature development and pathogen inactivation. The higher temperature brought by the biochar amendment can be attributed to several reasons 1) biochar has a porous structure; it retains water and various nutrients, improves aeration and pH, and, therefore, provides a habitat for microbial growth. A higher microbial activity leads to a higher composting temperature (Huiyong Yu et al., 2019); 2) Biochar fills the free space between large composting materials, therefore, reducing the heat loss to the surrounding environment (Godlewska et al., 2017). Similar findings were reported in previous studies. For instance, Chen et al. (2017) tested adding 10% biochar (by fresh weight)(equivalent to 26% v/v in our case) to layer manure compost and reported that there was a significant increase in temperature with the amendment of biochar. Wang et al. (2017) researched composting swine manure with biochar and found that the peak temperature (69.9 °C) reached with 10% (by dry weight) biochar addition was significantly higher compared to the peak temperature (66.9 °C) reached with no biochar addition. In another study (Sánchez-García et al., 2015), it was reported that 3% (by dry weight) of biochar addition to poultry manure yielded 5°C higher temperatures than the control (no biochar).

3.3.2. Oxygen concentrations of the mortality layer

Oxygen concentrations of the mortality layers are shown in Fig. 3.2. Oxygen concentrations ranged from 13.4 to 20.9%, which were within the acceptable range (>5%) (R. T. Haug, 1993). This indicates that the aeration (1.5 L per minute) was sufficient to maintain an aerobic mortality layer. After each turning, O_2 concentrations dropped and then gradually increased up to the ambient O_2 concentration (20.9%). It was mainly due to microbial activity. A higher microbial activity indicates a higher O_2 consumption (Godlewska et al., 2017). Biochar addition at 39% ratio showed significantly lower O_2 concentrations compared to control or 2.6% biochar addition during the three heating cycles ($P_{1st\ cycle}$= 0.0187, $P_{2nd\ cycle}$=0.0376, $P_{3rd\ cycle}$= 0.0371). The overall O_2 data was inversely proportional to the temperature data, indicating that the biochar amendment might have increased microbial activity, followed by the increased oxygen consumption and heat generation (Sanchez-Monedero et al., 2017).

3.3.3. Ammonia emissions from the surface of the compost material

Ammonia concentrations and cumulative ammonia emissions (per initial mortality weight) are shown in Fig. 3.3a and b, respectively. At the beginning of the process, the RSD of the data was high (0-7 days 0-145%) since while some test units were already producing ammonia, the ammonia generation in other test units was below the detection limits. Similar to the initial phase, at the end of the process, the RSD was high (52-80 days 0-173%) because some test units stopped generating ammonia a few days earlier than the other test units. From days # 9 to 45, the RSD of the data ranged from 0 to 61.2%. In each cycle, the highest ammonia concentrations were measured a couple of days (1-7 days) after recording the highest temperatures. A similar pattern can also be found in the previous studies, and it can be explained as that the temperature rises to the thermophilic phase that favors the volatilization of ammonia (Malińska et al., 2014). Chowdhury et al. (2014) reported that temperatures above 45 °C enhance NH_3 volatilization. pH also plays a role in NH_3 generation. It is known that the pH of the compost material drops at the beginning of a heating cycle due to volatile fatty acid production, but then it increases. A pH above neutral shifts the ammonium/ammonia equilibrium to the ammonia side (Neslihan Akdeniz, 2019; Johnson et al., 2005). Although temperature and pH contribute to NH_3 emissions, the adsorption of NH_3 and NH_4^+ by biochar pores has the potential to decrease NH_3 release, too (Guo et al., 2020). Dias et al. (2010) and Guo et al. (2020) indicated that acid groups on biochar surfaces trap NH_4^+ and prevent its volatilization. Meanwhile, multiple studies showed that biochar amendment increased the nitrate concentration in the final compost (Hagemann, Joseph, Schmidt, Kammann, Harter, Borch, Young, Varga, Taherymoosavi, and Elliott, 2017; Kammann et al., 2015), and it was probably because of two reasons 1) biochar amendment favors the nitrifying bacteria growth that transforms the ammonia to nitrate (Neslihan Akdeniz, 2019; Godlewska et al., 2017); 2) Biochar has a strong nitrate retention ability (Hagemann, Joseph, Schmidt, Kammann, Harter, Borch, Young, Varga, Taherymoosavi, and Elliott, 2017; Kammann et al., 2015).

The highest ammonia emissions (g NH_3 per initial mortality weight per day) were measured during the first heating period simply because more chicken tissues were available during this period. There was no significant difference in ammonia emissions of 13, 26, and 39% biochar added test units in the first heating period. Adding 13 or 26% biochar did not yield significantly lower ammonia emissions than adding 2.6% or no biochar, but the test units with 39% biochar

had the significantly lowest NH_3 emission rates (P=0.0008). Although some reductions in NH_3 emissions were recorded in the second and third heating periods, these reductions were not statistically significant ($P_{2nd\ cycle}$=0.8678, $P_{3rd\ cycle}$=0.5390).

The average cumulative ammonia emissions (g NH_3 per initial mortality weight) ranged from 0.60 to 1.43 g NH_3 per kg initial mortality weight. 26 and 39% biochar addition significantly reduced cumulative NH_3 emissions by 40.4% and 56.8%, respectively (corresponding P-values were 0.0228 and 0.0011, respectively). Other researchers reported similar results for other composting materials. Awasthi et al. (2018) indicated that adding biochar to biosolids could reduce ammonia emissions, which is important in odor management during the initial stages of the composting process. Steiner et al. (2010) found a 58% reduction in ammonia emissions during poultry litter composting with 20% biochar. Janczak et al. (2017) reported that adding 5% and 10% (by wet weight) of wood-derived biochar to poultry manure reduced ammonia emissions by 30% and 44%, respectively. This might be explained by the adsorption of NH_3 on the surface of the biochar, which leads to having lower NH_3 losses (Neslihan Akdeniz, 2019).

3.3.4. Physicochemical characteristics of leachate

The amount and the physicochemical characteristics of the leachate collected during each heating cycle are shown in Table 3.3. The amount of leachate collected varied over 11 weeks. In the first cycle, where the average COD values were the highest (ranged from 63.3-216 g/L), the control test units had more than twice the amount of leachate compared to the test units with 13% and 39% biochar. The pH values of the leachate samples were neutral and were not significantly different (P=0.832). Adding biochar at 13, 26, and 39% ratios resulted in having 71.2-89.6% lower total solids in the leachate. However, the volatile solid contents of the leachate samples were not significantly different.

COD concentrations varied. During the first cycle, COD concentrations were almost 1 to 3.3 times the concentrations reported by Xu et al. (2016) for swine slurry wastewater (~65 g/L). In the last cycle, average COD concentrations decreased below 20 g/L. Cumulative COD values were calculated to assess the overall effect of biochar amendment on leachate. Adding biochar at 13, 26, and 39% rates significantly lowered the cumulative COD values of leachate compared to control (P=0.0003). This might be attributed to the biochar's adsorption capacity (Godlewska et al., 2017). In this study, leachate formation was allowed to test if the biochar amendment could

decrease leachate generation and reduce the related environmental concern. If leachate presents after a heavy rainfall event, having biochar inside the pile can reduce the leachate's organic matter content.

3.3.5. Physicochemical characteristics of the finished compost

The physicochemical characteristics and nutrient value of finished compost are presented in Table 3.4. The optimum moisture content of the finished compost should be between 40 and 50% (MAFES, 2016). Overly wet compost would be too heavy to transport, while too dry compost would be dusty. The average moisture content of the finished compost samples ranged from 39.0% to 53.3%, which was almost within the optimum range. Biochar added test units had significantly higher moisture content than the control test units. Although this compost material would be harder to handle, biochar likely helped retain water, preventing over-drying of the compost material when environmental conditions are too dry to maintain the microbial activity (R. Li et al., 2015; Onwosi et al., 2017).

The pH values of the finished compost ranged from 6.6-7.2, which were within the expected range of 6-8 (Midwest Labs, 2019). Conductivity reflects the level of water-soluble ions in the compost material. The final EC values were below the upper limit of 4 mS/cm, which is considered to be tolerable by the plants with medium sensitivity (Lasaridi et al., 2006). The C:N ratio, which is often used as an indicator of compost stability, of the finished compost ranged from 17 to 21 (w/w). The C:N ratios were mostly within the range of the ideal C:N ratio of 10-20 for the finished compost (MAFES, 2016). The total and organic nitrogen contents of the 39% biochar added test unit were significantly higher than those of control test units, by 34.7% and 39.5%, respectively ($P_{\text{total N}}$= 0.027, $P_{\text{organic N}}$= 0.018). The result was consistent with the previous finding that the ammonia volatilization in the 39% biochar added test units was the minimum.

The average nutrient contents ($N+P_2O_5+K_2O$) of the samples were between 2.94 and 4.68 (% dry weight), which were within the typical range of 2-5 (% dry weight.) (Midwest Labs, 2019). Referring to the test standard from Midwest Labs, the nutrient index was calculated by dividing the total nutrients (N, P, K) by the amount of salt (sodium and chloride) in the samples (Midwest Labs, 2019). In this study, the nutrient index above 10 indicates that a toxic buildup of salt in the soil would be unlikely. Biochar amendment significantly increased potassium, iron, and manganese contents. Biochar’s surface may contain various functional groups attributed to its

high reactivity to bind metal cations (Guo et al., 2020). However, relevant studies mainly investigated biochar's effect in retaining heavy metals such as copper, zinc, and lead (Godlewska et al., 2017; Guo et al., 2020), while its capacities to retain potassium, iron, and manganese were not reported. Besides the retention capacity, biochar may contain these elements from its production. Prasad et al. (2018) tested biochars produced from woodchips, forest wood, and wood screening from tree branches and reported that the biochars contained low concentrations of N (0-2 mg/L) and P (3-11 mg/L) but generally high levels of K (25-990 mg/L). Brewer et al. (2015) measured a wide range of trace elements in hardwood char ash and found that potassium, calcium, silicon, and in smaller amounts iron and manganese were the most common elements. Surprisingly, no significant difference was found in the calcium contents of the finished compost samples. Rather than the biochar, chicken mortalities might have served as the primary source of calcium in the final product.

The finished compost is expected to have a rich brown color. Biochar addition significantly reduced "L" (lightness, O: black, 100: white). It had no effect on the "a," which refers to greenness (-) or redness (+), but significantly reduced "b," which expresses the distribution from blue (−) to yellow (+). As expected, biochar added units had a darker color. The purpose of measuring color was to provide data for future studies that would focus on developing correlations between compost maturity and its CIELAB color variables (M. A. I. Khan et al., 2009). Color might also be important in assessing consumer acceptance of the final product.

3.4. Conclusions

Adding wood-based biochar at a minimum 2.6% rate (v/v) increased the maximum temperatures (3.4-7.0 °C higher) reached during poultry mortality composting, which would be important in eliminating pathogens when dealing with diseased animal mortalities. The cumulative COD of the leachate collected from the test units with 13, 26, and 39% biochar was about five times less than that of the leachate collected from the control test units. 26% (40.4% less) and 39% (56.8% less) of biochar added test units had significantly lower cumulative ammonia emissions than control (corresponding *P*-values were 0.0228 and 0.0011, respectively). Total nitrogen, potassium, iron, and manganese contents of final compost in the test units with 39% biochar were significantly higher than those of the control test units. Adding biochar at a minimum rate of 13% by volume (5% by fresh weight) is recommended to maximize the

temperature profile and reduce the leachate COD. The impact of the final product on crop growth is currently being tested and will be reported in a separate manuscript. Future studies can investigate the effects of different biochar types (biochars made from cow manure or distiller's grain) on the mortality composting process.

3.5. Acknowledgment

This project was supported by the United States Department of Agriculture (USDA)-National Institute of Food and Agriculture (NIFA) through a Hatch grant provided to the Agricultural and Biological Engineering Department at the University of Illinois at Urbana-Champaign (no. ILLU-741-328).

3.6. Figures and Tables

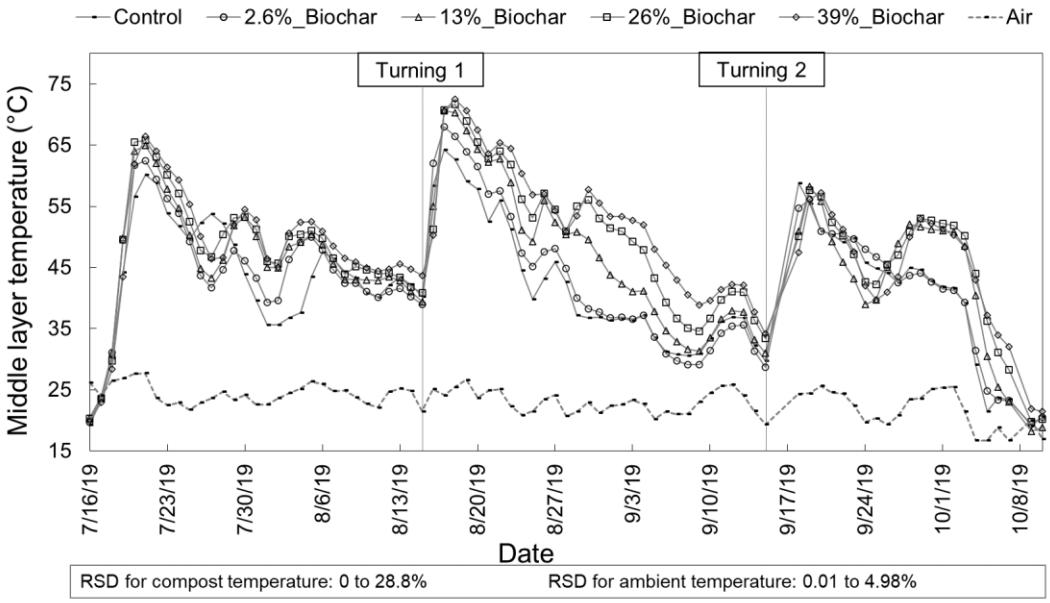

Fig. 3.1. Compost heating cycles and temperatures of the mortality layers. All experiments were conducted in triplicate. Standard error bars were not shown on the figures because they lowered the legibility of the figures. Relative standard deviations (%RSD= standard deviation/mean ×100) of the data provided on the graph.

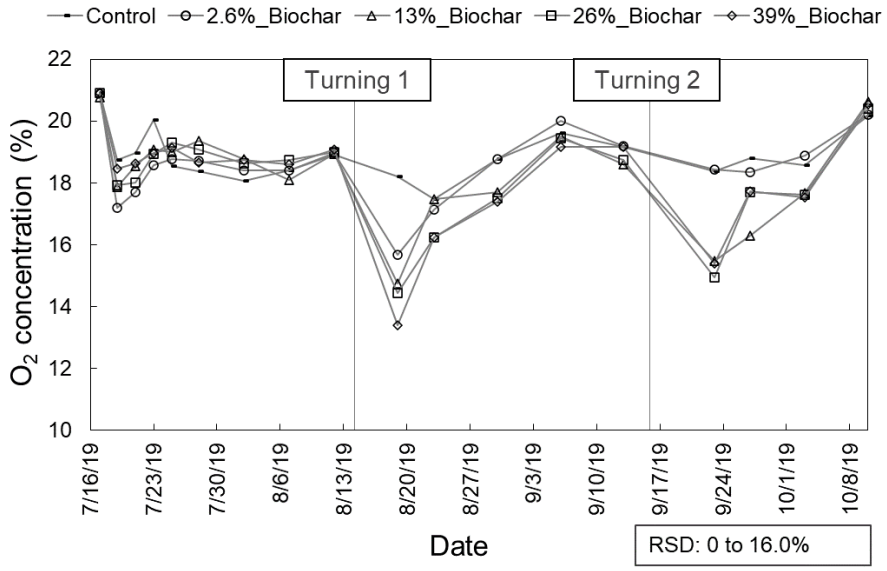

Fig. 3.2. Oxygen concentrations of the mortality layers. All experiments were conducted in triplicate. Standard error bars were not shown on the figures because they lowered the legibility of the figures. Relative standard deviation (%RSD= standard deviation/mean ×100) of the data provided on the graph.

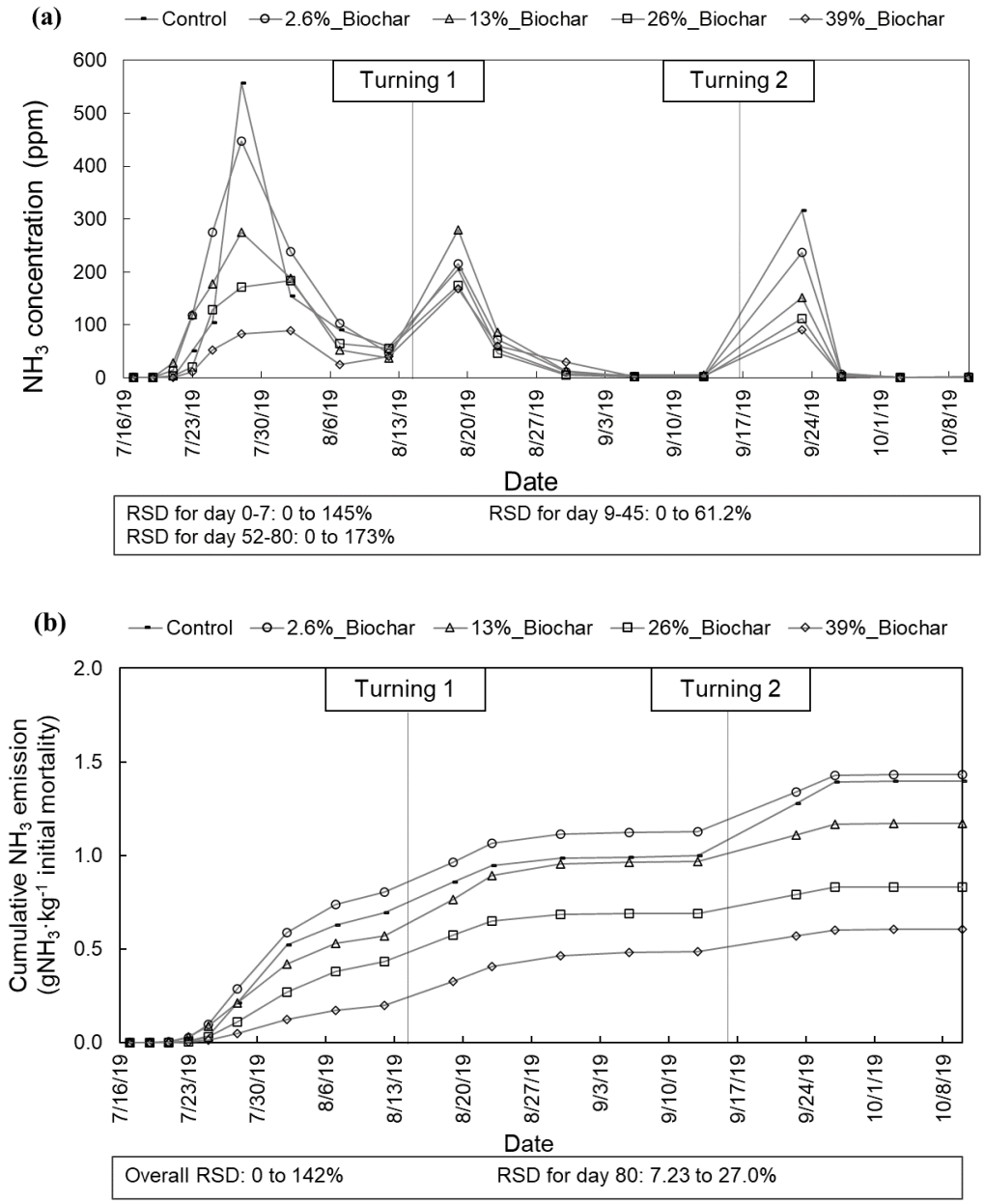

Fig. 3.3. Ammonia measurements from the surface of the compost units-ammonia concentrations (a), and cumulative ammonia emissions per mortality initial weight (b). All experiments were conducted in triplicate. Standard error bars were not shown on the figures because they lowered the legibility of the figures. Relative standard deviation (%RSD= standard deviation/mean ×100) of the data provided on the graph.

Table 3.1. Physicochemical characteristics of biochar and woodchips

Characteristics	**Biochar**	**Woodchip**
Moisture (%)	57.1 ± 0.88	30.4 ± 2.18
pH	7.71 ± 0.14	5.86 ± 0.12
Conductivity (mS/cm)	530 ± 13.1	326 ± 14.8
Bulk density (kg/m^3)	138 ± 18.6	201 ± 14.6
Water holding capacity (g water/g dw)	5.51 ± 0.37	1.50 ± 0.12
BET surface area (m^2/g)	397 ± 18.2	-
Total C (% dw)	67.8 ± 4.67	45.6 ± 0.11
Total N (% dw)	0.43 ± 0.08	0.57 ± 0.08
C/N	160 ± 2.68	80.4 ± 10.7
Color		
L	9.25 ± 1.52	34.2 ± 10.9
a	6.43 ± 1.72	8.61 ± 4.68
b	7.88 ± 0.67	17.7 ± 4.96

Table 3.2. Compost temperature-time criteria to eliminate pathogens

	Max temperature	Middle layer net heat unit[1]	Elving et al.'s (2012) AI H7N1 criteria[2]		EPA's (2003) Class A and B criteria[3]		
	(°C)	(°C ·day)	# of days above 67°C	yes/ no	# of days above 55 °C	Class A	Class B
Control	66.8± 0.21^{C}	1583±92^{B}	0.02 ± 0.04^{B}	N	4.15 ± 0.24^{C}	Y	Y
2.6% biochar	70.2± 1.40^{B}	1649±95^{B}	1.09 ± 1.04^{A}	N	6.10 ± 0.92^{B}	Y	Y
13% biochar	72.6± 0.62^{A}	1887±85^{A}	2.41 ± 0.31^{A}	Y	7.21 ± 0.41^{AB}	Y	Y
26% biochar	73.5± 0.66^{A}	2059±58^{A}	3.00 ± 0.31^{A}	Y	9.06 ± 1.28^{A}	Y	Y
39% biochar	73.8± 0.40^{A}	2123±89^{A}	3.19 ± 0.62^{A}	Y	9.77 ± 1.37^{A}	Y	Y

"Ctrl": no biochar, "WBC": Wood pallet biochar, "DGBC": distiller grain biochar, "CMBC": cow manure biochar

Within each column, means that are not connected by the same letter are significantly different ($P<0.05$).

[1] The "net" means the difference between the measured temperature and the ambient air temperature.

[2] Elving et al.'s (2012) reported that composting with its maximum temperature at 67 °C for 1 consecutive day is sufficient to inactivate avian influenza H7N1. If all replicates met the criteria, it is noted as Y, otherwise N.

[3] Class A: compost temperature of 55 ºC or higher for at least 3 consecutive days. Class B: compost temperature of at least 40 ºC for 5 or more consecutive days, exceeding 55 ºC for at least 4 hours during this period. If all replicates met the criteria, it is noted as Y, otherwise N.

Table 3.3. Leachate volume and characteristics

	Cycle	Control	1%	5%	10%	15%
Volume (mg/kg initial mortality)	1	117 ± 36.6^{A}	106 ± 22.0^{AB}	53.4 ± 14.4^{AB}	66.7 ± 15.9^{AB}	49.0 ± 20.0^{B}
	2	62.1 ± 10.1^{B}	63.4 ± 5.65^{B}	171 ± 10.2^{A}	150 ± 20.8^{A}	146 ± 22.5^{A}
	3	93.7 ± 19.1^{A}	109 ± 29.5^{A}	113 ± 21.0^{A}	103 ± 28.9^{A}	84.9 ± 13.1^{A}
pH	1	7.09 ± 0.19^{A}	7.05 ± 0.10^{A}	7.23 ± 0.11^{A}	7.09 ± 0.25^{A}	7.16 ± 0.34^{A}
	2	7.68 ± 0.27^{A}	7.86 ± 0.11^{A}	7.70 ± 0.28^{A}	7.51 ± 0.02^{A}	7.65 ± 0.23^{A}
	3	7.64 ± 0.27^{A}	7.72 ± 0.22^{A}	7.46 ± 0.09^{A}	7.53 ± 0.16^{A}	7.36 ± 0.34^{A}
Total solids (%)	1	27.4 ± 7.30^{A}	28.2 ± 11.0^{A}	5.57 ± 4.44^{B}	5.35 ± 3.74^{B}	5.45 ± 1.81^{B}
	2	1.27 ± 0.20^{A}	1.19 ± 0.54^{A}	0.33 ± 0.12^{B}	0.24 ± 0.14^{B}	0.20 ± 0.04^{B}
	3	1.14 ± 0.49^{A}	0.83 ± 0.34^{AB}	0.28 ± 0.05^{BC}	0.33 ± 0.17^{BC}	0.12 ± 0.03^{C}
Volatile solids (% d.b.)	1	98.8 ± 0.53^{A}	99.2 ± 0.34^{A}	98.7 ± 1.11^{A}	96.9 ± 1.64^{A}	99.0 ± 0.25^{A}
	2	89.6 ± 1.81^{A}	93.1 ± 3.82^{A}	87.8 ± 8.21^{A}	97.7 ± 3.29^{A}	96.2 ± 5.44^{A}
	3	86.2 ± 4.29^{A}	88.3 ± 0.46^{A}	91.5 ± 4.40^{A}	95.1 ± 1.54^{A}	88.1 ± 1.90^{A}
COD (g/L)	1	216 ± 84.8^{A}	187 ± 116^{A}	64.7 ± 54.1^{A}	63.3 ± 55.2^{A}	88.8 ± 31.1^{A}
	2	27.8 ± 4.88^{A}	28.5 ± 11.6^{A}	6.08 ± 3.05^{B}	5.98 ± 2.23^{B}	5.15 ± 0.79^{B}
	3	19.9 ± 10.3^{A}	14.9 ± 6.23^{A}	6.08 ± 1.11^{AB}	7.02 ± 3.85^{AB}	2.85 ± 1.04^{B}
Cum. COD[2]		28.0 ± 11.5^{A}	25.0 ± 17.8^{AB}	4.82 ± 2.27^{BC}	6.46 ± 5.30^{BC}	5.21 ± 2.09^{C}

Within each row, means that are not connected by the same letter are significantly different (P<0.05).

[1] Cumulative COD (g per kg initial mortality)

Table 3.4. Physicochemical characteristics of the finished compost samples

	Control	**2.6%**	**13%**	**26%**	**39%**
Moisture content (%)	39.0 ± 4.33^{B}	44.1 ± 1.21^{AB}	51.4 ± 4.01^{A}	51.6 ± 1.34^{A}	53.3 ± 5.94^{A}
Ash (% dw)	8.75 ± 1.13^{AB}	6.13 ± 1.20^{B}	10.3 ± 1.67^{A}	10.7 ± 0.54^{A}	10.3 ± 0.81^{A}
pH	6.83 ± 0.15^{A}	6.87 ± 0.31^{A}	6.87 ± 0.15^{A}	7.10 ± 0.00^{A}	7.00 ± 0.10^{A}
Conductivity (mS/cm)	1.81 ± 0.12^{B}	2.13 ± 0.17^{AB}	2.68 ± 0.22^{A}	2.50 ± 0.41^{A}	2.52 ± 0.37^{A}
Total N (% dw)	2.14 ± 0.11^{B}	2.63 ± 0.20^{AB}	2.64 ± 0.20^{AB}	2.66 ± 0.26^{AB}	2.88 ± 0.17^{A}
Organic N (% dw)	2.00 ± 0.09^{B}	2.47 ± 0.24^{AB}	2.50 ± 0.19^{AB}	2.57 ± 0.26^{A}	2.78 ± 0.15^{A}
Ammonium N (% dw)	0.14 ± 0.02^{A}	0.16 ± 0.05^{A}	0.15 ± 0.03^{A}	0.10 ± 0.03^{A}	0.10 ± 0.03^{A}
Nitrate N (% dw)	< 0.01	< 0.01	< 0.01	< 0.01	< 0.01
C:N ratio	19.0 ± 2.00^{A}	18.7 ± 1.53^{A}	19.7 ± 0.58^{A}	20.3 ± 0.58^{A}	20.0 ± 1.00^{A}
P as P_2O_5 (% dw)	0.61 ± 0.33^{A}	0.49 ± 0.10^{A}	0.46 ± 0.07^{A}	0.69 ± 0.19^{A}	0.69 ± 0.12^{A}
K as K_2O (% dw)	0.56 ± 0.04^{C}	0.63 ± 0.04^{BC}	0.64 ± 0.02^{BC}	0.69 ± 0.04^{AB}	0.75 ± 0.05^{A}
Sulfur (% dw)	0.23 ± 0.03^{A}	0.23 ± 0.02^{A}	0.22 ± 0.03^{A}	0.24 ± 0.02^{A}	0.27 ± 0.05^{A}
Calcium (% dw)	2.28 ± 0.34^{A}	1.47 ± 0.31^{A}	1.86 ± 0.25^{A}	2.48 ± 0.87^{A}	1.91 ± 0.19^{A}
Magnesium (% dw)	0.15 ± 0.02^{AB}	0.12 ± 0.02^{B}	0.14 ± 0.01^{AB}	0.19 ± 0.03^{A}	0.18 ± 0.02^{A}
Sodium (% dw)	0.13 ± 0.01^{A}	0.13 ± 0.01^{A}	0.12 ± 0.01^{A}	0.14 ± 0.01^{A}	0.14 ± 0.01^{A}
Zinc (ppm)	121 ± 29.9^{A}	102 ± 21.6^{A}	109 ± 33.5^{A}	160 ± 18.8^{A}	140 ± 15.6^{A}
Iron (ppm)	346 ± 23.3^{C}	492 ± 91.8^{BC}	684 ± 146^{AB}	931 ± 197^{A}	970 ± 79.2^{A}
Manganese (ppm)	77.0 ± 9.17^{C}	86.7 ± 10.1^{C}	169 ± 44.8^{B}	294 ± 25.5^{A}	344 ± 12.5^{A}
Color					
L	22.7 ± 5.76^{A}	16.9 ± 5.51^{B}	16.4 ± 5.64^{B}	11.9 ± 3.09^{C}	12.5 ± 2.97^{C}
a	5.61 ± 4.64^{A}	7.43 ± 4.02^{A}	5.28 ± 4.22^{A}	7.01 ± 3.88^{A}	5.76 ± 2.36^{A}
b	13.4 ± 2.68^{A}	11.8 ± 1.95^{A}	8.75 ± 3.00^{B}	8.41 ± 1.93^{B}	7.75 ± 1.35^{B}

Within each row, means not connected by the same letter are significantly different ($P<0.05$).

3.7. Appendix

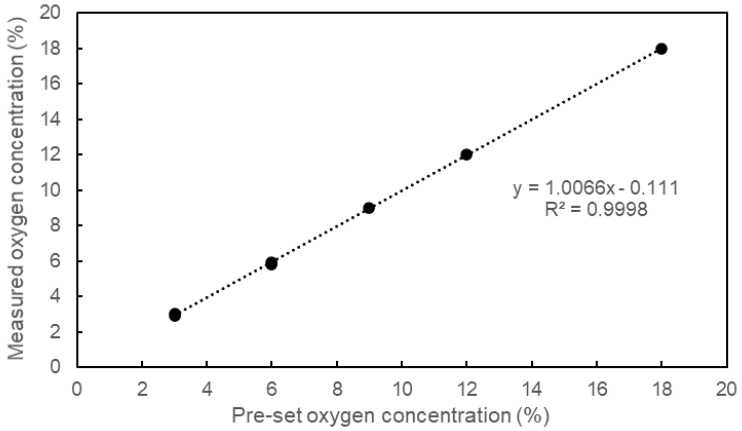

Fig. 3.4. Oxygen concentration calibration. Calibration levels were set at 3, 6, 9, 12, 18, 20.9% O_2 by volume. Calibration gases were prepared by diluting 20.9% O_2 with N_2 using an Environics Gas Dilution System (Environics 4040, Tolland, CT). The O_2 concentrations were measured by RKI - Eagle II® (Union City, CA)

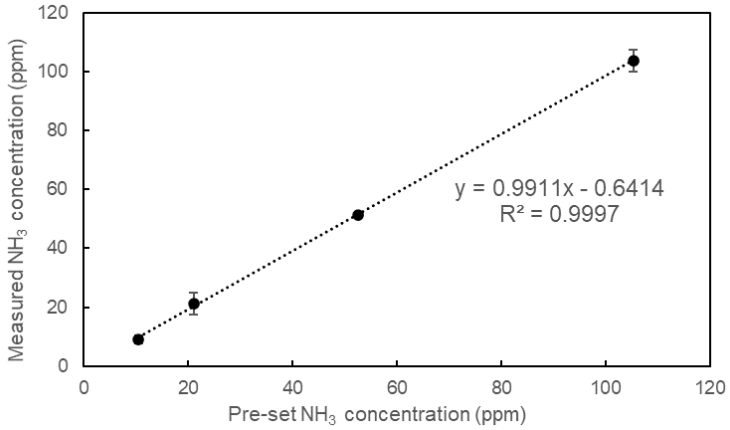

Fig. 3.5. Ammonia concentration calibration. Calibration levels were set at 10.53, 21.06, 52.65, and 105.3 ppm NH_3 by volume. Calibration gases were prepared by diluting 105.3 ppm NH_3 with N_2 using an Environics Gas Dilution System (Environics 4040, Tolland, CT). The NH_3 concentrations were measured by titrating the 0.005 M H_2SO_4 into 2% boric acid.

CHAPTER 4

COMPOSTING POULTRY MORTALITIES WITH COMMERCIALLY AVAILABLE BIOCHARS MADE FROM DIFFERENT FEEDSTOCKS

4.1. Introduction

Proper management of emergency animal mortalities is essential to reduce the impacts to surface and groundwater resources, reduce air emissions and decrease the spread of pathogens to the surrounding (NRCS - USDA, 2015). Composting has been successfully used in the U.S. for almost 20 years to control animal disease outbreaks and respond to natural disasters (Costa and Akdeniz, 2019; USDA-APHIS, 2017). For example, during the 2014-2016 highly pathogenic avian influenza (HPAI) outbreak in the U.S., which affected more than 50 million birds, composting was used to dispose of 85% of the mortalities (Costa et al., 2021; Costa and Akdeniz, 2019). African swine fever (ASF), affecting both domestic and feral swine, spread through China, Mongolia, Vietnam, Dominican Republic, Haiti, and parts of the European Union and caused the depopulation of millions of pigs (USDA-APHIS, 2021). The initial studies indicated that composting has the potential to eliminate the ASF virus (G. A. Flory, 2022). Most recently (March 2022), 42 confirmed HPAI positive cases have been reported in the U.S. So far, 12.8 million birds have been affected, and most of the depopulated birds have been disposed of onsite by composting (USDA-APHIS, 2022).

Although composting has been used to manage animal mortalities, even during disease outbreaks, it has limitations. One of the main concerns is having excess moisture, which reduces aeration, prevents reaching thermophilic temperatures, and increases leachate formation (Roy et al., 2018; Shan et al., 2021; Yuchuan Wang et al., 2021). Adding biochar as a co-composting material has been proposed to be an effective method to absorb excessive moisture, facilitating aeration of the compost material (Sanchez-Monedero et al., 2017). Micropores within the biochar structure provide a surface area for microbial growth (Sanchez-Monedero et al., 2017; Steiner, Sánchez-Monedero, et al., 2015). The changes in compost microbial activity can help meet the temperature-time criteria required to eliminate pathogens (N. Akdeniz, 2019). Even if the temperature increase is just a few degrees Celsius, it can significantly impact cumulative heat generation (Yuchuan Wang et al., 2021). Besides temperature increase, in some studies, it was

reported that the addition of biochar to poultry manure or litter compost could significantly reduce ammonia (NH_3) emissions (Agyarko-Mintah et al., 2017; N. Akdeniz, 2019).

The impact of biochar on livestock and poultry manure composting has been widely studied (W. Chen et al., 2017b; Guo et al., 2020; Janczak, Malinska, et al., 2017; Keiji Jindo et al., 2016; Lopez-Cano et al., 2016). Animal mortalities are another byproduct of animal production that need to be disposed of properly to prevent the spread of diseases. Co-composting animal mortalities with biochars has not been addressed except in our previously published study (Yuchuan Wang et al., 2021). Wang et al. (2021) reported that adding wood-based biochar at a minimum of 13% (v/v)(or 5% by fresh weight) increased compost temperatures by 3.4-7 °C and decreased leachate's chemical oxygen demand by 76.9-82.8% during poultry mortality composting.

Studies have shown that feedstock type affects biochars' characteristics (e.g., porosity, specific surface area, water absorption capacity) (Ji et al., 2022; Weber and Quicker, 2018). Wood-based biochars, which refer to biochars made of tree and forestry residues, have a higher specific surface area and porosity due to the thermal stability of lignin (Ji et al., 2022). Biochars made of non-woody feedstocks such as livestock manure or crop residues often contain more inorganic minerals (more ash), which can cause micropore-clogging, resulting in a lower surface area (Amalina et al., 2022; Ji et al., 2022; Özçimen and Ersoy-Meriçboyu, 2010).

In this pilot-scale study, three commercially available biochars made from different feedstocks, including wood pallets (WBC), distillers grain (DGBC), and cow manure (CMBC), were added to the poultry mortality composting bins. The goals of this study were 1) to measure physicochemical characteristics (e.g., water holding capacity, BET surface area, CHN content) of three commercially available biochars, 2) to compare the impact of co-composting poultry mortalities with WBC, DGBC, and CMBC on compost temperature development, ammonia emissions, and leachate production, 3) to test the effects of adding biochars on macro and micronutrient contents (e.g., N, P, K, Na, Mn, Fe) of the finished compost.

4.2. Material and methods

4.2.1. Compost materials

The experiment was conducted at the Agricultural and Biological Engineering Research and Training Farm, located a few miles south of the campus. Poultry mortalities were collected from the nearby Poultry Research Farm. After chickens were euthanized, mortalities were frozen at -20 °C. Poultry mortalities were thawed completely before being loaded into the composting bins. Woodchips were collected from the Ground Storage Barn on campus. Wood-based biochar (WBC) was produced by Chip Energy (Goodfield, IL) by gasification of wood pallets at 520 °C. DGBC and CMBC were produced by Ecochar (Evansville, IN) by gasification of distillers grains and cow manure at 815 °C and 760 °C, respectively.

4.2.2. Preparation of composting bins

The experiments were conducted in triplicate using 12 pilot-scale composting bins. There were four treatments: control (Ctrl), WBC, DGBC, and CMBC. While Ctrl refers to no biochar addition, WBC, DGBC, and CMBC stand for test units with corresponding types of biochar.

The composting bins were adapted from 32-gal bins. The outside of the bins was wrapped with an R19 fiberglass insulation roll (EcoRoll, OH). A steel mesh platform was placed 12 cm above the bottom of the bins to create an air plenum. A 1.2 cm diameter hole was drilled on the bottom edge of each bin to collect leachate samples. The hole was plugged with a rubber stopper when the leachate samples were not collected. About 30 L of woodchips were placed on the steel mesh. Four to five chicken mortalities (total weight of 9.83±0.45 kg) were placed on the woodchips. Biochar was not initially mixed with woodchips. Instead, a layer of biochar was placed both under (6 L) and above (3 L) the mortalities. The bottom layer helped capture leachate, and the top biochar layer served as a biofilter, reducing air emissions. For control bins, biochar was replaced with the same amount of woodchips. Another 15 L of woodchips were used to cap compost material. The biochar amendment accounts for about 13% of total compost material volume (chicken mortalities+woodchips) at the initial loading. This rate is equivalent to the recommendation by Wang et al. (2021). The initial carbon (C) to nitrogen (N) ratio was about 22, which was within the recommended range of 20-40 (NRAES, 1999). The initial moisture

content of the compost material (mortality, woodchips, and biochar) was calculated to be 59.8±1.02%, assuming the moisture content of the chicken mortalities was 70% (NRAES, 1999).

Compost bins were aerated at a 0.8 to 1.2 L/min aeration rate using a vacuum pump (Thomas Pump, Slidell, LA) equipped with a flowmeter (Cole-Parmer, IL). This airflow rate was chosen based on our previously published study (Yuchuan Wang et al., 2021). Airflow rates were checked every other day and adjusted if needed.

Composting experiments were continued for 80 days, from March 8 to May 26, 2021. The compost material went through three heating cycles. While the first and second heating cycles lasted for 25 days, the third cycle took 30 days. The bins were completely emptied, and the compost material was mixed at the end of each heating cycle. Large particles were manually broken into smaller pieces. The overall moisture content of the compost material was adjusted at the end of each cycle to 61.5±5.58%. During the first turning, about 9 L of fresh woodchips were mixed with the compost material in biochar-treated bins to compensate for the bulk volume loss. After reloading the compost material into the bins, an additional 6 L of fresh woodchips were added on top of all bins to cover the remaining chicken tissues.

4.2.3. Measurement of physico-chemical characteristics of woodchips and biochar

The physicochemical characteristics of woodchips and biochar samples, including pH, conductivity, bulk density, ash content, and water holding capacity, were measured according to the Test Method for the Examination of Composting and Compost (TMECC, 2002). For woodchips analysis, about 50 g of sample was mixed with deionized water (1:10 w/w), as described by TMECC, while 4 g of sample was used for biochar analysis. A bench-scale meter (Cole Parmer PC 100, IL) was used for pH and electrical conductivity (EC) measurements. For bulk density measurements, both woodchips and biochar samples were dried at 70°C for one day (Quincy Lab Inc, IL), and bulk density was measured as weight per unit volume using 500 mL beakers. Ash content was measured using a muffle furnace (Barnstead Thermolyne F6000, MN) at 550°C for 2 h. Water holding capacity was measured by soaking oven-dried woodchips and biochar samples with water, followed by draining excess water. The change in mass was used to calculate water holding capacity per g of initial dry weight.

Biochar samples were sent to the Microanalysis Laboratory at the University of Illinois for BET (Brunauer, Emmett, and Teller) surface area and CHN analyses. For surface area analysis,

samples were degassed at full vacuum at 300°C for 1 hour and then ran for a two-cycle N_2-gas mesopore analysis at liquid nitrogen temperatures. Samples were then degassed again at 300°C for 14 hours, and after that, degassed on the instrument for an additional 2.5 hours to clean up pores and run at the micropore region in CO_2 gas at ice water temperatures (Sigmund et al., 2017). CHN content was analyzed using an Exeter CHN Analyzer (CE440, UK).

4.2.4. Temperature measurements and assessment

Compost temperatures were measured every 30 min with pre-calibrated K-type thermocouples and recorded using 4-channel data loggers (Tekcoplus Ltd, Hong Kong). Thermocouples were inserted into PVC pipes to ensure consistent positioning and avoid condensation on the thermocouples (Costa et al., 2021; Yuchuan Wang et al., 2021). Three 1 mm small holes were drilled on PVC pipe to improve heat exchange. Each bin had two thermocouples: one measured the temperature in the center (middle layer), and the other measured the compost material's temperature 15 cm above the middle layer (top layer). Ambient temperature was also measured using K-type thermocouples in triplicate.

Cumulative heat generation was calculated by summing the difference between daily average compost temperature (middle and top layer) and daily average ambient temperature, as shown in Eq. 4.1. This calculation was adapted from Czekała et al. (2016), who used 4 h intervals instead of daily averages.

$$Cumulative\ heat\ generation\ (°C \cdot \text{day}) = \sum_{i=1}^{n} (T_{i,comp} - T_{i,air}) \qquad \text{Eq. 4.1}$$

where:

"n" is the number of days. $T_{i,\ comp,}$ and $T_{i,\ air}$ are the daily average temperature (°C) of compost and ambient air, respectively.

Class A and Class B criteria were used to assess bacterial and viral pathogen reduction (Costa et al., 2021; Glanville et al., 2016; USEPA, 2003; Yuchuan Wang et al., 2021). In addition, highly pathogenic avian influenza (AI H7N1) virus elimination criteria reported by Elving et al. (2012) was used to assess virus elimination.

4.2.5. Oxygen and ammonia concentration measurements

Oxygen and ammonia concentrations were measured every other day during the first 10 days of the composting process. After the first 10 days, measurements were done every 4-7 days. A stainless steel funnel was buried 5 cm below the surface of the compost material (Neslihan Akdeniz and Janni, 2012). Oxygen concentrations were measured using a portable gas monitor (RKI - Eagle II®, Union City, CA) connected to the funnels. Standard gases were used to calibrate Eagle (3, 6, 9, 12, 18, 20.9% O2, AirGas, IL)(Fig. 4.4) as reported by Wang et al. (2021).

An SKC pump (Eighty-Four, PA) at the 1 L/min airflow rate was connected to the funnels used to pull air samples for ammonia measurements. The air pulled by the pump went through a 100 mL impinger filled with 4% boric acid (Ricca Chemical, IL). Ammonia concentrations were measured by titrating collected samples with sulfuric acid (ThermoFisher Scientific, MA), as Meeker and Wagner (1933) explained. A calibration curve is shown in Fig. 4.5 at levels of 10.53, 21.06, 52.65, and 105.3 ppmv. The cumulative ammonia emissions were calculated in mg NH_3 per kg initial mortality, as reported by Wang et al. (2021).

4.2.6. Leachate

Leachate samples were collected every other day during the 80-day composting period, and they were stored at -20 °C. The pH and EC of leachate were measured by a PC100 pH/EC meter (Cole-Parmer, IL). Total solids and ash content were measured according to the EPA method #1684 (2001). The chemical oxygen demand (COD) was measured using Hach COD test kits (TNT 823, Hach, CO), a heating block (DRB200, Hach, CO), which holds the samples at 150 °C for 2 h, and a benchtop spectrophotometer (320-1,100 nm, DR3900, Hach, CO). The cumulative COD was calculated by summing up the total COD content of each heating cycle, as shown in Eq. 4.2.

$$COD_{total}\ (g) = \sum_{i=1}^{n} (COD_i \times Volume_i) \qquad \text{Eq. 4.2}$$

where:

n is the number of heating cycles (n=3), COD_i is COD at i^{th} heating cycle ($g \cdot L^{-1}$), and $volume_i$ is the leachate volume at i^{th} heating cycle (L).

The pathogen content in the leachate, including *E. coli* and coliform, was tested using the 3M Petrifilm E. coli/Coliform Count Plate (Saint Paul, MN). 1 ml leachate samples were placed on the petrifilm. The colony numbers were counted after 24 h incubation at 37 °C using the Thermo Scientific 320 Forma Direct Heat COIncubator (Waltham, MA). Trials with different pre-treatments were tested. In the first trial, there was no pre-treatment. Only leachate samples from the 3rd heating cycle were tested. In the second trial, leachates were centrifuged at 0, 4000, 7000 and 10,000 rpm for 1 min. A control sample from the second heating cycle was tested under those variations. In the last trial, all leachate samples within the same triplicate were mixed and centrifuged at 4000 rpm for 1 min. Centrifugation was done using the Eppendorf Minispin Centrifuge (Hamburg, German).

4.2.7. Physicochemical characteristics of the finished compost samples

After composting poultry mortalities for 80 days, bins were emptied, and compost material was mixed thoroughly. Five to six compost sub-samples were collected from each bin, and those sub-samples were combined and sent to the Midwest Laboratories (Omaha, NE) for analysis (Yuchuan Wang et al., 2021). pH, conductivity, total nitrogen, ammonium nitrogen, and other micro/macronutrients were analyzed according to the standard methods (EPA 200.7, 1994; NEMI-SM 2510B, 1997; NEMI-SM 4500 H+B, 2011; NEMI-SM 4500 NH3 C, 1997; PAI-DK01, 1994).

4.2.8. Statistical analysis

All experiments were run in triplicate. Data were analyzed by JMP Pro 15 (SAS Institute, Cary, NC, USA) using one-way analysis of variance (ANOVA) and Tukey HSD test at the 5% significance level. Data were log-transformed to improve their normality. Standard deviation (SD) bars were not shown on the figures because they overlapped and reduced the legibility of the manuscript. Instead, average relative standard deviations (AveRSD) were calculated to indicate the variance of each treatment in triplicate. The average standard deviations (AveSD), average relative standard deviations, and relative standard deviations (RSD) were calculated in Eq. 4.3 to Eq. 4.5.

$$AveSD = \sqrt{\sum_{i=1}^{n} \frac{SD_i^2}{n}} \quad \text{Eq. 4.3}$$

$$AveRSD = \frac{AveSD}{\mu} \times 100\% \quad \text{Eq. 4.4}$$

$$RSD = \frac{SD}{\mu} \times 100\% \quad \text{Eq. 4.5}$$

where:

"n" is the period of the experiment (80 days), "i" is the ith day, and "μ" is the average temperature of the entire composting period of each bin.

4.3. Results and discussion

4.3.1. Physicochemical characteristics of woodchips and biochar

The physicochemical characteristics of woodchips and biochar are shown in Table 4.1. All biochar types showed significantly higher ash content, carbon content, and water holding capacity than woodchips (p_{ash}<0.0001; p_{carbon}<0.0001; p_{WHC}<0.0001).

CMBC (cow manure biochar) had significantly higher pH and E.C. compared to WBC (wood-based biochar) and DGBC (distillers grain biochar) (p_{pH}<0.0001; p_{EC}<0.0001), but both pH and E.C. values of cow manure biochar were similar to those reported in the literature. Qin et al. (2019b) and Zhang et al. (2019) reported that cow manure biochar prepared at 700°C had pH values of 10.36 and 10.83, respectively. Gavili et al. (2018) reported that cattle manure biochar prepared at 600°C had an EC of 10 uS·cm^{-1}. The pH of feedstocks increases during gasification because of the detachment of acid groups and enrichment of alkaline species (Domingues et al., 2017; Weber and Quicker, 2018). EC is correlated with many factors, including nitrate, ammonia, potassium, sodium, chloride, and sulfate contents of the feedstocks (NRCS - USDA, 2014; Singh et al., 2017).

WBC had the highest BET surface area, while DGBC (distillers grain biochar) had the lowest (p<0.0001). Weber and Quicker (2018) and Wang et al. (2013) reported that wood-based biochars (pyrolysis/gasification temperatures ranging from 400 to 800°C) could have a wide range of BET surface areas ranging from nearly 0 m^2 ·g^{-1} to 800 m^2 ·g^{-1}. Wang et al. (2020) used only N_2 in the BET analysis of DGBC and reported a lower BET area of 0.921 m^2·g^{-1} compared

to the BET surface area reported in the current study. Qin et al. (2019) reported that by increasing pyrolysis temperatures of cow manure from 300°C to 700 °C, BET surface area increased from 3.52 to 121.1 $m^2 \cdot g^{-1}$. These values are comparable to those shown in Table 4.1. (760°C, 163 $m^2 \cdot g^{-1}$) since a rising temperature could result in biochars with a larger surface area (Weber and Quicker, 2018).

BET surface area can be connected to other biochar properties such as porosity and water holding capacity. Biochar's porosity is the result of the volatile gas release. A higher heating temperature within a certain range increased the porosity and BET surface area while reducing the bulk density (Weber and Quicker, 2018). As shown in Table 4.1, WBC has a significantly higher water holding capacity and lower bulk density compared to DGBC and CMBC ($p_{WHC}<0.0001$; $p_{bulk\ density}<0.0001$).

DGBC had more than seven times higher nitrogen than WBC and CMBC ($p<0.0001$). The value is similar to that of Fabbri et al. (2012), which reported the nitrogen content of distillers grain made at 350-400°C at about 7.5% (d.b.). Although in the present study, the DGBC was made at 815 °C, Weber and Quicker (2018) demonstrated that the nitrogen content tended to depend less on the heating temperature for plant-based raw materials.

4.3.2. The temperature profile in the composting pile

The compost temperatures measured at the middle (center) and upper layers are shown in Fig. 4.1. Heating cycles are separated by vertical lines marked with "Turning 1" and "Turning 2." The compost material went through three heating cycles during the study. During each heating cycle, middle layer compost temperatures increased above 70°C and then dropped back to the temperatures below 40°C. Ambient temperatures varied from 15 to 32°C with a relative standard deviation (RSD) of 2.1%.

During the first heating cycle, upper layer temperatures were about 11% lower than the temperatures measured at the middle layer. It was expected as the compost material was layered at the beginning of the experiments. While the middle layer was mainly the mortality layer, the upper layer had no animal tissues. This was not the case during the second and third heating cycles, as mortalities went through the initial degradation process, and were mixed homogenously with woodchips and biochar after the compost turning.

Maximum temperatures reached during the 80-day composting period are presented in Table 4.2. Table 4.2 also shows the net cumulative heat units (°C ·day) and if the bins met EPA's Class A and B criteria and Elving et al.'s AI H7N1 criteria (2012). All biochar-treated test units showed prolonged duration above 67 °C compared to control units (p=0.0029). WBC and CMBC addition significantly increased peak temperatures by 2.03-3.30 °C (p=0.0015). Composting bins amended with wood-based biochar had significantly higher heat units than control (p_{middle_layer}=0.0201; p_{top_layer}=0.0215), while there was no significant difference among heat units of DGBC, CMBC, and control (p_{middle_layer}=0.0749; p_{top_layer}=0.1909). Maintaining thermophilic temperatures is the primary mechanism for inactivating pathogens (R. Haug, 2018). Therefore, the improved temperature profile during the composting process can indicate an effective way to eliminate pathogens. Minimum temperature and times are required to meet the pathogen elimination criteria. All test units met the EPA Class A and Class B criteria. All units with biochar addition met Elving et al.'s (2012) criteria to inactivate avian influenza H7N1. The results are consistent with those from Wang et al. (2021), indicating that adding biochar at 13% v/v significantly increased compost temperatures, and the time compost temperature was above 67 °C.

Referring to Wang et al. (2021), biochar can improve the mortality compost temperature profile from two possible aspects: 1) reduce the heat loss due to the extra insulation it provides; 2) improving the composting environment due to its ability to retain the water and nutrients, adjust pH and microbial growth condition. The addition of the biochar can be seen as an additional insulation layer. However, unlike more woodchips or sands, biochar has a porous structure and does not count as an available carbon source because it is reluctant to degrade (Neslihan Akdeniz, 2019; Steiner et al., 2010b). A high C/N ratio can lower the biological degradation rate (Akratos et al., 2017; Nakasaki et al., 1992). Previous studies have confirmed that biochar can improve microbial activity during composting (Du, Zhang, Qu, et al., 2019; Keiji Jindo et al., 2012). However, little has been known regarding its real contribution to the actual temperature increase, excluding the influence of insulation.

4.3.3. Oxygen concentration in the composting pile

Oxygen concentration in the composting pile is shown in Fig. 4.2. The overall trend was similar to the previous study (Yuchuan Wang et al., 2021). During the 1st heating cycle, average

oxygen concentrations were above 15%. The mixing and moisture addition improved the composting condition at the 2nd heating cycle, resulting in higher oxygen consumption. Finally, oxygen consumption decreased during the 3rd heating cycle, indicating that the composting material was nearly mature.

Since the pile turning at the end of 1st heating cycle, biochar addition has shown significantly increased oxygen consumption during the 2nd heating cycle compared to control units (p=0.0088). Considering there has been no evidence that biochar could trap the oxygen from the air, the higher oxygen consumption can provide evidence of biochar's ability to improve the composting environment for microbial growth.

The air sampling method might be improved by placing an impermeable sheet on the pile top during the air sampling. Although the airflow coming out of the pile was assumed to be uniform, the actual fluxes at different pile surface locations can differ. As a result, it is possible to have air exchange on the pile top, causing a lower estimate of the oxygen consumption.

4.3.4. Ammonia emission from the composting pile

Fig. 4.3 indicated the ammonia concentration and cumulative ammonia emission. The ammonia concentrations were the highest during the 2nd heating cycle. During the 3rd heating cycle, the ammonia releases reduced to less than 40% of the previous heating cycles and were probably due to the depletion of raw materials as nitrogen sources. The increase in the compost temperature favored ammonia volatilization, resulting in the increased ammonia concentration in each heat cycle. Besides, although the pH of the composting was not measured along the process, previous studies have reported that the accumulation of ammonia in the composting pile can increase the pH of the composting material and facilitate the ammonia release (Hu et al., 2015; Janczak, Malinska, et al., 2017). Exclusively, biochar may reduce the ammonia emission by 1) its high adsorption capacity to retain the ammonia and ammonium and 2) the creation of a favorable condition for nitrifying bacteria, which convert ammonia to nitrate (Neslihan Akdeniz, 2019; W. Chen et al., 2017b). However, there was no significant difference in cumulative ammonia emissions among different treatments in the present study (p=0.5555), ranging from 265 to 315 $mgNH_3 \cdot kg^{-1}$ initial mortality. The previous study also indicated similar insignificance that at the wood-based biochar addition rate of 13% v/v (5% w/w), biochar addition did not reduce the cumulative ammonia emission (Yuchuan Wang et al., 2021).

Besides, woodchips and biochar may function as biofilter layers to reduce ammonia release (Neslihan Akdeniz et al., 2011; Baltrėnas et al., 2016). The present study indicates lower ammonia emission than Wang et al. (2021), which can be attributed to the increased absorption capacity of the biofilter layers. The composting was started with an average moisture content of 59.8±1.02% in the present study. Additional water was added to make the water content saturate during the pile turning. As a result, the overall moisture levels were higher than Wang et al. (2021), in which the moisture had generally been controlled below 53%. The higher moisture content may retain more ammonia in the composting pile. Besides, the present study had 9 L more woodchips added than Wang et al. (2021). Those woodchips with adjusted moisture functioned as an additional layer of the biofilter.

4.3.5. Leachate

Table 4.3 indicates the physicochemical characteristics of the leachate collected from the compost bin bottom during the entire experiment. Most of the leachate was generated during the 1st and 2nd heating cycles. The addition of wood-based and cow manure biochar significantly lowered the leachate generation during the 1st heating cycle (p=0.0050). The 1st heating cycle generated slightly acidic leachates. In contrast, the 2nd and 3rd cycles generated leachates with neutral or slightly basic pH levels, probably due to the dilution of the available chicken soft tissues during the later heating cycles. E.C. can be an indicator of salts or inorganic chemicals. Wood-based biochar significantly decreased leachate E.C. during the 1st and 2nd heating cycles (p_{1st}=0.0012; p_{2nd}=0.0209), indicating a lower nutrient loss or the environmental impact through the leaching. The total solids and ash content collected during the 1st heating cycle demonstrated a large standard deviation due to the immiscible liquid conditions. The COD concentrations in the leachate were found the highest during the 1st heating cycle when mortalities went through a preliminary degradation. Only the addition of wood-based biochar significantly reduced the COD concentration during the 1st heating cycle. Overall, wood-based biochar addition reduced the cumulative COD content from the control test units up to 87% (p=0.0215). The result is comparable to the previous study, in which the biochar addition at the same rate decreased the cumulative COD content by 83%. Biochar's ability to reduce its COD was also reported in another study (Lou et al., 2017). Besides the higher water holding capacity that helped to retain the leachate, biochar may reduce the leachate COD through other reported ways, including 1) the

adsorption of organic materials to biochar's surface, 2) the improved aerobic condition to degrade the COD (Laird et al., 2010; Lou et al., 2017). The latter mechanism can probably be indicated by the higher compost temperatures with the biochar amendment, shown in Table 4.2.

Leachate samples without pre-treatment resulted in high relative standard deviations of 81% to 200% (Table 4.4). Relative standard deviations for the *E.coli* test were reduced as the centrifugation rate increased, ranging from 4.6% to 67.7% (Table 4.5). For coliform, the relative standard deviation can be reduced except for the rate at 10,000 rpm. At 4000 rpm, the reduction of the relative standard deviation can reach 82.8%. Centrifugation can generally reduce the relative standard deviation of the pathogen test, probably because of the removal of irregularly suspended solids in the leachate. However, a high centrifugation rate may sediment the bacteria and impact the true result. 7000 and 10,000 rpm showed significant reductions in bacteria counts, while 4000 rpm did not. Hence, centrifugation of the leachate samples at 4000 rpm might be considered an approach to reduce the standard deviation of the measures without influencing the true reading. The rate of 4000 rpm to treat the leachate sample was also applied in another study (Ye et al., 2017). The mixing of the leachate samples before the centrifugation may furtherly decrease the relative standard deviation, as indicated in Table 4.6. *E.coli* was not tested due to the loss of its activity. Within the measure of coliform, the relative standard deviation for all samples can be reduced to within 57%, or with the mean of 26.3±14.8%. Although a true measurement of the *E.coli* and coliform could not be done to the activity loss after multiple trials, centrifuging the leachate samples at 4000 rpm with sample mixing was found to be appropriate when testing the complicated leachate samples.

4.3.6. Final compost

Table 4.7 shows the physicochemical characteristics and nutrient contents of the finished compost. There is no significant difference among the moisture contents. Cow manure added compost has the highest ash content, pH, and E.C. Wood-based biochar significantly changed neither potassium nor sodium content from the control units in the final compost (p_K=0.4596; p_{Na}=0.9370). CMBC had a higher E.C., as indicated in Table 4.1; therefore, its addition was likely to increase the E.C. of the final compost. In the current study, due to extra woodchips for balancing the compost volume, the control and wood-based biochar amended treatment at 13% (v/v) showed lower nitrogen contents compared to the previous study (Yuchuan Wang et al.,

2021). Overall, all biochar-treated units indicate significantly higher total nitrogen or organic nitrogen content than the control (p_{TN}<0.0001; p_{ON}<0.0001). Test units with distillers grain biochar showed the greatest final improvement in the nitrogen content (p=0.0009). Besides biochar's ability to retain the nitrogen, another reason might be that the fresh distillers' grain biochar had the highest initial nitrogen content (Table 4.1). The high nitrogen content in the final compost also decreased its C/N ratio. The average nutrient values ($N+P_2O_5+K_2O$) of the control, wood-based, and cow manure biochar test units were within the medium range of 2 to 5 (% dry weight). Distillers' grain test units had the highest of 5.40 ± 0.76. All control test units had nutrient indexes above 10, indicating the unlikely situation of salt injury. The nutrient index was calculated by dividing the total nutrient amount (N+P+K) by the salt (sodium and chloride). For one test unit of wood-based biochar and two of the cow manure biochar, the nutrient indexes were found between 5 and 10. However, these composts can still be applied to soils with high salts, poor water quality, or drainage. Generally, adding all biochar can increase the iron and manganese contents compared to the control test units (p_{Fe}=0.0008; p_{Mn}=0.0007). Some studies reported biochar could capture the metal ions during composting (Guo et al., 2020; Saifullah et al., 2018); however, contents that elevated these three properties may also come from the biochar (Yuchuan Wang et al., 2021).

4.4. Conclusion

Wood-based biochar had the highest BET surface area and was 1.4 and 28 times greater than cow manure and distillers grain biochar, respectively. At the addition rate of 13% by volume, test units with wood-based biochar, distillers grain biochar, and cow manure biochar showed higher oxygen consumption (p=0.0088) and more durable compost temperatures above 67 °C to eliminate avian influenza (H7N1) viruses than the those of the control (p=0.0029), which had no biochar addition. Test units with wood-based and cow manure biochar significantly increased the composting peak temperatures by 2.03-3.30 °C (p=0.0015). Wood-based biochar resulted in a higher heat unit generation during the composting process (p_{middle_layer}=0.0201; p_{top_layer}=0.0215). None of the biochar amended test units significantly reduced ammonia concentrations and emissions (p=0.5555). Wood-based biochar significantly reduced the cumulative COD content of leachate by 87% compared to the control (p=0.0215). In the final compost, all biochar-treated test units had significantly higher total and organic nitrogen contents than the control

(p_{TN}<0.0001; p_{ON}<0.0001), and test units with distillers grain biochar had the highest nitrogen content (p=0.0009). All biochar additions increased the iron and manganese contents (p_{Fe}=0.0008; p_{Mn}=0.0007).

4.5. Acknowledgment

This project was supported by the United States Department of Agriculture (USDA)-National Institute of Food and Agriculture (NIFA) through a Hatch grant provided to the Agricultural and Biological Engineering Department at the University of Illinois at Urbana-Champaign (no. ILLU-741-328).

4.6. Figures and Tables

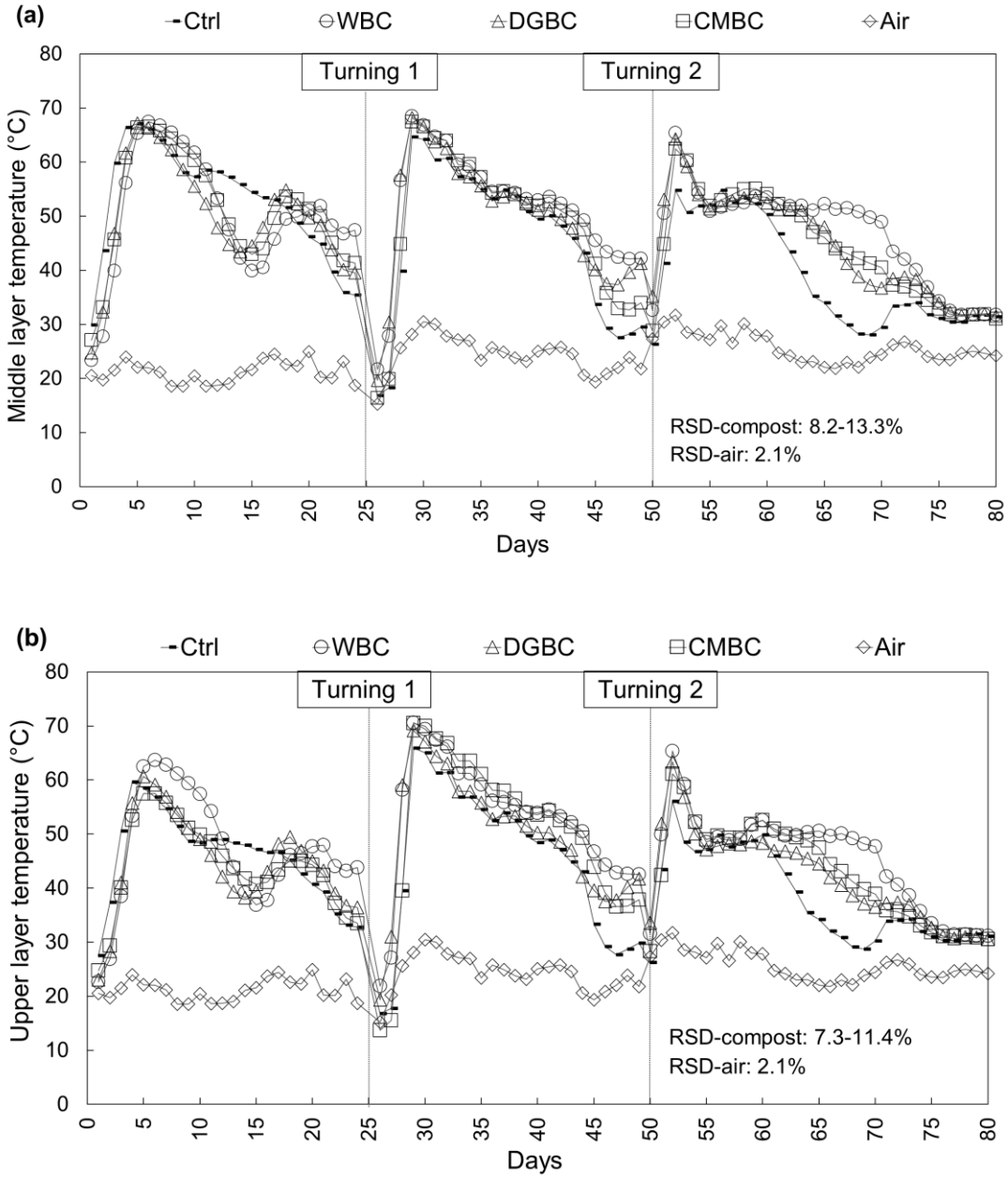

Fig. 4.1. (cont.)

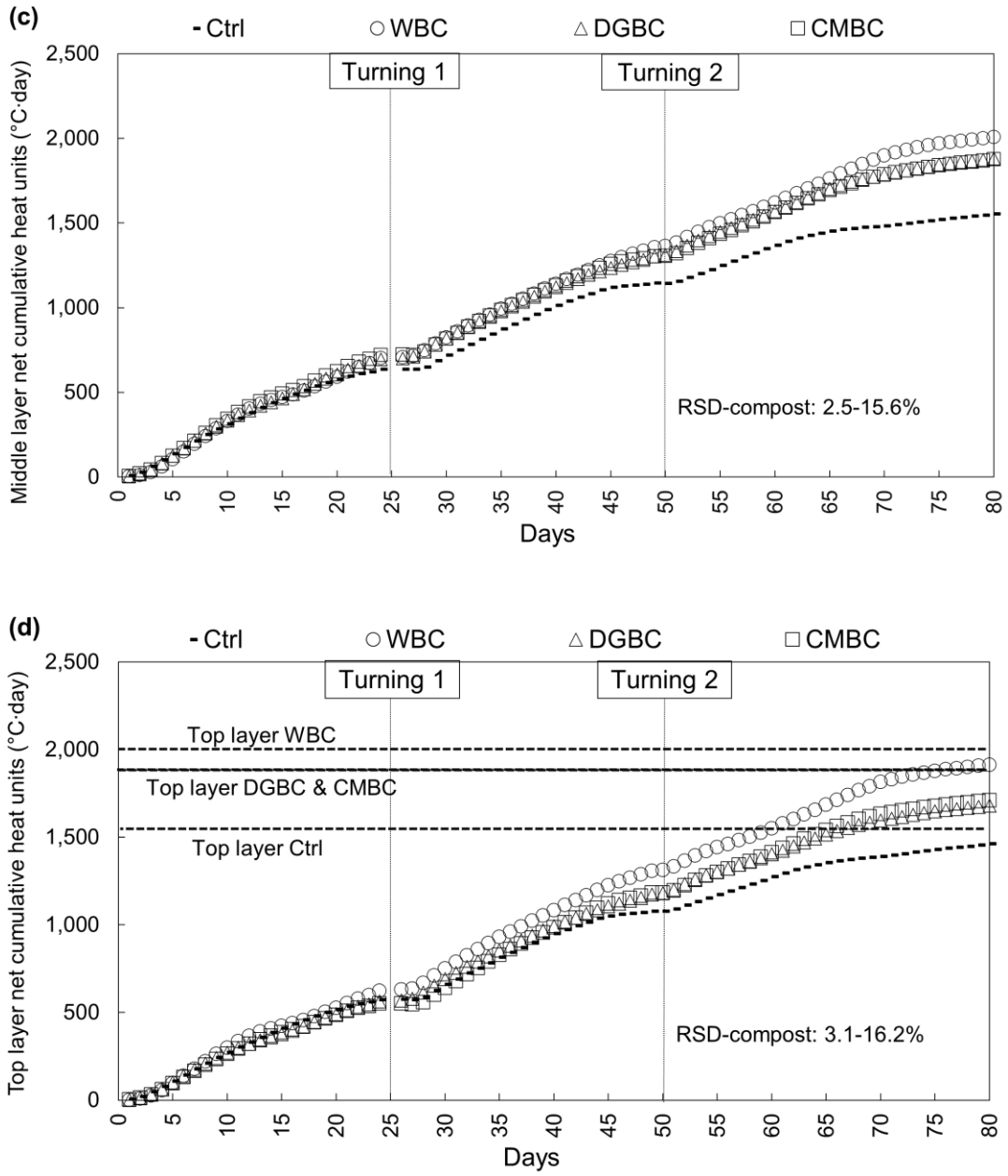

Fig. 4.1. The compost temperature profile of different treatments during 11 weeks. The middle layer temperature (a), the upper layer temperature (b), the net cumulative heat units (°C ·day) of the middle layer (c) and the net cumulative heat units (°C ·day) of the top layer (d). Since standard deviation bars overlap and reduce the visual quality, they were not shown in the graph. Instead, relative standard deviations (RSD) are reported. The "net" means the difference between the measured temperature profile and the ambient air temperature profile.

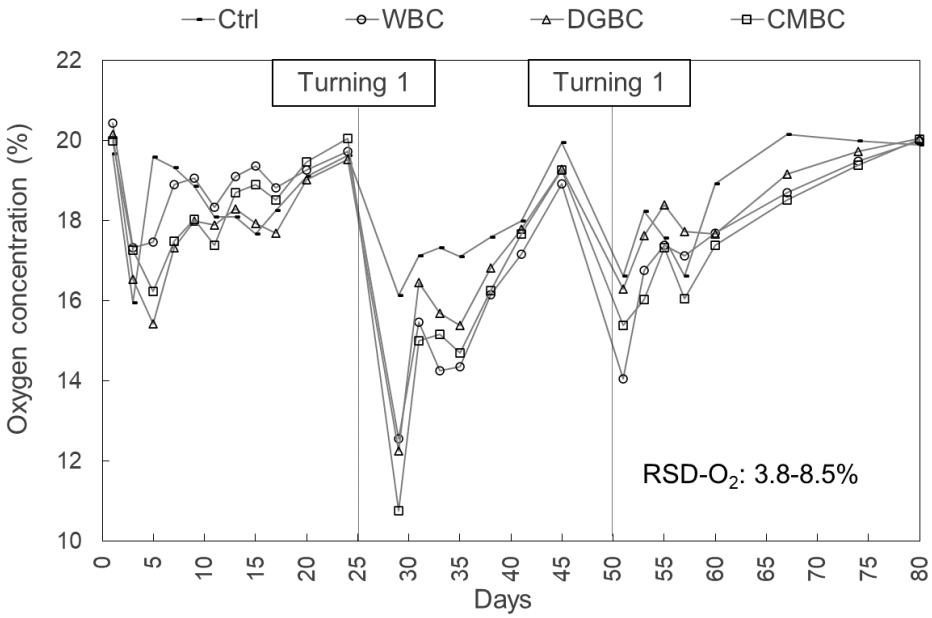

Fig. 4.2. Oxygen concentrations measured at the compost top layer.

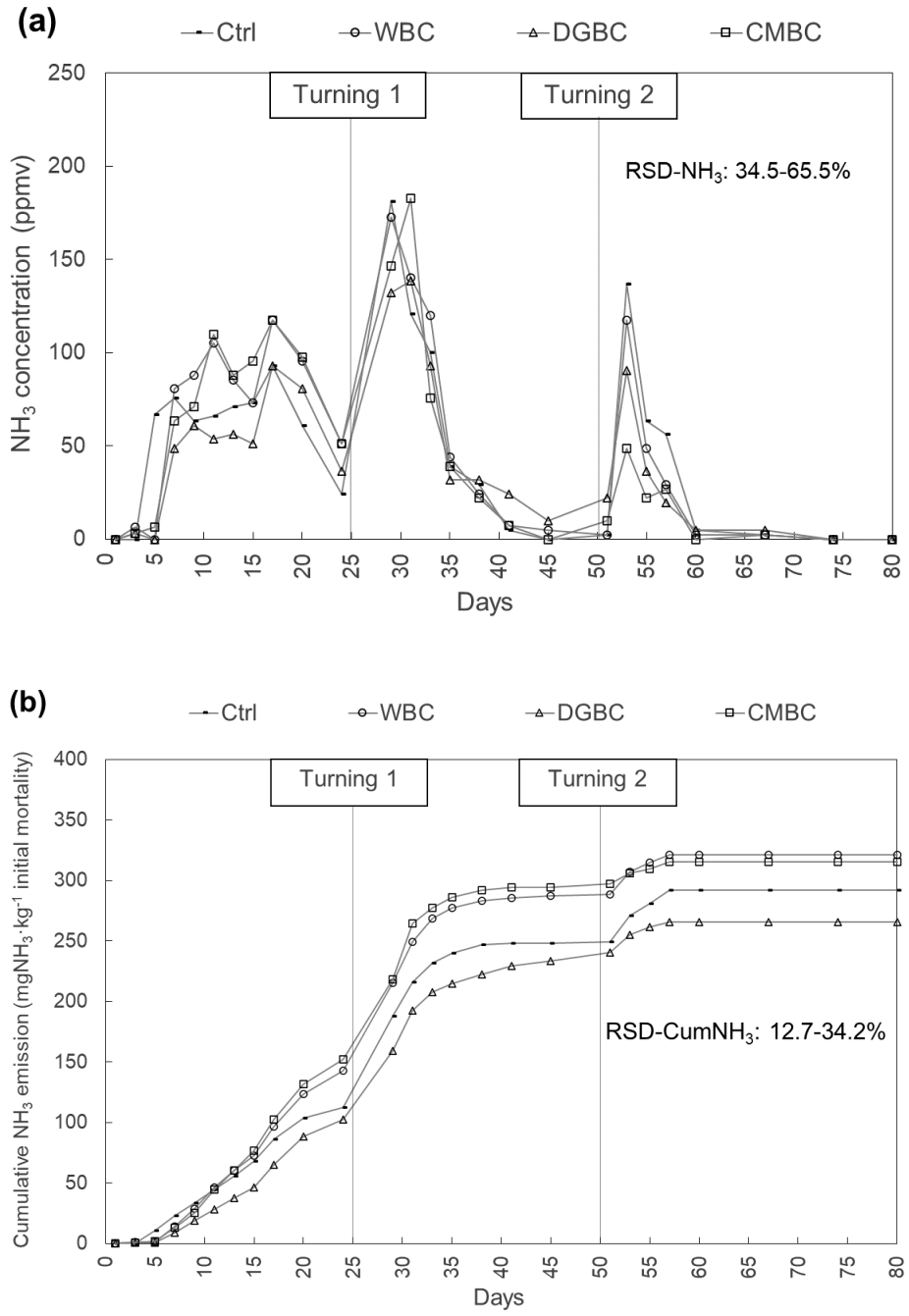

Fig. 4.3. Ammonia concentrations as time (a) and cumulative ammonia emissions as time (b).

Table 4.1. Physicochemical characteristics of biochar and woodchips.

Characteristics	**Woodchips**	**WBC**	**DGBC**	**CMBC**
Ash (%)	1.35 ± 0.31 ^{A}	12.71 ± 3.76 ^{B}	15.50 ± 1.94 ^{B}	18.94 ± 0.95 ^{B}
pH	5.69 ± 0.03 ^{D}	7.53 ± 0.04 ^{B}	6.94 ± 0.03 ^{C}	10.87 ± 0.03 ^{A}
EC ($uS \cdot cm^{-1}$)	0.34 ± 0.0 ^{C}	0.33 ± 0.0 ^{C}	0.79 ± 0.00 ^{B}	7.84 ± 0.05 ^{A}
Bulk density ($kg \cdot m^{-3}$)	190 ± 3.84 ^{B}	135 ± 8.19 ^{C}	254 ± 5.58 ^{A}	267 ± 3.44 ^{A}
Water holding capacity (g water $\cdot g^{-1}$ d.b.)	1.18 ± 0.22 ^{C}	5.75 ± 0.77 ^{A}	2.68 ± 0.12 ^{B}	3.33 ± 0.09 ^{B}
BET surface area ($m^2 \cdot g^{-1}$)	-	397 ± 18.2 ^{A}	13.7 ± 4.05 ^{C}	163 ± 12.0 ^{B}
Total C (% d.b.)	45.6 ± 0.11 ^{C}	67.8 ± 4.67 ^{A}	67.8 ± 2.03 ^{A}	59.37 ± 2.40 ^{B}
Total H (% d.b.)	5.53 ± 0.04 ^{A}	1.66 ± 0.49 ^{B}	1.95 ± 0.60 ^{B}	1.18 ± 0.07 ^{B}
Total N (% d.b.)	0.57 ± 0.08 ^{BC}	0.43 ± 0.08 ^{C}	6.87 ± 0.60 ^{A}	0.86 ± 0.02 ^{B}

Within each row, means that are not connected by the same letter are significantly different ($P<0.05$).

Table 4.2. Compost temperature-time criteria to eliminate pathogens.

	Max temperature	Middle layer net heat unit[1]	Top layer net heat unit	Elving et al.'s (2012) AI H7N1 criteria[2]		EPA's (2003) Class A and B criteria[3]		
	(°C)	(°C ·day)	(°C ·day)	# of days above 67°C	yes/ no	# of days above 55 °C	Class A	Class B
Control	70.27 ± 0.58^{C}	1541 ± 240^{B}	1499 ± 235^{B}	1.12 ± 0.16^{B}	N	8.26 ± 2.33^{A}	Y	Y
WBC	72.30 ± 0.61^{AB}	2007 ± 83^{A}	1914 ± 60^{A}	3.36 ± 0.58^{A}	Y	9.67 ± 1.45^{A}	Y	Y
DGBC	71.15 ± 0.35^{BC}	1857 ± 47^{AB}	1655 ± 96^{AB}	2.33 ± 0.60^{A}	Y	7.65 ± 0.51^{A}	Y	Y
CMBC	73.57 ± 0.72^{A}	1865 ± 109^{AB}	1702 ± 119^{AB}	3.33 ± 1.18^{A}	Y	10.23 ± 0.81^{A}	Y	Y

"Ctrl": no biochar, "WBC": Wood pallet biochar, "DGBC": distiller grain biochar, "CMBC": cow manure biochar

Within each column, means that are not connected by the same letter are significantly different ($P<0.05$).

[1] The "net" means the difference between the measured temperature and the ambient air temperature.

[2] Elving et al.'s (2012) reported that composting with its maximum temperature at 67 °C for 1 consecutive day is sufficient to inactivate avian influenza H7N1. If all replicates met the criteria, it is noted as Y, otherwise N.

[3] Class A: compost temperature of 55 ºC or higher for at least 3 consecutive days. Class B: compost temperature of at least 40 ºC for 5 or more consecutive days, exceeding 55 ºC for at least 4 hours during this period. If all replicates met the criteria, it is noted as Y, otherwise N.

Table 4.3. Leachate volume and characteristics.

	Cycle	Ctrl	WBC	DGBC	CMBC
Volume ($mg \cdot kg^{-1}$ initial mortality)	1	2285 ± 360 ^{A}	900 ± 60 ^{B}	1730 ± 510 ^{AB}	1080 ± 366 ^{B}
	2	1630 ± 342 ^{A}	1437 ± 103 ^{A}	1533 ± 359 ^{A}	1373 ± 131 ^{A}
	3	330 ± 26 ^{A}	527 ± 241 ^{A}	520 ± 347 ^{A}	540 ± 419 ^{A}
pH	1	6.34 ± 0.71 ^{A}	6.18 ± 0.34 ^{A}	6.40 ± 0.85 ^{A}	6.61 ± 0.60 ^{A}
	2	7.75 ± 0.20 ^{A}	7.55 ± 0.12 ^{A}	7.65 ± 0.41 ^{A}	7.92 ± 0.14 ^{A}
	3	7.72 ± 0.08 ^{A}	7.56 ± 0.17 ^{A}	7.54 ± 0.27 ^{A}	7.38 ± 0.23 ^{A}
EC ($mS \cdot cm^{-1}$)	1	4.91 ± 0.84 ^{A}	0.68 ± 0.20 ^{C}	2.62 ± 0.59 ^{B}	1.38 ± 0.95 ^{BC}
	2	2.30 ± 0.53 ^{A}	1.15 ± 0.42 ^{B}	2.52 ± 0.23 ^{A}	2.32 ± 0.61 ^{A}
	3	1.60 ± 0.39 ^{AB}	1.12 ± 0.28 ^{B}	2.35 ± 0.54 ^{A}	2.31 ± 0.74 ^{A}
Total solids (%)	1	15.4 ± 14.3 ^{A}	0.84 ± 0.67 ^{A}	22.3 ± 17.8 ^{A}	9.4 ± 14.0 ^{A}
	2	0.36 ± 0.12 ^{A}	0.24 ± 0.11 ^{A}	0.42 ± 0.18 ^{A}	0.37 ± 0.19 ^{A}
	3	0.42 ± 0.27 ^{AB}	0.22 ± 0.07 ^{B}	0.75 ± 0.16 ^{A}	0.80 ± 0.15 ^{A}
Ash (% d.b.)	1	3.46 ± 5.08 ^{A}	5.50 ± 3.73 ^{A}	1.27 ± 1.88 ^{A}	8.91 ± 13.64 ^{A}
	2	16.89 ± 5.07 ^{A}	7.62 ± 3.33 ^{A}	17.37 ± 2.46 ^{A}	23.86 ± 11.89 ^{A}
	3	13.38 ± 4.12 ^{A}	12.12 ± 3.38 ^{A}	12.47 ± 3.27 ^{A}	16.82 ± 1.21 ^{A}
COD ($g \cdot L^{-1}$)	1	265 ± 70.6 ^{A}	71.8 ± 51.4 ^{A}	254 ± 99 ^{A}	242 ± 89 ^{A}
	2	5.61 ± 3.35 ^{A}	9.15 ± 5.94 ^{A}	6.50 ± 2.94 ^{A}	8.87 ± 8.33 ^{A}
	3	3.75 ± 0.99 ^{AB}	2.42 ± 0.54 ^{B}	5.10 ± 1.34 ^{A}	4.31 ± 0.69 ^{AB}
Cum. COD[2]		632 ± 246 ^{A}	79.7 ± 44.3 ^{B}	481 ± 269 ^{A}	330 ± 218 ^{AB}

Within each row, means that are not connected by the same letter are significantly different ($P<0.05$).

[1] Cumulative COD (g per kg initial mortality)

Table 4.4. Pathogen colony counts without centrifugation/mixing

Rpm, 1 min	Ctrl	WBC	DGBC	CMBC
E. Coli counts	0.1 ± 0.2^{A}	0.4 ± 0.4^{A}	0.8 ± 0.8^{A}	0.7 ± 0.7^{A}
Coliform counts	1.1 ± 1.6^{A}	2.0 ± 1.8^{A}	23.9 ± 19.8^{A}	16.7 ± 13.5^{A}

Within each row, means that are not connected by the same letter are significantly different ($P<0.05$).

Table 4.5. The effects of centrifugation rates on the pathogen colonies

Rpm, 1 min	0	4,000	7,000	10,000
E. Coli counts	3.7 ± 2.3^{AB}	5.3 ± 0.6^{A}	2.5 ± 1.3^{AB}	1.3 ± 1.2^{B}
Coliform counts	31.7 ± 7.4^{A}	22.7 ± 5.0^{AB}	15.5 ± 1.3^{BC}	7.7 ± 0.6^{C}

Within each row, means that are not connected by the same letter are significantly different ($P<0.05$).

Table 4.6. Coliform counts with samples homogenization and centrifugation at 4,000 rpm for 1 min

	Week	Control	WBC	DGBC	CMBC
	1 to 2	0.0 ± 0.0^{C}	25.3 ± 4.0^{B}	0.0 ± 0.0^{C}	75.0 ± 21.2^{A}
Coliform	3 to 4	2.7 ± 1.5^{B}	9.7 ± 2.3^{A}	13.7 ± 5.0^{A}	13.0 ± 2.6^{A}
counts	5 to 8	14.7 ± 4.6^{B}	15.0 ± 2.6^{B}	28.3 ± 1.5^{A}	0.0 ± 0.0^{C}
	9 to 12	6.7 ± 2.1^{B}	4.7 ± 1.5^{B}	5.7 ± 1.2^{B}	373.3 ± 28.9^{A}

Within each row, means that are not connected by the same letter are significantly different ($P<0.05$).

Table 4.7. Physicochemical characteristics of the finished compost samples.

	Ctrl	**WBC**	**DGBC**	**CMBC**
Moisture content (%)	38.53 ± 3.77^{A}	45.07 ± 6.39^{A}	44.9 ± 8.43^{A}	48.13 ± 3.47^{A}
Ash (% d.b.)	5.38 ± 0.34^{B}	6.74 ± 0.46^{B}	8.21 ± 2.76^{AB}	11.21 ± 0.65^{A}
pH	7.10 ± 0.26^{B}	6.63 ± 0.40^{B}	6.57 ± 0.55^{B}	8.20 ± 0.26^{A}
EC ($uS \cdot cm^{-1}$)	1.89 ± 0.02^{B}	2.07 ± 0.26^{B}	2.45 ± 0.72^{B}	4.35 ± 0.42^{A}
Total N (% d.b.)	1.71 ± 0.04^{C}	2.29 ± 0.23^{B}	3.28 ± 0.29^{A}	2.27 ± 0.20^{B}
Organic N (% d.b.)	1.62 ± 0.01^{C}	2.20 ± 0.22^{B}	3.18 ± 0.28^{A}	2.27 ± 0.20^{B}
C:N ratio	28.3 ± 0.58^{A}	22.3 ± 2.08^{B}	15.67 ± 1.15^{C}	22.3 ± 1.53^{B}
P as P_2O_5 (% d.b.)	0.66 ± 0.44^{A}	0.55 ± 0.10^{A}	1.26 ± 0.38^{A}	0.89 ± 0.25^{A}
K as K_2O (% d.b.)	0.53 ± 0.02^{C}	0.63 ± 0.08^{BC}	0.85 ± 0.13^{B}	1.65 ± 0.28^{A}
Sulfur (% d.b.)	0.18 ± 0.01^{A}	0.21 ± 0.03^{A}	0.22 ± 0.01^{A}	0.22 ± 0.05^{A}
Calcium (% d.b.)	1.83 ± 0.27^{A}	2.00 ± 0.19^{A}	1.73 ± 0.04^{A}	2.14 ± 0.41^{A}
Magnesium (% d.b.)	0.19 ± 0.01^{B}	0.23 ± 0.04^{B}	0.31 ± 0.05^{AB}	0.42 ± 0.12^{A}
Sodium (% d.b.)	0.14 ± 0.01^{B}	0.15 ± 0.02^{B}	0.21 ± 0.05^{AB}	0.28 ± 0.03^{A}
Zinc (ppm)	274 ± 70.4^{A}	369 ± 90.2^{A}	571 ± 92.1^{A}	489 ± 212^{A}
Iron (ppm)	149 ± 40.15^{C}	416 ± 109^{BC}	1660 ± 796^{A}	737 ± 330^{AB}
Manganese (ppm)	$< 20.0^{B}$	128 ± 38.0^{A}	61.7 ± 12.7^{A}	99.0 ± 33.1^{A}

Within each row, means not connected by the same letter are significantly different ($P<0.05$).

4.7. Appendix

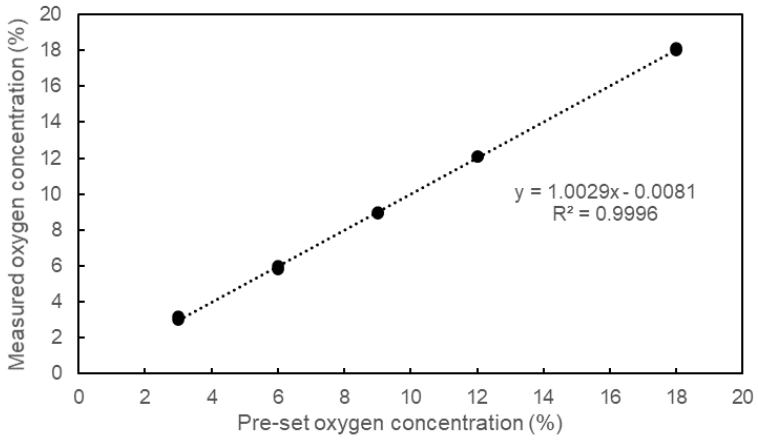

Fig. 4.4. Oxygen concentration calibration. Calibration levels were set at 3, 6, 9, 12, 18, 20.9% O_2 by volume. Calibration gases were prepared by diluting 20.9% O_2 with N_2 using an Environics Gas Dilution System (Environics 4040, Tolland, CT). The O_2 concentrations were measured by RKI - Eagle II® (Union City, CA)

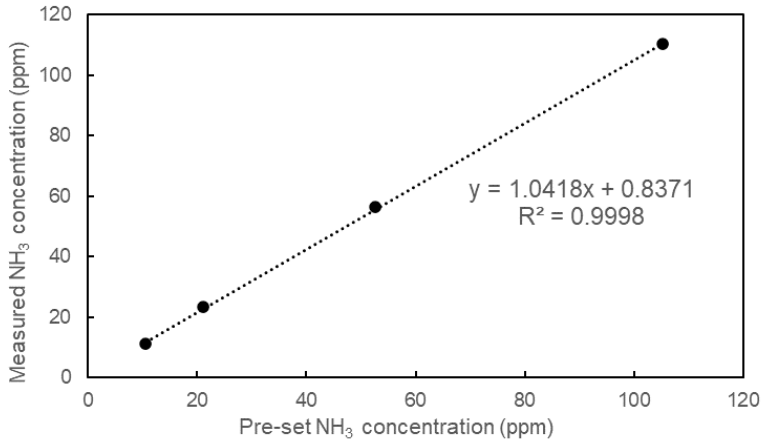

Fig. 4.5. Ammonia concentration calibration. Calibration levels were set at 10.53, 21.06, 52.65, and 105.3 ppm NH_3 by volume. Calibration gases were prepared by diluting 105.3 ppm NH_3 with N_2 using an Environics Gas Dilution System (Environics 4040, Tolland, CT). The NH_3 concentrations were measured by titrating the 0.005 M H_2SO_4 into 4% boric acid.

CHAPTER 5

MODELING OF BIOCHAR'S ROLE IN INCREASING THE TEMPERATURE DURING CO-COMPOSTING

5.1. Introduction

A high compost temperature is desired because it positively reflects the thermophilic bacteria activity and pathogen inactivation efficiency (Arvanitoyannis and Ladas, 2008; Medina et al., 2019). While composting can be inactive during cold weather, multiple previous studies introduced biochar as a co-composting material, resulting in increased compost temperatures (Godlewska et al., 2017; Yuchuan Wang et al., 2021). Liu et al. (2019) reported that adding bamboo-derived biochar at 10% (w/w) significantly increased the compost temperatures and duration at ambient temperatures of 0°C and 5°C, and both conditions met the Class A criteria with biochar addition. Biochar's improvement in compost temperature is likely to overcome the constraint of composting. Regarding the reasons for biochar's ability to increase the compost temperature, previous studies concluded two possible reasons: 1) biochar can increase the microbial activity, resulting in an increased heat generation, and 2) biochar can fill the free space of the compost materials, resulting in an increased insulation and a reduced heat loss (Godlewska et al., 2017; H. Liu et al., 2019; Huiyong Yu et al., 2019).

Nevertheless, it is unclear how much each aspect contributes to the temperature increase. The change in microbial activity can be an aspect of many possible reasons, such as biochar's high porosity, large surface area, and suitable size scale for microbial communities (Wei et al., 2014). A large portion of the contribution of this aspect can indicate that the temperature increase is a unique characteristic of biochar. On the other hand, if biochar's effect of increasing the insulation is the primary aspect to increase the compost temperature, biochar can likely be replaced by similar small particle materials such as sand and soil due to their lower prices.

In multiple studies, heat transfer modeling has been studied and successfully implemented to predict compost temperature. However, finding a universal solution is challenging because the composting model can differ in configuration, operation, and mathematical expressions (Mason and Milke, 2005). Hopefully, Guardia et al. (2012) developed the in-vessel composting heat transfer model with aeration, and the configuration of the model was similar to that of our two

previous studies. The model will partially rely on continuous measurements during the experiment, such as the oxygen content and ambient air temperature. With the input of experimental conditions, the compost temperature will be simulated from the first day of composting. The main difference in configuration between our studies and Guardia et al. (2012) was that a lid was applied to cap the composter on the top in Guardia et al. (2012), and this might result in a different scenario when calculating the heat transfer profile on the surface of the compost pile.

Known that the biochar addition has shown the increased temperature during the composting process. The purpose of this study is to 1) construct a valid heat transfer model for in-vessel aerated composting without the lid and 2) investigate mathematically the contribution of adding biochar to the compost temperature using the data measured from the previous two studies, from aspects of A) biochar increasing the insulation, and B) biochar increasing the microbial activity.

5.2. Material and methods

5.2.1. Source of the data

The data used for the heat transfer modeling was obtained from the author's previous composting experiment in CHAPTER 3 and CHAPTER 4. Both experiments were carried out in the Agricultural research training farm located at the University of Illinois Urbana-Champaign. Chicken mortality, woodchips, and biochar were composted in pilot-scale in-vessel composters for 80-84 days.

5.2.2. Composter configuration

Composters were made from 32-gallon bins. All the composters were placed on two layers of wood pallets, about 20 cm from the ground, to reduce the heat loss. The sidewall of the composters was wrapped by a layer of the R19 fiberglass insulation (EcoRoll, OH). Aeration at 0.8-1.5 $L \cdot min^{-1}$ was applied from the bottom of each composter to supply air flowing through the composting materials. The aeration line consisted of a vacuum pump (Thomas Pump, Slidell, LA), airflow meter (Cole-Parmer, IL), and PVC tubes for connection. Inside the composter, a steel mesh platform was made 12 cm above the bottom to create the air plenum. Another 1.2 cm

diameter hole was drilled for leachate sample collection on the sidewall near the bottom. A rubber stopper was plugged into the hole when leachate was not collected.

5.2.3. Compost materials

Chicken mortalities were collected from the nearby Poultry Research farm. Chickens were euthanized and frozen at -20 °C when not in use. Before the initial loading of the compost materials, chicken mortalities were thawed at the ambient temperature for two days. Woodchips were a mixture of different types of wood and were collected from the Ground Storage Barn in the university.

Three types of biochar were used in the two studies, including wood-based material (WBC), distillers' grains (DGBC), and cow manure (CMBC). WBC was produced by Chip Energy (Goodfield, IL) by gasification of wood pallets at 520 °C. DGBC and CMBC were produced by Ecochar (Evansille, IN) by gasification of distillers' grains and cow manure at 815 °C and 760 °C, respectively.

5.2.4. Treatments

The experiment from CHAPTER 3 consisted of 15 composters with five treatments and three replicates for each treatment. Treatment included: "Ctrl_1" - control, no biochar was added to the composting, "2.6%WBC" - compost materials were added with 2.6% (v/v, biochar volume/woodchips, and chicken mortality volume) wood-based biochar. "13%WBC_1" - compost materials were added with 13% (v/v) wood-based biochar, "26%WBC" - compost materials were added with 26% (v/v) wood-based biochar, and "39%WBC" - compost materials were added with 39% (v/v) wood-based biochar

The experiment from CHAPTER 4 consisted of 12 composters with four treatments and three replicates for each treatment. Treatment included: "Ctrl_2" – control, no biochar was added to the composting, "13%WBC_2" - compost materials were added with 13% (v/v) wood-based biochar, "13% DGBC" - compost materials were added with 13% (v/v) distillers grain biochar, "13% CMBC" - compost materials were added with 13% (v/v) cow manure biochar. In the study of Wang et al. (2021), biochar was added at the weight basis of 2.6%, 13%, 26%, and 39% (v/v). The addition at biochar of 13% (v/v) was recommended as the minimum addition rate.

5.2.5. Process maintenance

In the experiment of CHAPTER 3, the steps of the initial loading were:

- Place 22.5 L woodchips (15 cm thickness) on the steel platform as the bottom layer.
- Place half dosage of biochar on the woodchips layer.
- Place 4 to 5 chicken mortalities (8.8±0.4 kg) on the biochar or woodchips layer.
- Place another half dosage of biochar on the woodchips layer.
- Finally, place another 22.5 L woodchips as the top layer.

The initial moisture was estimated at around 50%, with a C/N ratio of about 22. Aeration was kept at 1.5 $L \cdot min^{-1}$. The experiment lasted for 84 days with three heating cycles separated by two turning on day 31 and day 63. Compost materials were thoroughly mixed, weighed, and reloaded into composters. Moisture content was adjusted to about 50% during each turning by adding the tap water. After the loading, about 6 L woodchips were added to cover the top surface of compost materials.

In the experiment of CHAPTER 4, the steps of the initial loading were:

- Place 30 L woodchips on the steel platform as the bottom layer.
- Place 6 L of biochar on the woodchips layer. For control, it was replaced with 6 L woodchips.
- Place 4 to 5 chicken mortalities (9.83±0.45 kg) on the biochar or woodchips layer.
- Place 3 L biochar on the woodchips layer. For control, it was replaced with 3 L woodchips.
- Finally, place another 15 L woodchips as the top layer.

The initial moisture was estimated at around 60%, with a C/N ratio of about 22. Aeration was kept at 0.8-1.2 $L \cdot min^{-1}$. The experiment lasted for 80 days with three heating cycles on day 25 and day 50. During the 1^{st} turning only, 9 L woodchips were added to all biochar treated units and mixed with the compost materials. Moisture content was adjusted to about 62% during each turning, and about 6 L woodchips were added to cover the top surface of compost materials after the loading.

5.2.6. Data measurement

Temperatures were monitored every 30 min using pre-calibrated K-type thermocouples and 4-channel data loggers (Tekcoplus Ltd, Hong Kong). Thermocouples were inserted into a PVC tube to avoid moisture and deformation. Three 1 mm small holes were drilled near the sensor tip to improve the heat exchange inside and outside the PVC tube. Compost temperatures were measured at the center of the materials. For the experiment of CHAPTER 4, an additional measurement was set up at 15 cm above the center. The measurement procedure of oxygen was the same as Wang et al. (2021). The humidity of the aerated air was measured by a humidity meter (DHT11, HiLetgo, Shenzhen), which was placed by the air pump.

The data used for the heat transfer modeling in this composting experiment included: compost temperatures on the first day (the starting point), all compost temperatures (used for water loss calibration), ambient air temperature, the oxygen concentration inside the compost pile, aeration rate, the dimension of the composter, weights and volumes of compost materials, compost materials densities, and conductive and convective coefficients of compost materials, air, moisture, and insulation layer.

5.2.7. Heat transfer modeling

5.2.7.1. Pore space determination

All nomenclature information is shown in Table 5.1. Excluding the portion of biochar, the pore space fraction (θ) was estimated at 65%, based on the ratio of compost material bulk density ($\rho_{comp,b}$) to the actual density ($\rho_{comp,s}$), as shown in Eq. 5.1. Assuming the θ is constant over positions and time.

$$\theta = \frac{\rho_{comp,b}}{\rho_{comp,s}} \qquad \text{Eq. 5.1}$$

The addition of biochar will change θ, and the final value was calculated instead. The pore space fraction of biochar was assumed to be 80%, according to (Leng et al., 2021). Our mixing test indicated that the pore space of the compost could hold about 13% (v/v) biochar in the pore space without increasing the height. Therefore, biochar addition within 13% (v/v) decreases the overall pore space, and the updated θ at X% (v/v) biochar addition rate was calculated as:

$$\theta = \theta_{comp}\theta_{bc}\frac{X\%}{13\%} \quad \text{Eq. 5.2}$$

Where θ_{comp}= 65% and θ_{bc}= 80%. For biochar addition rate beyond 13% (v/v), the updated θ at X% (v/v) biochar addition rate was calculated as:

$$\theta = \theta_{comp}\theta_{bc} + (X - 13\%)(\theta_{bc} - \theta_{comp}\theta_{bc}) \quad \text{Eq. 5.3}$$

5.2.7.2. The net heat transfer rate (H_{net})

The heat transfer model was constituted to simulate the temperature change during the composting process using R 4.1.2. The modeling fellow the general approach by De Guardia et al. (2012) with modifications. Assuming the overall heat transfer has reached a steady-state, the overall heat transfer rate equation is shown in Eq. 5.4.

$$H_{net} = H_{bio} - H_{eva} - H_{btm} - H_{top} - H_{wall} \quad \text{Eq. 5.4}$$

where H_{bio} is the biologically generated heat due to the degradation of compost materials ($kJ \cdot h^{-1}$), H_{eva} is the heat loss from water evaporation from the compost material. H_{btm} and H_{top} are the heat losses from the compost pile top and bottom surfaces. H_{wall} is the heat loss from the composter wall. Finally, H_{net} is the net heat transfer rate of all abovementioned rates. Radiation heat loss is neglected because the surface temperature of the compost materials was assumed to be equal to the ambient air temperature. Ahn et al. (2007) counted in the radiation heat loss from the surface of compost materials because its temperature was equivalent to the compost temperature, which was higher than the ambient temperature. However, results indicated that less than 5% of the total heat loss was attributed to radiation loss.

5.2.7.3. Heat generation from biodegradation (H_{bio})

The microbial activity resulted in the heat generation during the composting process, which was reflected by the oxygen consumption. Assuming the air pumped in from the bottom of the composters traveled uniformly through the composting materials, the measured oxygen concentration (C_{o2}, %) from the top surface of the pile can be converted to the total oxygen consumption rate (rO_2, mol $O_2 \cdot h^{-1}$) by the microbes. It was reported by Bailey and Ollis (1986)

and applied by de Guardia et al. (2012), 440 kJ·mol^{-1} O_2 was the biological heat generation amount by consuming the oxygen (h_{bio}). The heat generation rate can be expressed as:

$$H_{bio} = rO_2 \cdot h_{bio} \quad \text{Eq. 5.5}$$

Where for rO_2, it is calculated by the ideal gas law. Standard air pressure (P, 1 atm), aeration rate ($\dot{Q}_{air}$, 0.8-1.2 L·min^{-1}), ideal gas law constant (R=0.0821 atm·L·mol^{-1}·K^{-1}) and the temperature of the inlet air ($T_{a,in}$, K) were used to calculate the rO_2 as shown. $T_{a,in}$ is assumed equal to the ambient air temperature T_{amb}, and a sensitive test on it will be discussed later.

$$rO_2 = \frac{P \cdot (20.9\% - C_{o2}) \cdot \dot{Q}_{air}}{RT_{a,in}} \quad \text{Eq. 5.6}$$

5.2.7.4. Heat loss from water evaporation (H_{eva})

Water evaporation resulted in the moisture loss of the compost materials, taking away the heat and leading to higher humidity in the air flowing out from the top surface of the pile. The heat exchange rate (H_{eva}, kJ·h^{-1}) was calculated from the water mass in the air entering ($\dot{m}_{w,in}$, g·h^{-1}) and leaving ($\dot{m}_{w,out}$, g·h^{-1}) the compost materials, and the latent heat of water evaporation (L_{eva}, kJ·kg^{-1} water evaporated). L_{eva} is dependent on the compost temperature (T, °C) and can be calculated by Eq. 5.8.

$$H_{eva} = (\dot{m}_{w,out} - \dot{m}_{w,in}) \cdot L_{eva} \quad \text{Eq. 5.7}$$

$$L_{eva} = 2501 - 2.65 * T \quad \text{Eq. 5.8}$$

In this study, the air humidity leaving from the top of the compost pile was not recorded. However, considering the retention time of the air in the compost materials was about 32 min, the same assumption was made as de Guardia et al. (2012), which assumed the air leaving the pile was saturated with vapor. For saturated air, the vapor content ($f_{w,sa}$,kg vapor·kg^{-1} dry air) was dependent on the temperature of compost materials (T), and was calculated by following the equation suggested by de Guardia et al. (2012), shown in Eq. 5.9. The mass of dry air coming into the compost pile ($\dot{m}_{da,in}$, g·h^{-1}) is equivalent to the mass going out and can be calculated from the ideal gas law using air flow rate ($\dot{Q}_{air}$, L·min^{-1}), air pressure (P, 1 atm), the temperature of the incoming air in the bottom chamber of the composter ($T_{a,in}$, °C), and molar mass of the air

(M_{air}, 29 g·mol^{-1}). $T_{a,in}$ is assumed equal to T_{amb}. The vapor content of the air going out of the pile ($\dot{m}_{w,out}$, g·h^{-1}) was calculated from $\dot{m}_{da,in}$ and $f_{w,sa}$.

$$\dot{m}_{w,out} = \dot{m}_{da,in} \cdot f_{w,sa} = \dot{m}_{da,in} \cdot 0.00464 \cdot e^{(0.05859*T)} \quad \text{Eq. 5.9}$$

$$\dot{m}_{da,in} = \frac{\dot{Q}_{air} P}{R T_{a,in}} \cdot M_{air} \quad \text{Eq. 5.10}$$

The vapor content of air coming into the pile ($\dot{m}_{w,in}$, g·h^{-1}) can be calculated by multiplying the $\dot{m}_{w,out}$ by the average relative humidity of air entering the compost materials ($RH_{a,in}$, %), which was measured to be 54.4±5.39%.

$$\dot{m}_{w,in} = RH_{a,in} \cdot \dot{m}_{w,out} \quad \text{Eq. 5.11}$$

5.2.7.5. Heat loss from at the compost pile bottom surface (H_{btm})

Since compost materials were loaded on the steel mesh above the air chamber in the composter bottom, convective heat transfer happened on the bottom. There were two components of the convection: 1) The convection between the compost materials and the ambient air ($H_{conv,m}$, kJ·h^{-1}), and 2) The convection between the compost materials and the air going through the pile ($H_{conv,ba}$), known as the sensible heat. In this case, both terms are positive because the heat was transferred from the surrounding environment to the compost materials. The heat transfer rate can be written as:

$$H_{btm} = H_{conv,m} + H_{conv,ba} \quad \text{Eq. 5.12}$$

The calculation of $H_{conv,m}$ was different from De Guardia et al. (2012), in which the convective heat transfer was considered at the pile surface only. In the present study, the conduction inside the compost pile along the longitudinal direction was considered as part of the thermal resistance against the surface convection. The overall equation can be written as:

$$H_{conv,m} = \frac{1}{R_d + R_w + R_{ai} + R_{ao}} A_c (T - T_{amb}) \quad \text{Eq. 5.13}$$

A_c (m^2) is the cross-sectional area of the compost pile and was used as the effective contact area of the convective heat transfer. The inlet air temperature $T_{a,in}$ (°C) was assumed to be equal to T_{amb}. R_d, R_w, R_{ai} and R_{ao} were the thermal resistance (m^{2}K·W^{-1}). R_d is the resistance for dry compost materials, including woodchips, chicken mortalities, and biochar, and was calculated

from the compost materials' heights (L_{wood}, $L_{chicken}$, L_{bc}, m), the actual height of the compost pile (L_{tot}), thermal conductivities (k_{wood}=0.16, $k_{chicken}$=0.17, k_{bc}=0.13, $W \cdot m^{-1}K^{-1}$)(Datta, 2002; Siripon et al., 2007; Usowicz et al., 2016), the effective length of the longitudinal conductive heat transfer on the pile surface (L_s, m) and the pore space fraction (θ, %), shown in Eq. 5.14. The addition of biochar may not increase overall height because they fill the pore inside. Therefore, L_{tot} may not be the sum of L_{wood}, $L_{chicken}$ and L_{bc}. L_s is the thickness of compost materials to the surface between the uniform compost temperature and the ambient air temperature (discuss later).

$$R_d = \left(\frac{L_{wood}}{k_{wood}} + \frac{L_{chicken}}{k_{chicken}} + \frac{L_{bc}}{k_{bc}}\right)\left(\frac{L_s}{L_{tot}}\right)(1-\theta) \quad \text{Eq. 5.14}$$

R_w is the thermal resistance for the moisture content of compost materials and was calculated from L_s, thermal conductivity of water (k_w, 0.64 $W \cdot m^{-1}K^{-1}$)(Datta, 2002), overall moisture content of compost materials (Υ_w, %) and θ. The equation is shown as:

$$R_w = \left(\frac{L_s}{k_w}\right)\Upsilon_w(1-\theta) \quad \text{Eq. 5.15}$$

R_{ai} is the thermal resistance for air inside the compost pile and was calculated from L_s, thermal conductivity of air (k_a, 0.027 $W \cdot m^{-1}K^{-1}$)(Datta, 2002) and θ, shown as:

$$R_{ai} = \left(\frac{L_s}{k_a}\right)\theta \quad \text{Eq. 5.16}$$

R_{ao} is the thermal resistance for air outside the compost pile, and was calculated from the convective coefficient of air (h_{air}). The default h_{air} was set at 7 $W \cdot m^{-1}K^{-1}$, validated by De Guardia et al. (2012).

$$R_{ao} = \frac{1}{h_{air}} \quad \text{Eq. 5.17}$$

The calculation of $H_{conv,ba}$ is related to the sensible heat of the air, which contained the portions of vapor ($\dot{m}_{w,in}$, $g \cdot h^{-1}$, $C_{p,v}$=1.871 $kJ \cdot kg^{-1}K^{-1}$) and dry air ($\dot{m}_{da,in}$, $C_{p,da}$=1.005 $kJ \cdot kg^{-1}K^{-1}$)(de Guardia et al., 2012). The inlet air temperature $T_{a,in}$ was assumed to be equal to T_{amb}. The heat exchange rate equation can be written as:

$$H_{conv,ba} = \left(\dot{m}_{da,in} \cdot C_{p,da} + \dot{m}_{w,in} \cdot C_{p,v}\right) \cdot \left(T - T_{a,in}\right) \quad \text{Eq. 5.18}$$

5.2.7.6. Heat loss from at the compost pile top surface (H_{top})

The top surface heat transfer had similar terms as the bottom surface. The overall heat transfer rate can be written as:

$$H_{top} = H_{conv,m} - H_{conv,ta} \quad \text{Eq. 5.19}$$

$H_{conv,ta}$ is the heat transfer rate between the air flowing out of the top surface and ambient air ($kJ \cdot h^{-1}$), and it is a new term we included in addition to the method by De Guardia et al. (2012). In this case, it has the minus sign because the heat was transferred to the surrounding environment. In the case of ongoing composting, the air leaving the compost pile had a warm temperature and would heat the ambient air on the top surface, reducing the heat exchange rate between compost materials and the ambient air. The equation of $H_{conv,ta}$ ($kJ \cdot h^{-1}$) can be written as:

$$H_{conv,ta} = \left(\dot{m}_{da,in} \cdot C_{p,da} + \dot{m}_{w,out} \cdot C_{p,v}\right) \cdot (T - T_{amb}) \quad \text{Eq. 5.20}$$

5.2.7.7. Heat loss from conduction through the composter wall (H_{wall})

Heat exchange on the transverse direction through the conduction happened on the sidewall of the composter through the insulation layer between the compost material (T) and the ambient air (T_{amb}). r_{ext} (0.36 m) is the inner radius of the compost material pile, while r_{int} (0.21 m) is the outer radius of the compost composter. The difference between r_{ext} and r_{int} represents the thickness of the insulation layer ($r_{ext} - r_{int}$), which had the thermal conductivity (k_{ins}) of 0.028 $kJ \cdot m^{-1}K^{-1}h^{-1}$ (R19). L_{tot} is the height of the compost material.

$$H_{wall} = k_{ins} \cdot 2 * \pi \cdot L_{tot} * \left(\frac{T - T_{amb}}{\ln\left(\frac{r_{ext}}{r_{int}}\right)}\right) \quad \text{Eq. 5.21}$$

5.2.7.8. The daily change of compost temperature

The compost temperature was updated in a daily basis, and can be calculated as the equation below after knowing the overall heat transfer exchange rate:

$$T(t+dt) = T(t) + \frac{H_{net}(t) \cdot dt}{m_{dw} \cdot C_{p,dw} + m_{dc} \cdot C_{p,dc} + m_{dbc} \cdot C_{p,dbc} + m_w(t) \cdot C_{p,w}} \quad \text{Eq. 5.22}$$

Where $T(t+dt)$(K) is the compost temperature predicted for the next day, $T(t)$ is the compost temperature of the current day. m_{dw} (kg) and $C_{p,dw}$ (1.35 kJ·kg^{-1}K^{-1})(Anusha et al., 2011) are the dry weight and heat capacity of dry woodchips, m_{dc} and $C_{p,dc}$ (1.9 kJ·kg^{-1}K^{-1})(Siripon et al., 2007) are the dry weight and heat capacity of dry chicken, and m_{dbc} and $C_{p,dbc}$ (2.7 kJ·kg^{-1}K^{-1})(Usowicz et al., 2016) are dry biochar's dry weight and heat capacity, assuming the dry weights do not change over time. $m_w(t)$ and $C_{p,dw}$ (4.18 kJ·kg^{-1}K^{-1}) are the weight and heat capacity of water content of all the compost materials. $m_w(t)$ changed as time and cannot be calculated from $\dot{m}_{w,out}$ merely because moisture was also lost through the leaching. The water losses during each heating cycle were recorded. Assuming the rate of water loss is proportional to the vapor pressure, a trendline (R^2=0.9997) was made between the compost temperature (T) and its corresponding vapor pressure from 0 to 100 °C as Eq. 5.23. The daily moisture loss was calibrated using the temperature data from the actual measurement instead of the simulation.

$$\text{VaporPressure} = (1.58 \cdot 10^{-6}) \cdot T^3 - (8.28 \cdot 10^{-5}) \cdot T^2 + (2.59 \cdot 10^{-3}) \cdot T - 2.36 \cdot 10^{-3} \quad \text{Eq. 5.23}$$

5.2.8. Statistical analysis

The significance test was performed by one-way analysis of variance (ANOVA) and Tukey HSD test at the 5% significance level using JMP Pro 15 (SAS Institute, Cary, NC, USA).

5.3. Results and discussion

5.3.1. The physical meaning of L_s and the corresponding layer

The convection by the ambient air at the pile surface results in the temperature gradient inside the compost materials. Wang et al. (2016) mentioned the concept of virtual boundary in the compost heat transfer model. The temperature was considered uniform, and there was no heat flux within the virtual boundary or toward the inner side of the compost. L_s in this case, was the thickness of the compost material outside the virtual boundary layer. Heat was transferred

through conduction along L_s and exchanged with the ambient air on the surface through convection.

In the studies of our previous chapters, compost materials had a thickness between the center and the surface of about 23 cm. Temperature was measured in the core, and the spot at 15 cm above the core. It was found that if the compost was well mixed, the mean temperature difference between these two locations was within 3.7%, while the difference in total heat unit was only 1.1% (10800 and 9969 °C· day). Hence, we considered the compost temperatures between these two locations to be uniform and the same for the downside of the compost materials within 15 cm thickness. L_s was determined to be 8 cm, which was the difference between the compost half thickness and the thickness between the two temperature measurement locations (15 cm).

L_s can be smaller if considering the virtual boundary layer affected a larger region. The choice of a smaller L_s reduced the thermal resistance of conduction through the layer of L_s, increasing the heat lost at the pile surface, and finally, resulting in a lower simulated compost temperature. What comes with it is that the actual compost temperature should also be averaged due to the lower temperature of the virtual boundary layer.

The determination of L_s is important in our heat transfer calculation because compost materials within this layer formed a composite layer to reduce the heat loss. This is different from de Guardia et al. (2012) and Ahn et al. (2007), which assumed that the compost surface temperature was the same as the compost temperature. Therefore, the conduction effect of the compost materials was not counted in their studies. The composite layer of L_s consisted of dry wood, chicken mortality, biochar, moisture, and the air and had a pore space of 65%. Air was the most effective part of the insulation because it had the lowest thermal conductivity and largest volume. In Wang et al. (2016) and van Ginkel (1996), the porosity of the compost material was considered to increase the convective heat loss as it increased. In our case, the airflow within the compost pile was considered aligned with the height due to the aeration. On the top surface where the air was flowing out, the warmer air coming from the pile kept replacing the air above the pile surface, resulting in a weak contact between the inner compost surface to the ambient air. On the other hand, air aerated into the bottom surface contacted with the inner surface of the compost. This part of the heat exchange has been included in the calculation of the sensible heat

(Eq. 5.24), and the air would not have the chance to exchange heat with the ambient air until being emitted from the top surface.

5.3.2. Comparison between simulated and measured data

Fig. 5.1 showed the simulated temperature profiles for all treatments of the two composting experiments. The comparison between the simulated and the measured data is shown in Table 5.2. The R^2 values of the linear regression between the simulated and measured data were significantly lower during the 1st heating cycle (p<0.0001). At the same time, there was no significant difference between the values of the 2nd and 3rd heating cycles (p=0.229). On the other hand, during the 3rd heating cycle, the R^2 values of simulated treatment from Wang et al. (2021)(CHAPTER 3) were significantly lower than those from CHAPTER 4 (p=0.0066). The average RSME for all simulations was 13.5±5.08°C, indicating the average temperature difference between simulated and measured data. However, regarding the total heat unit generation, the average difference between simulation and measurement was 10.7±8.56%, indicating the average temperature difference (RSME) was around 5.3°C if the average compost temperature was 50°C. The difference in estimating RSME may indicate that the simulation changed the skewness of the real measurement. As shown in Fig. 3.1 and Fig. 4.1, more rapid increases in the compost temperature can be found after the pile turning. On the one hand, this was probably because turning refilled the air in the compost pile and broke the steady-state. The increased oxygen content can boost heat generation while a relatively higher oxygen concentration will still be observed. On the other hand, our modeling predicted the temperature increment in the next day based on the current day's value; therefore, the temperature change was always delayed. Consequently, the difference caused by skewness resulted in the pairs of a high temperature and a low temperature, thus resulting in a higher RMSE. As evidence, it happened all to the simulation results that the time taken to reach peak temperatures was 8.37±4.79 days longer than the real measurement.

Overall, the simulation of the 2nd heating cycle had the best fit regarding all the criteria mentioned in Table 5.2. The complete regression fittings are shown in Table 5.3. R^2, RMSE, the difference in the maximum temperature and total heat unit, and delay in the date of reaching the maximum temperature were 0.85±0.08, 12.6±3.17°C, 6.08±4.30°C, 7.30±4.24% and 5.44±2.19,

respectively. De Guardia et al. (2012) also reported the difference in maximum temperature in their study, and it ranged from 1.2 to 12.3 °C. All the materials were layered during the 1st heating cycle, meaning that carbon, nitrogen, and moisture were not homogenized. During the 3rd heating cycle, thermophilic bacteria maintained a high activity since the previous two heating cycles. However, primary degradation of chicken mortality and woodchips during the previous two cycles limited heat generation. Therefore, the 2nd heating cycle, with sufficient raw compost materials being well-mixed, is more suitable for further model analyses.

Fig. 5.2 indicated the heat loss proportion during the 2nd heating cycle through the sidewall, surface, and evaporation. The heat loss through the sidewall conduction accounted for 11.2 to 19.1% of total heat loss and was relatively stable in each study, with a standard deviation of less than 2%. Fig. 5.2A had a significantly higher proportion of evaporation heat loss than Fig. 5.2B (p<0.0001). The reason was the higher aeration rate applied in the study of Fig. 5.2B (1.5 $L \cdot min^{-1}$) than that of Fig. 5.2A (0.8-1.2 $L \cdot min^{-1}$). A higher aeration rate indicates stronger forced convection between the moisture in the compost pile and the air flowing through. Evaporation took away a large amount of the heat due to the latent heat, and the vapor was lost from the top surface of the compost pile. Among the two studies with different aeration rates, evaporation accounted for 30.5 to 52.1% of the total heat loss. At last, the heat loss from the surfaces, which included the loss from the sensible heat and on-surface contact, accounted for 34.1 to 51.4% of the total heat loss.

Considering similar cases of in-vessel composting, Weppen (2001) reported that evaporation counted for 35% of the total heat loss, which was similar to the case in Fig. 5.2B. However, about 60% of the heat was lost due to conduction. This was probably because the composter was enclosed, and therefore, most of the heat was lost from the composter wall. Regarding the heat loss through evaporation, Ahn et al. (2007) conducted a large scale 275 kg initial compost materials. They reported that it could vary from 17% to 54% when the aeration was changed from a low (about 0.04 $L \cdot min^{-1}kg^{-1}$ compost) level to a high level (about 0.12 $L \cdot min^{-1}kg^{-1}$). A larger conduction heat loss of (33.1%-52.6%) was reported in the same study.

5.3.3. Sensitivity of h_{bio}, h_{hair}, $T_{a,in}$ and θ

The heat generation per mole of oxygen consumed (h_{bio}) was assumed to be 440 kJ·mol^{-1} O_2. As shown in Fig. 5.3A, a decrease of h_{bio} by 20% (352 kJ·mol^{-1} O_2) decreased the total heat unit by 8.2%, while an increase of h_{bio} by 20% (528 kJ·mol^{-1} O_2) increased the total heat unit by 6.3%. The change in magnitude is smaller for a higher h_{bio} because a higher generation of heat (H_{bio}) increased the compost temperature, and meanwhile increased the heat loss from H_{eva}, H_{btm}, H_{top} and H_{ins}. The test showed a similar result to de Guardia et al. (2012), in which the same changes made to h_{bio} resulted in the peak compost temperature changing roughly around 5 °C. Since both h_{bio} and rO_2 were the only two parameters for calculating the H_{bio}. The sensitivity of h_{bio} is same for rO_2, which indicates the oxygen consumption rate of the compost materials.

The convective heat transfer coefficient of air (h_{air}) was assumed to be 7 W·m^{-2}K^{-1}. As shown in Fig. 5.3B, a decrease of h_{air} by 71% (2 W·m^{-2}K^{-1}) increased the total heat unit by 2.3%, while an increase of h_{air} by 614% (50 W·m^{-2}K^{-1}) decreased the total heat unit by 1.0%. The role of h_{air} in surface heat loss was not significant due to its much smaller thermal resistance (0.14 m^{2}K·W^{-1}) compared to that of the L_s layer (1.81 m^{2}K·W^{-1}) at 13% (v/v) mixing rate. As a comparison, de Guardia et al. (2012) indicated that a change of h_{air} at 50% resulted in roughly 5-10 °C peak temperature difference as a response. This was probably because the inner conductive resistance of compost materials was not considered in their case. However, de Guardia et al. (2012) had a different composter configuration because a lid was placed on the top of the composter. The lid decreased the heat loss of inner compost compared to the case without a lid.

The inlet air temperature from the bottom surface ($T_{a,in}$) was assumed to be equal to T_{ain}. Since the bottom space of composters was confined, the insulation provided by the composter wall could reduce the heat loss and result in a higher inlet air temperature. As shown in Fig. 5.3C, an increase of $T_{a,in}$ by 5°C increased the total heat unit by 1.5%, while an increase of $T_{a,in}$ by 10 °C increased the total heat unit by 3.0%. A higher $T_{a,in}$ reduced the loss as the air sensible heat.

The pore space porosity of L_s layer (θ) was 65% for control units. After mixing with 13% (v/v) biochar, the pore space was reduced to 52%. A decrease of θ to 26% and 5% decreased the total heat units by 6.2% and 18.0%, respectively. An increase of θ to 78% and 91% increased the total heat unit by 3.6% and 4.8%, respectively. The decrease of θ can be understood as filling the pore space with smaller particles such as biochar, soil, and sand. In the extreme case, the L_s layer can be considered a composite plate with lower thermal resistance than air-filled insulation. The corresponded conductive resistances along L_s at these θ values were plotted in Fig. 5.3E, which indicated a linear relationship. The addition of 13% (v/v) biochar with mixing decreased longitudinal conductive resistance by 12.6%. The assumption behind a high θ was that the L_s layer could still maintain a weak mixing between ambient air and the air inside the compost pile. In such a case, the improvement in heat unit becomes lower at a high θ level.

5.3.4. Biochar's impact on compost's heat profile

Fig. 5.4 demonstrates the simulation data of biochar's role in improving the compost temperature. Fig. 5.4A demonstrated the data from CHAPTER 4, while Fig. 5.4B-E demonstrated the data from Wang et al. (2021)(CHAPTER 3). Data of "Ctrl_X" and "X%WBC" were the same as those shown in Fig. 5.1. Regarding the total heat unit generation, in the study of CHAPTER 4, biochar's (wood-based) addition at 13% (v/v)("13%WBC") increased the total heat unit by 17.9% compared to the control (Fig. 5.4A). In the study of Wang et al. (2021), biochar addition at 2.6% (v/v)("2.6%WBC") increased the total heat unit by 1.64%, while 13%, 26%, and 39% (v/v) obtained a higher increase by 11.8±1.45% (Fig. 5.4B-E). For biochar addition at 2.6% (v/v), the cumulative oxygen consumption was 13.1% higher than the control. As the addition rate increased to 13%, 26%, and 39% (v/v), the cumulative oxygen consumption was 38.1% to 61.1% higher than the corresponding control. The higher oxygen consumption is an indicator of improved microbial activity. However, it is unknown if the improved microbial activity contributed to a higher compost temperature.

"Ctrl+X%WBCmix" indicates the simulations of biochar's addition into control units at different rates with thoroughly mixing but without changing the oxygen profile. The label "mix" indicates that a portion of biochar would fill into the pore space of compost materials, which was assumed to be 13% (v/v). At the rate of 2.6% (v/v)(Ctrl+2.6%WBCmix), the total heat units were reduced by 0.39%, while at the rate of 13% (v/v), the total heat units were reduced by

2.58±0.25% (Fig. 5.4A and Fig. 5.4C). As the rate increased to 39% (v/v), the total heat unit was reduced by 3.40%. Within a certain range (13% v/v in this study), biochar mixing filled the pore space of the compost materials; however, it decreased the overall thermal resistance along the longitudinal direction because it replaced the fraction or air, which had a much lower thermal conductivity. The continuous increase in the total heat loss at higher mixing rates was because, at 26% or 39% (v/v), biochar addition also increased the height of the compost pile, leading to higher conduction heat losses from the sidewall. "Ctrl+X%WBCsurface" indicates the cases in which biochar was added by layering onto the top and bottom surface without changing the oxygen profile. In this case, biochar's addition only served as an additional insulation layer. The total heat units increased by 1.29% at 2.6% (v/v) and gradually increased to 8.0% up to 39% (v/v). In these cases, adding the thickness to the surface was equivalent to increasing L_s. This will lead to increased thermal resistance against the surface heat loss so that the increased compost temperature.

Thus, in the case of mixing, biochar addition tended to increase the heat loss in our experimental cases, in which woodchips and chicken mortalities were used as the base compost materials. However, biochar's improvement in microbial activity generated more heat to increase the compost temperature. Although layering the biochar on the compost surface can also improve the compost temperature profile, its effect was 53.6±19.8% of biochar's treatment in our cases. Actually, biochar was usually thoroughly mixed with compost materials, and thereby the process was referred to as "co-composting" (Giagnoni et al., 2020). In the case of adding insulation to the outer layer, more commonly used materials can be used instead, considering biochar's high production cost.

5.4. Conclusion

A heat transfer model was constructed to simulate the compost temperature from two previous experiments, which used woodchips, chicken mortalities, and biochar as compost materials. The representative heating cycle selected for the primary simulation analyses had an average R^2 value of 0.85. Results indicated that biochar additions ranged from 2.6% to 39% increased the overall heat loss because they decreased the thermal resistance along the longitudinal direction by replacing the air insulation; the decrease was 12.6% at 13% (v/v) rate. However, biochar's ability to increase microbial activity produced more heat and increased the cumulative heat unit by

11.8%. In comparison, layering biochar outside the surface of compost material can increase the cumulative heat unit by up to 8.0% within the test range. In the future, biochar's influence on compost temperature profile can be conducted on compost materials with different configurations, such as manure, sewage sludge, wheat straw, and sawdust.

5.5. Acknowledgment

This project was supported by the United States Department of Agriculture (USDA)-National Institute of Food and Agriculture (NIFA) through a Hatch grant provided to the Agricultural and Biological Engineering Department at the University of Illinois at Urbana-Champaign (no. ILLU-741-328).

5.6. Figures and Tables

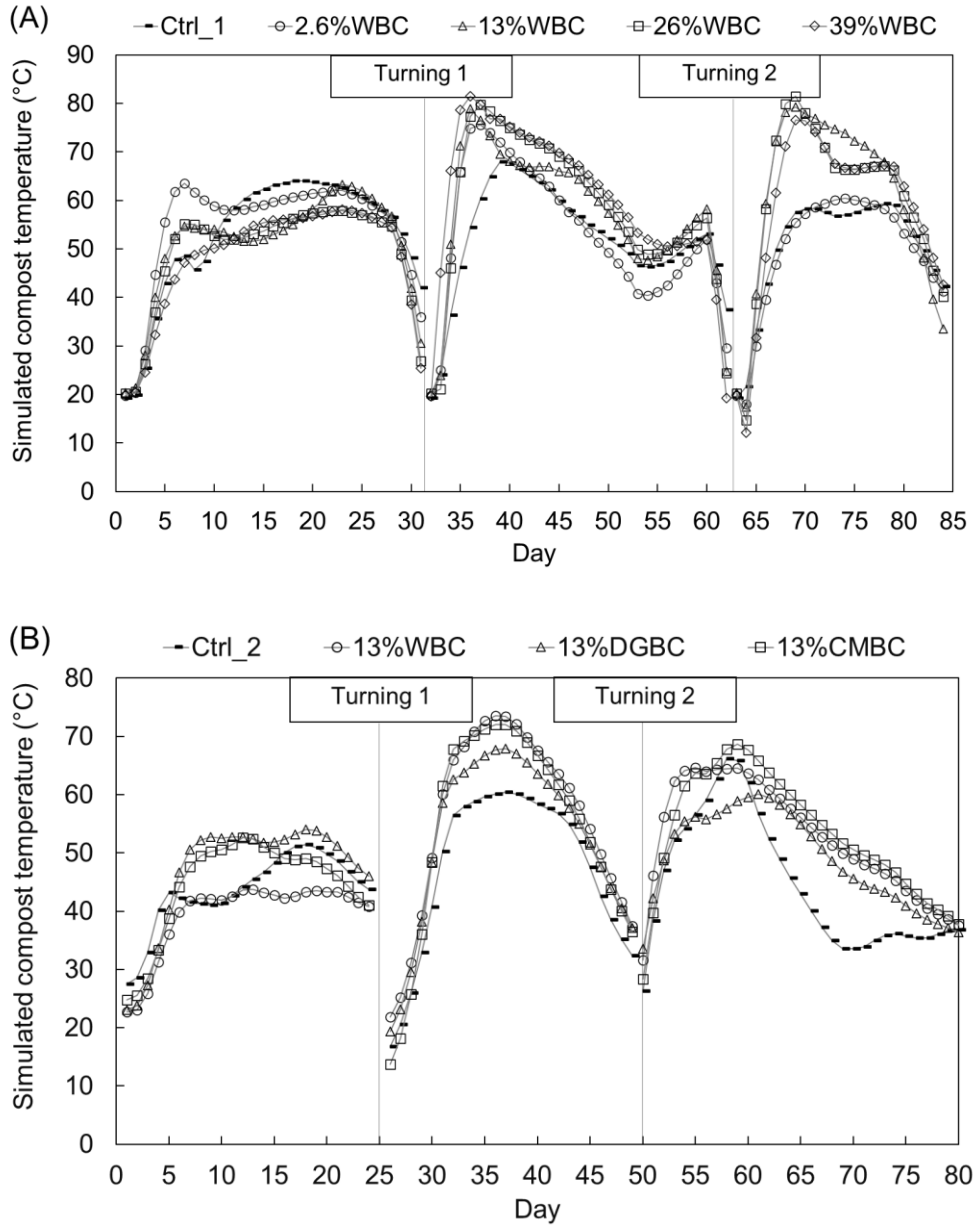

Fig. 5.1. Simulated compost temperatures as time. (A) Wood-based biochar was added at different rates ranging from 2.6% to 39% (v/v.), and (B) Biochar were made from different feedstocks and added at the same rate of 13%% (v/v) ("Ctrl": no biochar, "WBC": wood-based biochar, "DGBC": distiller grain biochar, "CMBC": cow manure biochar)

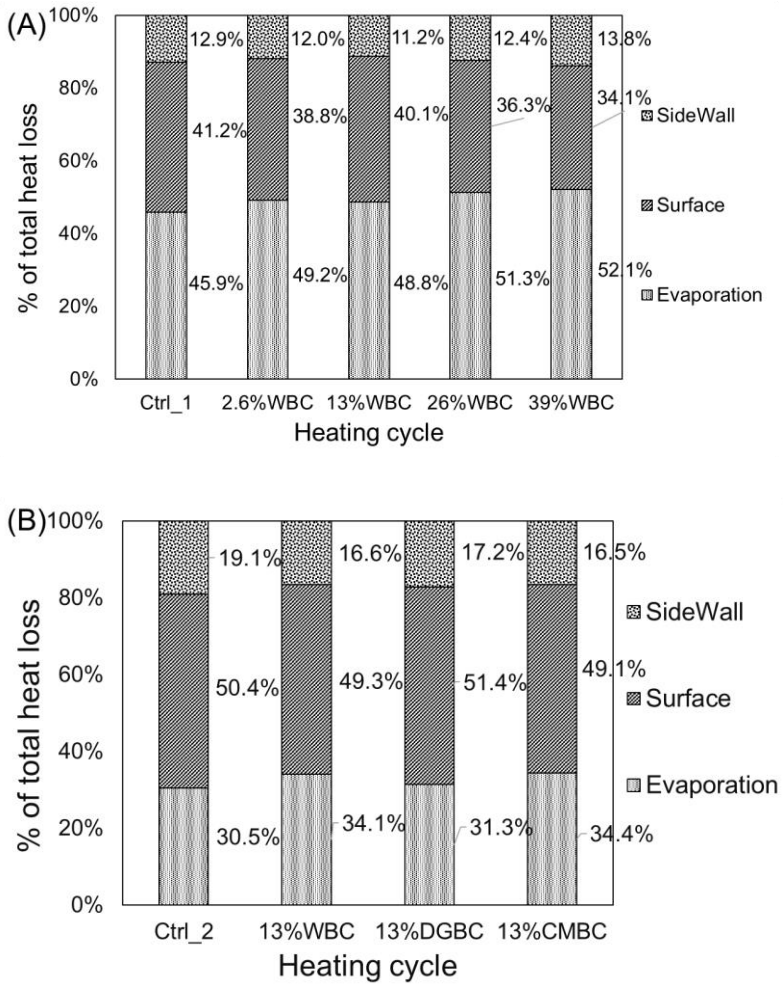

Fig. 5.2. The ratio of heat loss during the 2nd heating cycle of the two compost experiments. ("SideWall": conduction heat loss in the transverse direction through the insulated composter wall, "Surface": convection heat loss in the longitudinal direction through the top and bottom surface, "Evaporation": heat loss through the water evaporation)

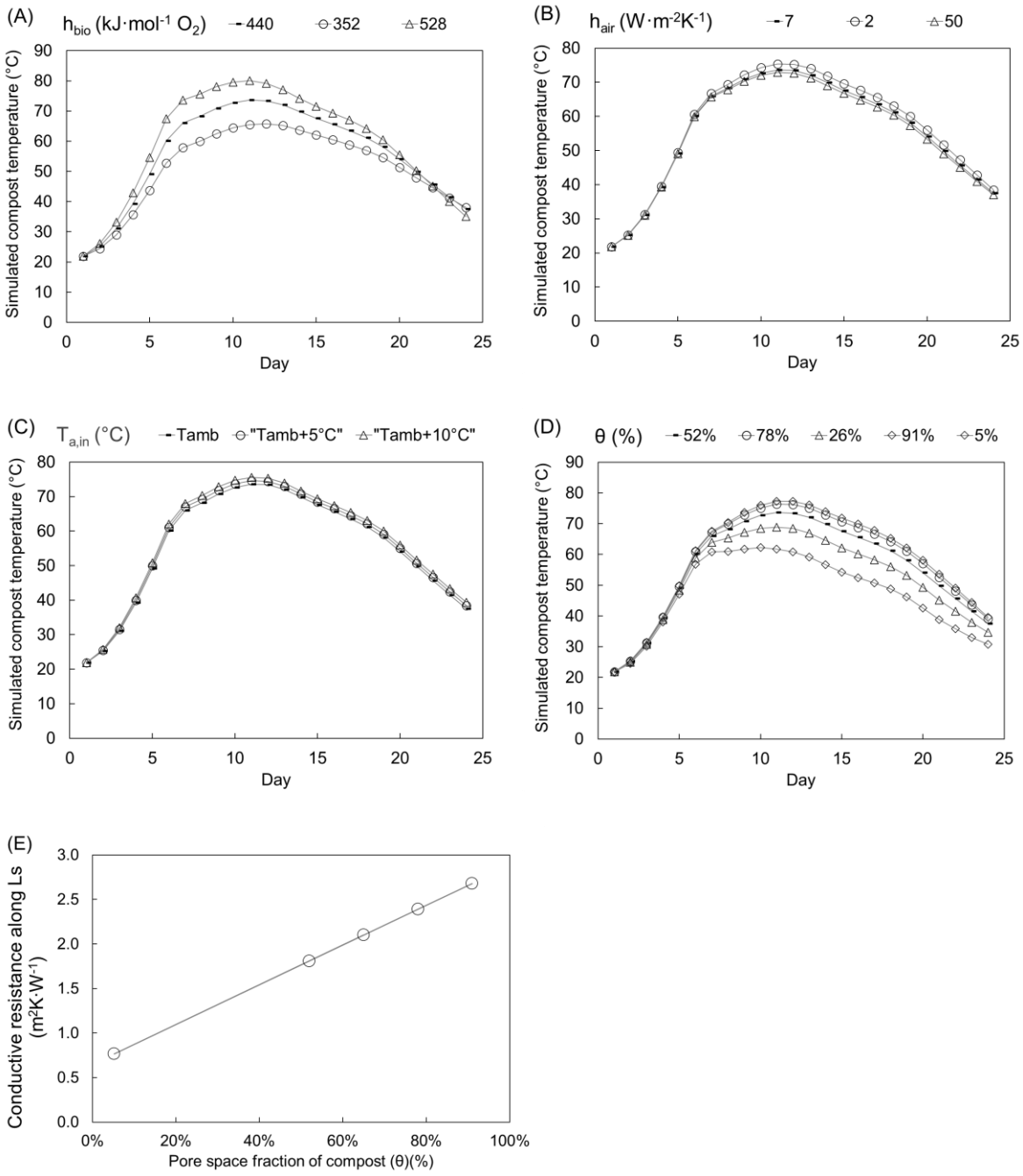

Fig. 5.3. (A)-(D) Sensitivity tests of parameters h_{bio}, h_{hair}, $T_{a,in}$ and θ, using the condition of 13% (v/v) biochar addition at the 2nd heating cycle, from CHAPTER 4, and (E) Conductive resistance along L_s (Longitudinal) as the change of pore space fraction θ.

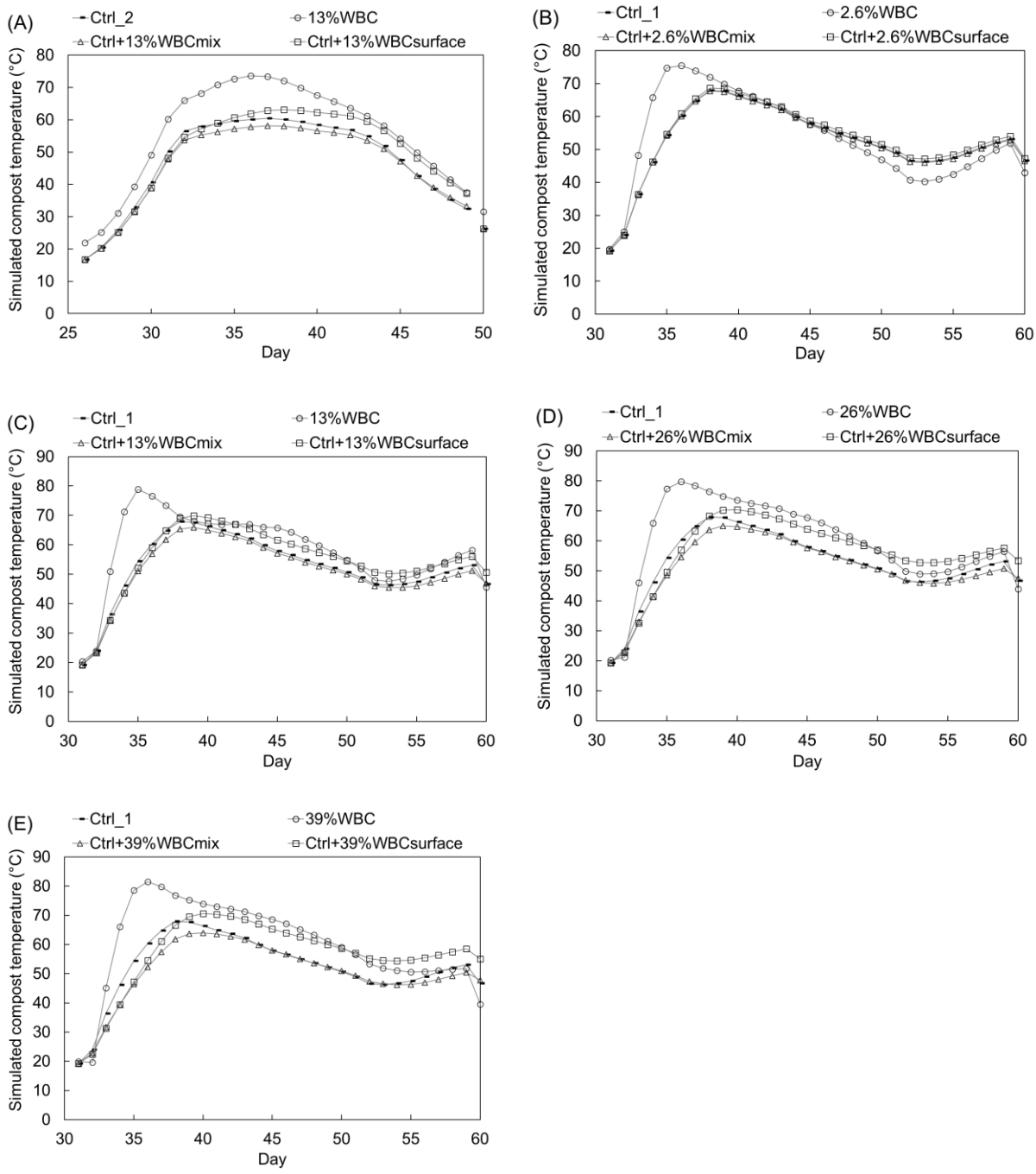

Fig. 5.4. Simulation of biochar role in improving the compost temperature. (A) from CHAPTER 4, (B)(C)(D)(E) from Wang et al. (2021)(CHAPTER 3). “Ctrl_X”: control, no biochar, same as the line in Fig. 5.1, “X%WBC”: adding X% (v/v) wood-based biochar, same as the lines in Fig. 5.1, “Ctrl+X%WBCmix”: simulation case of adding X% wood-based biochar to control and mixing thoroughly, keeping the oxygen profile of control, “Ctrl+X%WBCsurface”: simulation case of adding X% wood-based biochar to control units by layering outside the top and bottom surface, keeping the oxygen profile of control.

Table 5.1. Nomenclature

θ	Overall pore space faction of compost materials (%)
θ_{bc}	Pore space faction of biochar (%)
θ_{comp}	Pore space faction of compost without biochar (%)
$\rho_{comp,b}$	Bulk density of compost materials ($kg \cdot m^{-3}$)
$\rho_{comp,s}$	Actual density of compost materials ($kg \cdot m^{-3}$)
Υ_w	Overall moisture content of compost materials (%)
A_c	Effective contact area on the top and bottom of the composting pile (m^2)
C_{o2}	Measured oxygen concentration (%)
$C_{p,da}$	Specific heat of dry air ($kJ \cdot kg^{-1}K^{-1}$)
$C_{p,dbc}$	Specific heat of dry biochar ($kJ \cdot kg^{-1}K^{-1}$)
$C_{p,dc}$	Specific heat of dry chicken ($kJ \cdot kg^{-1}K^{-1}$)
$C_{p,dw}$	Specific heat of dry woodchips ($kJ \cdot kg^{-1}K^{-1}$)
$C_{p,v}$	Specific heat of vapor ($kJ \cdot kg^{-1}K^{-1}$)
$C_{p,w}$	Specific heat of water ($kJ \cdot kg^{-1}K^{-1}$)
$f_{w,sa}$	Vapor content in saturated gas (kg vapor$\cdot kg^{-1}$ dry air)
H_{bio}	Heat generation rate from biodegradation ($kJ \cdot h^{-1}$)
H_{btm}	Heat transfer rate from the bottom surface of the compost pile ($kJ \cdot h^{-1}$)
$H_{conv,ba}$	Heat transfer rate between compost materials and incoming air as sensible heat ($kJ \cdot h^{-1}$)
$H_{conv,ta}$	Heat transfer rate between the air flowing out of the top surface and ambient air ($kJ \cdot h^{-1}$)
$H_{conv,m}$	Heat transfer rate between compost materials and ambient air on pile surface ($kJ \cdot h^{-1}$)
H_{eva}	Heat transfer rate from water evaporation ($kJ \cdot h^{-1}$)
H_{net}	Net heat transfer rate from all aspects ($kJ \cdot h^{-1}$)
H_{top}	Heat transfer rate from the top surface of the compost pile ($kJ \cdot h^{-1}$)
H_{wall}	Heat transfer rate of conduction through the composter wall ($kJ \cdot h^{-1}$)
h_{air}	Convective heat transfer coefficient of air ($W \cdot m^{-2}K^{-1}$)
h_{bio}	Heat generation per mole of oxygen consumed ($kJ \cdot mol^{-1}$ O_2)
k_a	Thermal conductivity of air ($W \cdot m^{-1}K^{-1}$)
k_{bc}	Thermal conductivity of the biochar ($W \cdot m^{-1}K^{-1}$)
$k_{chicken}$	Thermal conductivity of the dry chicken ($W \cdot m^{-1}K^{-1}$)
k_{ins}	Thermal conductivity of the wall insulation (0.028 $kJ \cdot m^{-1}K^{-1}h^{-1}$)(R19)
k_w	Thermal conductivity of water ($W \cdot m^{-1}K^{-1}$)
k_{wood}	Thermal conductivity of the dry wood ($W \cdot m^{-1}K^{-1}$)
L_{bc}	Height of the biochar layer (m)
$L_{chicken}$	Height of the chicken layer (m)

Table 5.1. (cont.)

L_{eva}	Latent heat of evaporation (kJ·kg^{-1} water evaporated)
L_s	Thickness of compost materials to the surface in between the virtual boundary layer and the pile surface (m)
L_{tot}	Actual height of the compost pile (m)
L_{wood}	Height of the woodchips layer (m)
M_{air}	Molar mass of air (29 g·mol^{-1})
m_{dbc}	Mass of dry biochar (kg)
m_{dc}	Mass of dry chicken (kg)
m_{dw}	Mass of dry woodchips (kg)
m_w	Mass of water in composting materials (kg)
$\dot{m}_{da,in}$	Dry air mass in (g·h^{-1})
$\dot{m}_{w,in}$	Mass of water in the air coming in (g·h^{-1})
$\dot{m}_{w,out}$	Mass of water in the air coming out (g·h^{-1})
P	Standard air pressure, 1 atm
$\dot{Q}_{air}$	Air pump aeration rate (L·min^{-1})
R	Ideal gas law constant, 0.0821 atm·L·mol^{-1}·K^{-1}
R_{ai}	Thermal resistance of air inside the compost pile (m^{2}K·W^{-1})
R_{ao}	Thermal resistance of air outside the compost pile (m^{2}K·W^{-1})
R_d	Overall thermal resistance of dry compost materials including woodchips, chicken mortalities, and biochar (m^{2}K·W^{-1})
R_w	Thermal resistance of the moisture content of compost materials (m^{2}K·W^{-1})
$RH_{a,in}$	Relative humidity of the air in the bottom chamber of the composter (%)
r_{ext}	External radius of the insulation wall, 0.36 m
r_{int}	Internal radius of the insulation wall, 0.21 m
rO_2	Oxygen consumption rate (mol O_2·h^{-1})
T	Composting pile temperature (°C)
T_{amb}	Ambient air temperature (°C)
$T_{a,in}$	Air temperature in the bottom chamber of the composter (°C)

Table 5.2. R^2 of linear regression equations, root-mean-square deviation (RMSE), and the difference in maximum temperatures and total heat units between values from simulations versus actual measurements.

	Examinations	Heating cycle 1	Heating cycle 2	Heating cycle 3
Ctrl_1	R^2	0.139	0.700	0.351
	RMSE	15.3	17.2	19.7
	Max. Temp. Diff. (°C)	3.92	3.71	0.54
	Total heat unit Diff. (%)	20.0	10.0	11.8
	Max. Temp. Day Diff.	13	6	7
2.6%WBC	R^2	0.536	0.9071	0.620
	RMSE	12.7	15.6	19.2
	Max. Temp. Diff. (°C)	0.99	7.56	4.21
	Total heat unit Diff. (%)	22.0	10.7	4.77
	Max. Temp. Day Diff.	18	4	9
13%WBC	R^2	0.362	0.912	0.6842
	RMSE	10.36	15.6	25.3
	Max. Temp. Diff. (°C)	1.73	8.15	20.1
	Total heat unit Diff. (%)	9.35	14.9	32.9
	Max. Temp. Day Diff.	17	3	4
26%WBC	R^2	0.450	0.921	0.499
	RMSE	8.80	14.1	23.6
	Max. Temp. Diff. (°C)	7.90	8.05	23.9
	Total heat unit Diff. (%)	3.75	6.10	26.0
	Max. Temp. Day Diff.	17	3	4
39%WBC	R^2	0.315	0.901	0.483
	RMSE	10.3	12.2	23.7
	Max. Temp. Diff. (°C)	8.32	9.02	19.3
	Total heat unit Diff. (%)	0.15	7.48	19.7
	Max. Temp. Day Diff.	17	3	3
Ctrl_2	R^2	0.230	0.824	0.886
	RMSE	11.6	7.99	7.63
	Max. Temp. Diff. (°C)	11.6	4.88	10.74
	Total heat unit Diff. (%)	19.2	4.8	11.1
	Max. Temp. Day Diff.	13	8	7
13%WBC	R^2	0.248	0.799	0.753
	RMSE	13.42	10.67	8.52
	Max. Temp. Diff. (°C)	21.8	4.04	0.78
	Total heat unit Diff. (%)	19.2	2.70	10.4
	Max. Temp. Day Diff.	7	7	4

Table 5.2. (cont.)

	Examinations	Heating cycle 1	Heating cycle 2	Heating cycle 3
13%DGBC	R^2	0.162	0.773	0.923
	RMSE	10.5	9.90	7.80
	Max. Temp. Diff. (°C)	9.86	0.82	3.72
	Total heat unit Diff. (%)	1.18	3.7	2.5
	Max. Temp. Day Diff.	13	8	10
13%CMBC	R^2	0.212	0.898	0.945
	RMSE	9.67	10.07	11.86
	Max. Temp. Diff. (°C)	9.46	3.04	6.85
	Total heat unit Diff. (%)	6.7	0.5	11.6
	Max. Temp. Day Diff.	6	7	8

Table 5.3. Regression fittings with equations

	Heating cycle 1	Heating cycle 2	Heating cycle 3
Ctrl_1	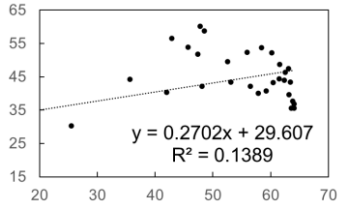	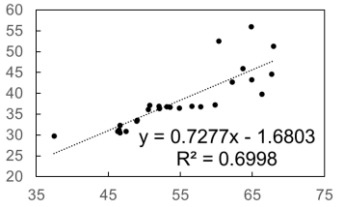	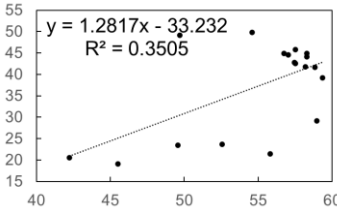
2.6% WBC	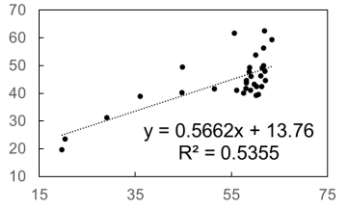	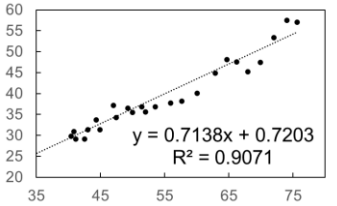	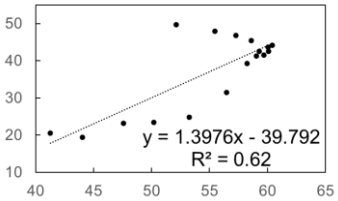
13% WBC	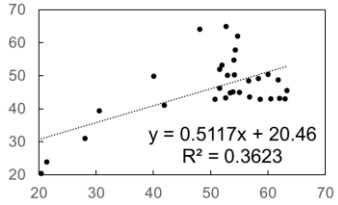	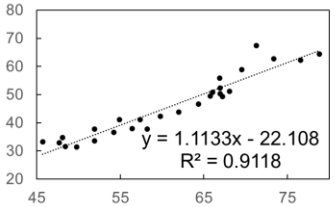	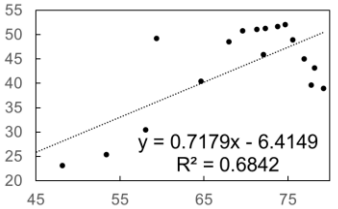
26% WBC	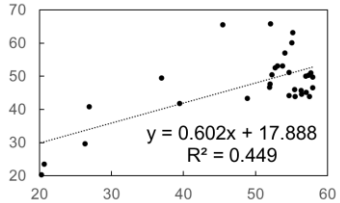	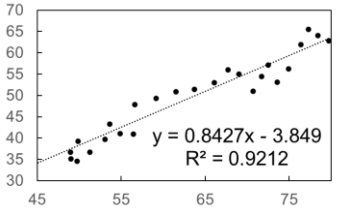	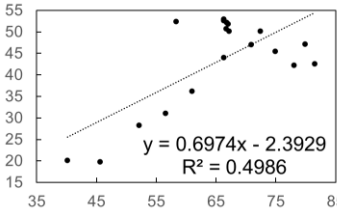
39% WBC	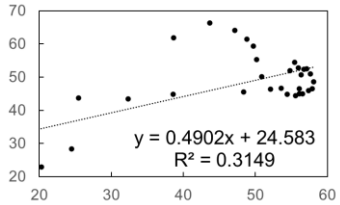	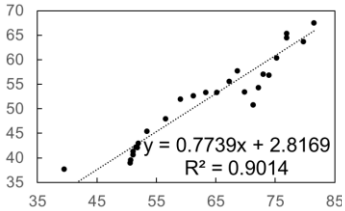	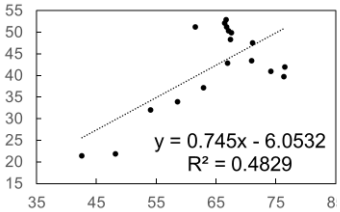
Ctrl_2	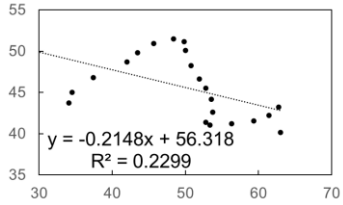	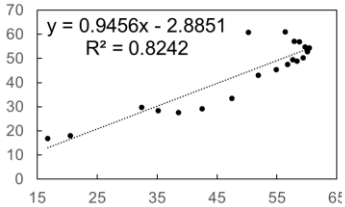	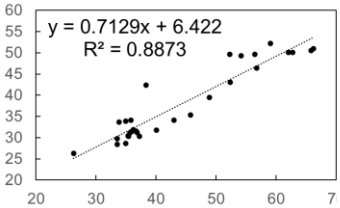
13% WBC	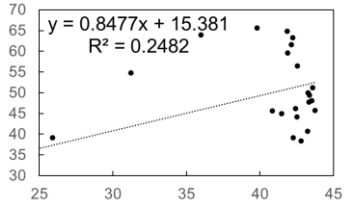	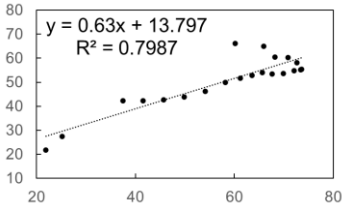	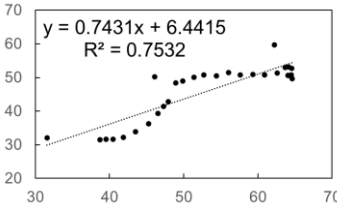

Table 5.3. (cont.)

	Heating cycle 1	Heating cycle 2	Heating cycle 3
13% DGBC	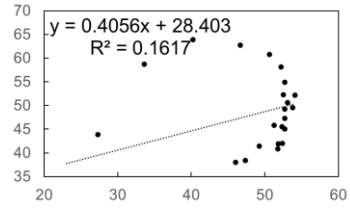	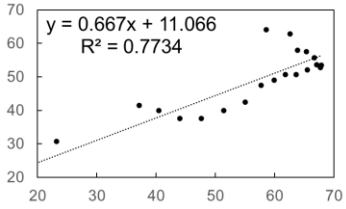	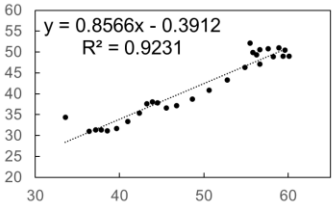
13% CMBC	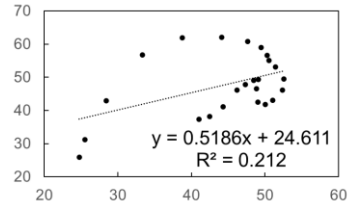	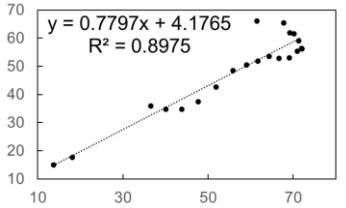	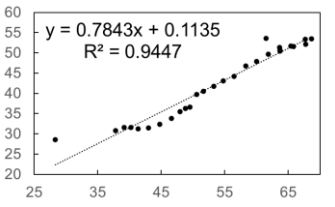

CHAPTER 6

CROP GROWTH USING POULTRY MORTALITIES CO-COMPOSTED WITH BIOCHARS

6.1. Introduction

Adding biochar to composting process can bring multiple benefits such as increasing microbial activity, increasing compost temperature, enhancing water holding capacity, and reducing nutrient losses by leaching (Yuchuan Wang et al., 2019). In some previous studies, the finished compost was called COMBI (Agegnehu et al., 2017; Yuchuan Wang et al., 2019). COMBI is different from the mixture of biochar and mature compost because biochar was added from the beginning and went through the entire composting process. During the process, aging can happen to fresh biochar particles and grant them organic coatings, making the biochar more hydrophilic and enabling better retention ability of essential nutrients such as N (Hagemann, Joseph, Schmidt, Kammann, Harter, Borch, Young, Varga, Taherymoosavi, Elliott, et al., 2017). Therefore, COMBI is expected to combine the benefits of individual compost and biochar and bring extra benefits to the soil and plant growth.

Nevertheless, the effect of COMBI to plant growth has not been widely studied yet. Wang et al. (2019) conducted a meta-analysis of COMBIs' effect to plant growth on 14 existing articles of 233 observations. Although COMBI increased plant productivity by 22.8% in general, the authors suggested more studies were still needed to obtain more solid analysis results (Yuchuan Wang et al., 2019). The investigation of COMBI's effect can have many variations due to the difference in its making, such as the biochar type, dosing rate, compost type, COMBI application rate, and plant type. As one part of the category, COMBI produced from the animal mortality composting has never been studied. Fortunately, COMBI from animal mortality composting has been generated from the author's previous study. Compared to the control without any biochar, adding biochars made from wood pallets, distillers grains, and cow manure to the poultry mortality composting at the 13% rate (by volume) significantly increased the nitrogen content by 33%-92%. The objective of this study is to investigate if the application of COMBI from poultry mortality with different types of co-composted biochars can increase crop productivity and nutrient contents.

6.2. Material and methods

6.2.1. Compost materials and the soil

The making process of mature compost was mentioned in CHAPTER 4. Composting materials included woodchips, chicken mortalities, and biochar. There were four kinds of composts, differentiated by the addition of biochar, including no biochar (Ctrl), wood-based biochar (WBC), distillers grain biochar (DGBC), and cow manure biochar (CMBC). All mature composts were mixed thoroughly within the same treatment. Hard pieces like bones and large woodchips were manually removed. After that, composts were ground and screened by a 3.35 mm sieve. Pulverized topsoil was collected from the Landscape Recycling Center at Urbana, Illinois, and screened through a 2 mm sieve to remove larger particles. The ground composts were mixed with soil at 10% (w/w)(30% v/v). The final mixtures were named "Ctrl-COMP", "WBC-COMP", "DGBC-COMP", and "CMBC-COMP".

6.2.2. Plant growth experiment

Buttercrunch lettuce (*Lactuca sativa* var. capitata) was grown under five different treatments, named "Soil", "Ctrl-COMP", "WBC-COMBI", "DGBC-COMBI", and "CMBC-COMBI". There were six replicates for each treatment. Initially, three lettuce seeds were sowed into 30 rockwool cubes, which were placed inside a container with water to maintain the moisture. For the first 2-4 days, the container was capped, and its inside temperature was maintained at room temperature to allow the seeds to germinate. After that, shoots in the cube were thinned to one with the best growth condition. The container with cubes was placed under the light at 200 $\mu mol \cdot m^{-2} \cdot s^{-1}$ for 16 h daily to allow further growth of the shoots. After another ten days, 24 cubes with the best growth condition were transferred to twenty-four 1 L pots, filled with "Soil", "Ctrl-COMP", "WBC-COMBI", "DGBC-COMBI", and "CMBC-COMBI". All pots were placed under the light at 200 $\mu mol \cdot m^{-2} \cdot s^{-1}$ for 16 h daily for four weeks to allow the complete growth of lettuce.

During the four-week growth period, each lettuce was applied with about 2.5 g of commercial fertilizer (8-15-36 for N-P-K) and equivalent mineral fertilizer (2% N, 3.2% Ca, 1.2% Mg, and 0.1% Fe). All soils were watered to field capacity once moisture of any pot dropped to 60%.

6.2.3. Measurements

Temperature and moisture were monitored by the DHT11 Temperature Humidity Sensor (HiLetgo Technology Co., Ltd). The moisture contents of 3 pots per treatment were recorded. Each pot was inserted with one soil moisture sensor, and soil moisture was measured by the HOBOnet Soil Moisture EC-5 Sensor (Onset, MA). All sensors were programmed and connected to Arduino Mega R3 boards (Somerville, MA, US). The calibrations of the moisture sensors to the water content of the soils are shown in Fig. 6.3.

For different soil mixtures, ash contents were measured by heating the sample at 550 °C for two hours using a muffle furnace (Barnstead Thermolyne F6000, MN). For pH and electrical conductivity (EC), samples were mixed with deionized water at 1:10 w/w (TMECC, 2002) and measured by PC100 pH/Conductivity meter (Cole Parmer, IL). Water holding capacity was measured by saturating samples with water for at least one day, followed by the draining of excess water. Wet samples were weighed and dried. Water holding capacity was calculated based on the change of water mass after the drying and the dry sample weight in g water of initial dry weight in (g water $\cdot g^{-1}$ dry weight).

Leaf chlorophyll was measured one day before the harvest using MC-100 Chlorophyll Concentration Meter (Apogee Instruments, Inc., UT). Within each pot, three leaves were measured, and readings were averaged into one. Three leave samples (1-2 g) were taken from the lettuce in each pot during the harvest period. They were ground and mixed before the chemical analyses. The harvested fresh lettuces were measured for their growth index. Roots were thoroughly washed to remove the soil. The dry weights were measured by drying the sample at 105°C for one day (Quincy Lab Inc, IL). Ash contents were measured by heating the sample at 550 °C for two hours using a muffle furnace (Barnstead Thermolyne F6000, MN).

Soluble sugar was measured, referring to Salehi et al. (2016). 1 g grounded lettuce leaf sample was mixed with 20 ml distilled water and heated at 100 °C for one hour in the water bath. Samples were then filtered. 0.5 ml supernatant was taken and mixed with 1.5 ml distilled water and 0.5 ml anthrone solution (1 g anthrone in 50 ml ethyl acetate), and 5 ml concentrated H_2SO_4. The solution was placed in a 100 °C water bath for 1 min. After cooling down, the optical

density value was measured using the spectrophotometer (DR 3900, Hach, DO) at 630 nm. The soluble sugar calibration curve is shown in Fig. 6.4.

Nitrate content was measured referring to Liu et al. (2016). 1 g leaf sample was grounded in every 6 ml liquid. 0.2 ml supernatant was mixed with 0.8 ml 5% (w/v) salicylic acid in concentrated H_2SO_4. After 20 min, 19 ml 2N NaOH was added to raise the pH of the test solution to 12. The final solution was cooled down and measured under the wavelength of 410 nm using the spectrophotometer (DR 3900, Hach, DO). The nitrate calibration curve is shown in Fig. 6.5.

Crude fiber content was measured referring to Chen and Yang (2018). Leaf samples were mixed with 1.25% H_2SO_4 and boiled for 30 min. The liquid portion was drained and replaced with 1.25% NaOH with another 30 min boiling. Again, the liquid portion was drained, and the sample was washed with deionized water. The remaining solid sample was heated using the muffle furnace at 600 C for 30 min, and the final weight was recorded as the crude fiber content.

Finally, soil samples and ground dry lettuce samples were sent to Midwest Laboratories (Omaha, Nebraska) to analyze physicochemical characteristics. Physicochemical characteristics of the soil are as follows: ash content 88.6± 0.09% dw, pH 7.57±0.06, conductivity 0.29±0.03 mS/cm, total N 0.47±0.05% dw, organic N 0.46±0.05% dw, C:N ratio 15.7±4.73% dw, P as P_2O_5 0.21±0.04% dw, K as K_2O 0.31±0.02% dw, S 0.08±0.02% dw, Ca 4.63±1.19% dw, Na 0.07±0.00% dw, Mg 1.33±0.45% dw, Fe 198550±4445 ppm, Cu 58.3±31.3 ppm, Zn 80.3±6.43 ppm, Mn 899±513 ppm. Physicochemical characteristics of composts are shown in Table 6.3.

6.2.4. Statistical analysis

All results were analyzed by JMP (SAS Institute, Cary, NC, USA) using the one-way analysis of variance (ANOVA) and Tukey HSD test at the 5% significance level. Log-transform was applied to data with skewed distribution.

6.3. Result and discussion

Temperature and relative humidity were kept at around 22°C and 56% most of the time (Fig. 6.1). Photos of all pots during the day of harvest are shown in Fig. 6.2.

Table 6.1 indicate the physicochemical characteristic of different soil mixtures. Compared to the soil, composts had higher total and organic nitrogen contents, organic matter content, EC, and water holding capacity (p<0.0001 for all), and lower ash content and bulk density (p<0.0001 for both). The pH of soil mixtures with compost was slightly decreased (p<0.0001). However, it was maintained within the neutral level, and the difference was within 6%. The increased water holding capacity (29% to 34%) indicated that compost could help mitigate the drought and retain more water-soluble nutrients. Biochar influence was not significant probably because of its low rate (3.9%) in the soil mixture.

Table 6.2 indicates the final growth and quality indices and micro/macro nutrient and heavy metal contents of harvested lettuce. Regarding the growth indices, although "CMBC-COMBI" significantly increased the lettuce height by 10% (p=0.007), there was no significant difference between the different treatments in diameter (p=0.209), dry shoot weight (p=0.164), shoot ash content (p=0.481) and dry root weight (p=0.417). Regarding the quality indices, "WBC-COMBI" significantly increased the crude fiber content by 85.8% compared to "Soil" (p=0.0005). Compared to "Ctrl-COMP", "WBC-COMBI" and "DGBC-COMBI" significantly decreased the leaf nitrate content by 26.8% and 34.1%, respectively (p=0.01). A lower nitrate level indicates a reduced amount of nitrite that can be formed. Although nitrate is relatively unharmful to humans, its conversion to nitrite by the salivary enzymes and oral bacteria brings risks such as gastric and bladder cancers (Colla et al., 2018). Regarding the micro/macro nutrient and heavy metal contents. "WBC-COMBI" and "DGBC-COMBI" had significantly lower leaf N content compared to other treatments (p<0.001). Considering stoichiometry, up to 87% of N might be attributed to the nitrate content (Buchholz, 1993). Besides, "DGBC-COMBI" and "CMBC-COMBI" increased the P content from "Soil" by 20.3% and 29.7%, respectively (p=0.0036). Regarding alkaline metal elements, there were variations in Mg and Na. For "Ctrl-COMP" and "CMBC-COMBI", the Na contents were significantly higher than those in other treatments (p<0.001). High sodium content can adversely affect plant growth because it increases soil salinity (Saifullah et al., 2018). Although many previous studies reported that biochar addition could remediate salt-affected soils (Chaganti and Crohn, 2015; Lashari et al., 2015), biochar addition can also aggravate the salt concern because some of them can be high in salinity (Saifullah et al., 2018). However, the inhibition caused by the salinity was not significantly indicated. A significant difference in leave samples among different treatments was found for Fe,

Mn, Cu, and Zn for other metal contents. Their contents in the soil mixture may be the reason for the significance (Ferri et al., 2012; Peralta-Videa et al., 2009; Zhou et al., 2016).

6.4. Conclusion

We tested COMBI's effect on lettuce growth. The COMBI used in this study was produced from chicken mortalities. To produce COMBI, wood-based biochar, distiller grain biochar, and cow manure biochar were added as co-composting materials. Adding composts to soil increased its water holding capacity by 29% to 34%. However, biochar did not significantly increase the water holding capacity. Lettuce yield was not inhibited by adding composts. The use of COMBI made from wood-based biochar and distillers grain biochar significantly reduced the nitrate content in lettuce leaves by 26.8% and 34.1%, respectively. Lettuce's essential metal content can be influenced because mixing soil with compost changes their concentration profiles.

6.5. Acknowledgment

This project was supported by the United States Department of Agriculture (USDA)-National Institute of Food and Agriculture (NIFA) through a Hatch grant provided to the Agricultural and Biological Engineering Department at the University of Illinois at Urbana-Champaign (no. ILLU-741-328).

6.6. Figures and Tables

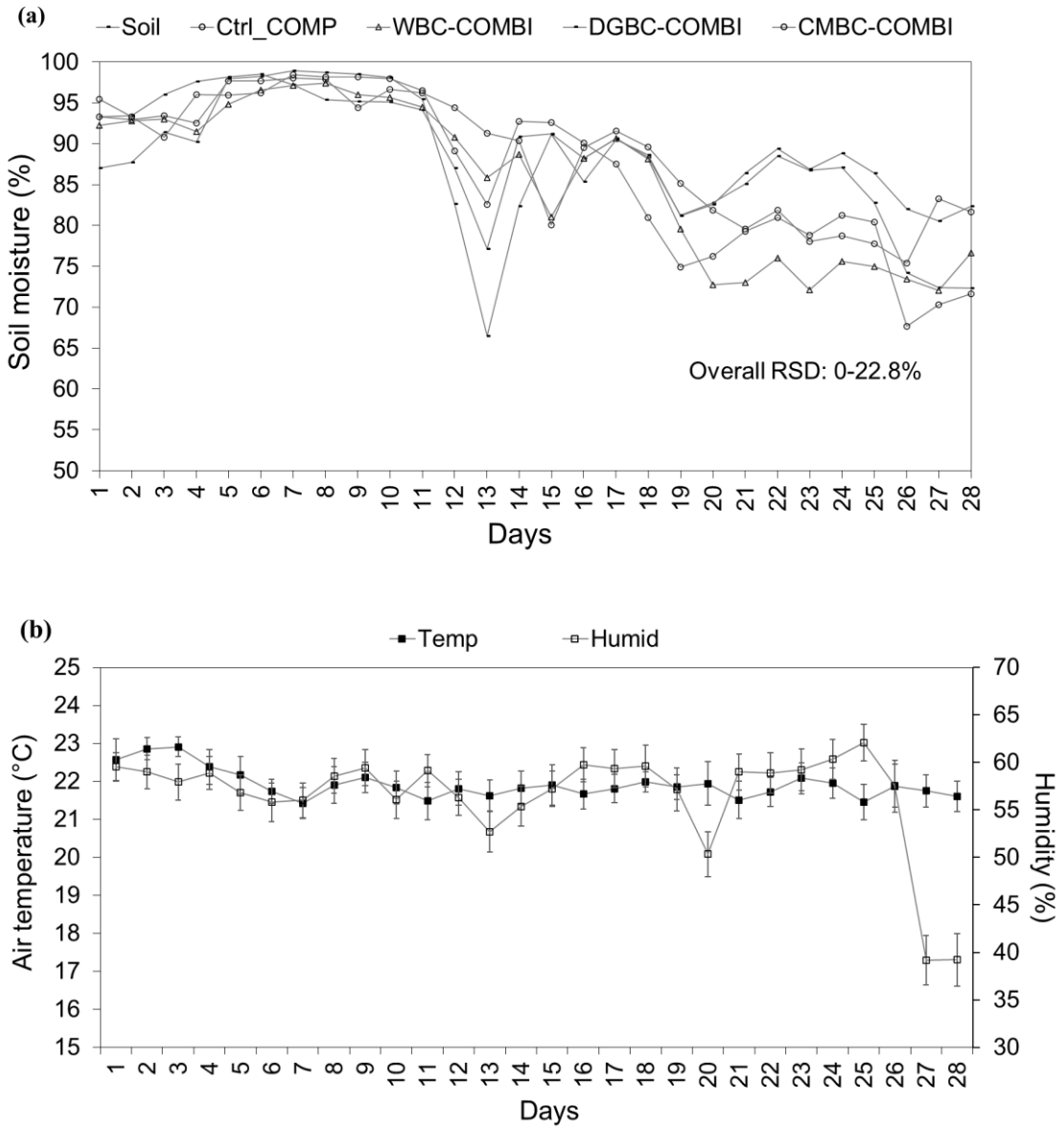

Fig. 6.1. Soil moisture as time (each treatment had three replicates, shown in averages) (a), air temperature, and humidity as time (b). ("Soil": soil only, "Ctrl-COMP": soil + combi without biochar, "WBC-COMBI": soil + combi with wood-based biochar, "DGBC-COMBI": soil + combi with distillers grain biochar, "CMBC-COMBI": soil + combi with cow manure biochar)

Soil

Ctrl-COMP

WBC-COMBI

DGBC-COMBI

CMBC-COMBI

Fig. 6.2. Lettuce before harvesting. (“Soil”: soil only, “Ctrl-COMP”: soil + combi without biochar, “WBC-COMBI”: soil + combi with wood-based biochar, “DGBC-COMBI”: soil + combi with distillers grain biochar, “CMBC-COMBI”: soil + combi with cow manure biochar)

Table 6.1. Physicochemical characteristics of different soil mixtures. ("Soil": soil only, "Ctrl-COMP": soil + combi without biochar, "WBC-COMBI": soil + combi with wood-based biochar, "DGBC-COMBI": soil + combi with distillers grain biochar, "CMBC-COMBI": soil + combi with cow manure biochar)

	Soil	**Ctrl-COMP**	**WBC-COMBI**	**DGBC-COMBI**	**CMBC-COMBI**
Ash (%)	85.1 ± 1.23 ^{A}	75.9 ± 0.85 ^{D}	77.8 ± 0.66 ^{C}	76.5 ± 0.78 ^{CD}	80.1 ± 0.92 ^{B}
pH	7.58 ± 0.03 ^{A}	7.22 ± 0.02 ^{C}	7.20 ± 0.03 ^{C}	7.20 ± 0.01 ^{C}	7.36 ± 0.01 ^{B}
EC (mS/cm)	0.96 ± 1.70 ^{D}	1.70 ± 0.05 ^{B}	1.56 ± 0.02 ^{C}	1.67 ± 0.02 ^{B}	1.78 ± 0.01 ^{A}
Bulk density (kg/m^3)	0.84 ± 0.04 ^{A}	0.61 ± 0.04 ^{C}	0.75 ± 0.01 ^{B}	0.73 ± 0.01 ^{B}	0.75 ± 0.02 ^{B}
Water holding capacity (g water/g dw)	0.69 ± 0.05 ^{B}	0.90 ± 0.08 ^{A}	0.89 ± 0.05 ^{A}	0.92 ± 0.04 ^{A}	0.89 ± 0.03 ^{A}

Within each row, means that are not connected by the same letter are significantly different (P<0.05).

Table 6.2. Final growth and quality indices, and micro/macro nutrient and heavy metal contents of lettuce's leaves. ("Soil": soil only, "Ctrl-COMP": soil + combi without biochar, "WBC-COMBI": soil + combi with wood-based biochar, "DGBC-COMBI": soil + combi with distillers grain biochar, "CMBC-COMBI": soil + combi with cow manure biochar)

	Soil	**Ctrl-COMP**	**WBC-COMBI**	**DGBC-COMBI**	**CMBC-COMBI**
Height (cm)	21.6 ± 1.10 ^{B}	22.3 ± 0.73 ^{AB}	22.1 ± 0.66 ^{B}	22.3 ± 0.36 ^{AB}	23.8 ± 1.56 ^{A}
Diameter (cm)	34.3 ± 1.64 ^{A}	34.4 ± 1.77 ^{A}	32.9 ± 2.10 ^{A}	31.7 ± 3.89 ^{A}	33.6 ± 4.19 ^{A}
Dry shoot weight (g)	4.49 ± 0.10 ^{A}	4.09 ± 0.50 ^{A}	4.56 ± 0.50 ^{A}	4.20 ± 0.34 ^{A}	3.71 ± 0.23 ^{A}
Shoot ash (%)	28.4 ± 4.06 ^{A}	26.5 ± 5.77 ^{A}	24.9 ± 2.98 ^{A}	25.3 ± 3.09 ^{A}	23.0 ± 5.46 ^{A}
Dry root weight (g)	0.62 ± 0.22 ^{A}	0.49 ± 0.12 ^{A}	0.59 ± 0.13 ^{A}	0.59 ± 0.10 ^{A}	0.48 ± 0.12 ^{A}
Chlorophyll ($nmol \cdot cm^{-2}$)	351 ± 26.7 ^{A}	351 ± 35.4 ^{A}	364 ± 28.0 ^{A}	402 ± 65.3 ^{A}	349 ± 37.4 ^{A}
Soluble sugar (% dw)	71.8 ± 5.54 ^{A}	74.2 ± 10.2 ^{A}	55.5 ± 7.0 ^{A}	54.5 ± 13.3 ^{A}	68.3 ± 7.19 ^{A}
Crude fiber (% dw)	3.05 ± 0.8 ^{B}	2.48 ± 0.4 ^{B}	5.66 ± 0.3 ^{A}	4.26 ± 1.7 ^{AB}	3.51 ± 1.1 ^{B}
NO_3^- (% dw)	22.0 ± 5.48 ^{AB}	29.6 ± 5.97 ^{A}	16.1 ± 1.20 ^{B}	14.5 ± 4.11 ^{B}	25.0 ± 11.1 ^{AB}
N (% dw)	5.70 ± 0.09 ^{A}	5.63 ± 0.07 ^{A}	5.29 ± 0.13 ^{B}	5.37 ± 0.08 ^{B}	5.75 ± 0.08 ^{A}
P (% dw)	0.53 ± 0.04 ^{C}	0.62 ± 0.02 ^{ABC}	0.55 ± 0.02 ^{BC}	0.63 ± 0.06 ^{AB}	0.68 ± 0.03 ^{A}
K (% dw)	10.5 ± 0.48 ^{A}	10.9 ± 0.91 ^{A}	10.5 ± 0.32 ^{A}	9.95 ± 0.38 ^{A}	10.4 ± 0.47 ^{A}
B (ppm)	38.3 ± 2.08 ^{A}	41.3 ± 3.21 ^{A}	35.7 ± 1.53 ^{A}	37.0 ± 2.65 ^{A}	35.3 ± 2.52 ^{A}
S (% dw)	0.29 ± 0.02 ^{A}	0.33 ± 0.01 ^{A}	0.29 ± 0.02 ^{A}	0.29 ± 0.02 ^{A}	0.31 ± 0.02 ^{A}
Ca (% dw)	1.04 ± 0.04 ^{A}	0.96 ± 0.50 ^{A}	0.98 ± 0.04 ^{A}	1.13 ± 0.08 ^{A}	0.94 ± 0.06 ^{A}
Na (% dw)	0.37 ± 0.02 ^{C}	0.53 ± 0.04 ^{B}	0.39 ± 0.02 ^{C}	0.43 ± 0.02 ^{C}	0.63 ± 0.04 ^{A}
Mg (% dw)	0.41 ± 0.02 ^{AB}	0.47 ± 0.03 ^{A}	0.39 ± 0.02 ^{B}	0.44 ± 0.03 ^{AB}	0.38 ± 0.02 ^{B}
Fe (ppm)	115 ± 2.00 ^{A}	104 ± 8.89 ^{AB}	86.0 ± 12.3 ^{B}	86.0 ± 7.94 ^{B}	84.7 ± 6.51 ^{B}
Cu (ppm)	9.67 ± 1.15 ^{A}	8.00 ± 0.00 ^{B}	7.67 ± 0.58 ^{B}	7.00 ± 0.00 ^{B}	7.00 ± 0.00 ^{B}
Zn (ppm)	94.0 ± 5.57 ^{C}	137 ± 10.3 ^{A}	108 ± 4.73 ^{BC}	95.0 ± 7.00 ^{C}	115 ± 7.55 ^{B}
Mn (ppm)	33.3 ± 2.52 ^{A}	29.0 ± 1.73 ^{AB}	28.0 ± 2.00 ^{AB}	27.0 ± 2.00 ^{B}	26.7 ± 2.08 ^{B}

Within each row, means that are not connected by the same letter are significantly different ($P<0.05$).

6.7. Appendix

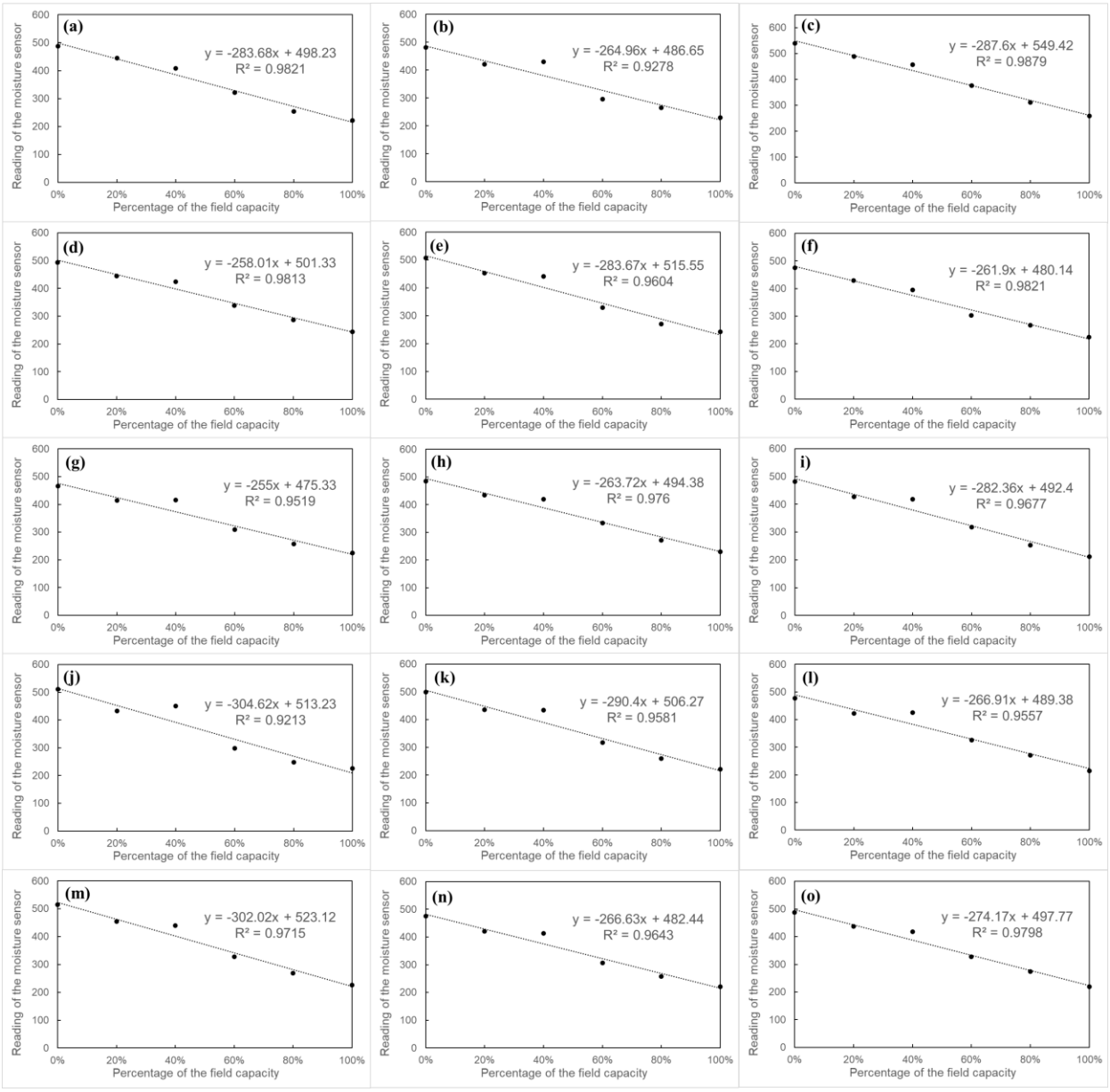

Fig. 6.3. Moisture sensor calibration. (a-c: Soil, d-f: Ctrl-COMP, g-i: WBC-COMBI, j-l: DGBC-COMBI, and m-o: CMBC-COMBI)

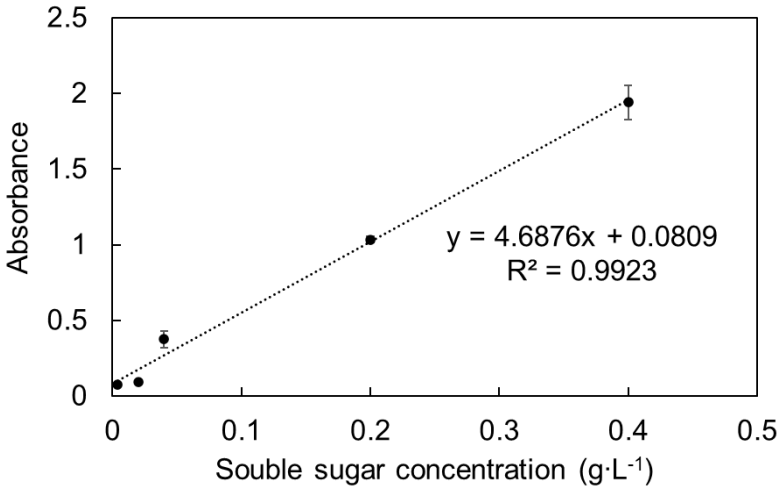

Fig. 6.4. Soluble sugar concentration calibration. Calibration was done using the glucose at 0.4, 0.2, 0.04, 0.02 and 0.004 g glucose·L^{-1}. Each concentration had 3 replicates)

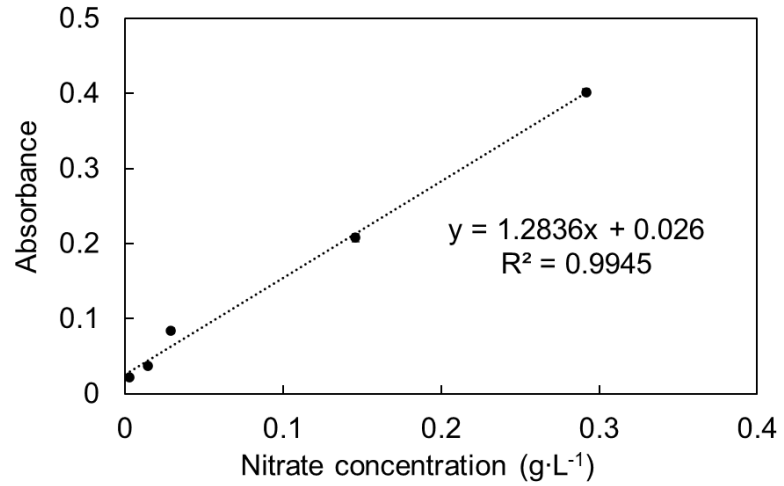

Fig. 6.5. Nitrate concentration calibration. Calibration was done using $NaNO_3$ at 0.292, 0.146, 0.029, 0.015 and 0.003 g NO_3^-·L^{-1}. Each concentration had 3 replicates)

Table 6.3. Physicochemical characteristics of soil and finished composts with complete Tukey test results. ("Soil": soil only, "Ctrl-COMP": soil + combi without biochar, "WBC-COMBI": soil + combi with wood-based biochar, "DGBC-COMBI": soil + combi with distillers grain biochar, "CMBC-COMBI": soil + combi with cow manure biochar)

	Soil	**Ctrl-COMP**	**WBC-COMBI**	**DGBC-COMBI**	**CMBC-COMBI**
Moisture content (%)	14.8±5.40^{B}	38.53±3.77^{A}	45.07±6.39^{A}	44.9±8.43^{A}	48.13±3.47^{A}
Ash (% dw)	88.6±0.09^{A}	5.38±0.34^{C}	6.74±0.46^{C}	8.21±2.76^{BC}	11.21±0.65^{A}
pH	7.57±0.06^{AB}	7.10±0.26^{BC}	6.63±0.40^{BC}	6.57±0.55^{C}	8.20±0.26^{A}
Conductivity (mS/cm)	0.29±0.03^{C}	1.89±0.02^{B}	2.07±0.26^{B}	2.45±0.72^{B}	4.35±0.42^{A}
Total N (% dw)	0.47±0.05^{D}	1.71±0.04^{C}	2.29±0.23^{B}	3.28±0.29^{A}	2.27±0.20^{B}
Organic N (% dw)	0.46±0.05^{D}	1.62±0.01^{C}	2.20±0.22^{B}	3.18±0.28^{A}	2.27±0.20^{B}
C:N ratio	15.7±4.73^{B}	28.3±0.58^{A}	22.3±2.08^{AB}	15.7±1.15^{B}	22.3±1.53^{AB}
P as P_2O_5 (% dw)	0.21±0.04^{B}	0.66±0.44^{A}	0.55±0.10^{AB}	1.26±0.38^{A}	0.89±0.25^{A}
K as K_2O (% dw)	0.31±0.02^{D}	0.53±0.02^{C}	0.63±0.08^{BC}	0.85±0.13^{B}	1.65±0.28^{A}
S (% dw)	0.08±0.02^{B}	0.18±0.01^{A}	0.21±0.03^{A}	0.22±0.01^{A}	0.22±0.05^{A}
Ca (% dw)	4.63±1.19^{B}	1.83±0.27^{A}	2.00±0.19^{A}	1.73±0.04^{A}	2.14±0.41^{A}
Na (% dw)	0.07±0.00^{D}	0.14±0.01^{C}	0.15±0.02^{BC}	0.21±0.05^{AB}	0.28±0.03^{A}
Mg (% dw)	1.33±0.45^{C}	0.19±0.01^{B}	0.23±0.04^{BC}	0.31±0.05^{BC}	0.42±0.12^{B}
Fe (ppm)	19850±4445^{A}	149±40.15^{D}	416±109^{CD}	1660±796^{A}	737±330^{BC}
Cu (ppm)	58.3±31.3^{B}	< 20.0^{A}	< 20.0^{A}	< 20.0^{A}	< 20.0^{A}
Zn (ppm)	80.3±6.43^{B}	274±70.4^{A}	369±90.2^{A}	571±92.1^{A}	489±212^{A}
Mn (ppm)	899±513^{A}	< 20.0^{C}	128±38.0^{B}	61.7±12.7^{BC}	99.0±33.1^{B}

Within each row, means not connected by the same letter are significantly different (P<0.05).

CHAPTER 7

SUMMARY AND FUTURE WORK

In conclusion, wood-based biochar addition at a minimum of 13% (by volume) or 5% (by fresh weight) is recommended to improve the composting process (e.g., temperature, leachate COD, final N content). The temperature improvement by adding biochar, which is critical in eliminating foreign animal diseases such as avian influenza, was likely the result of enhanced microbial activity. COMBI did not have an adverse effect on crop growth under the controlled conditions studied. Future research can include:

1. Investigating biochar's influence on the temperature profile using different compost materials, such as manure, sewage sludge, wheat straw, and sawdust.
2. Growing plants using different COMBIs, and under different experimental conditions, such as the drought condition.

REFERENCE

Abbott, L. K., Macdonald, L. M., Wong, M. T. F., Webb, M. J., Jenkins, S. N., Farrell, M. (2018). Potential roles of biological amendments for profitable grain production – A review. *Agric. Ecosyst. Environ.*, *256*(January), 34–50. https://doi.org/10.1016/j.agee.2017.12.021

Agegnehu, G., Bass, A. M., Nelson, P. N., Bird, M. I. (2016). Benefits of biochar, compost and biochar–compost for soil quality, maize yield and greenhouse gas emissions in a tropical agricultural soil. *Sci. Total Environ.*, *543*, 295–306. https://doi.org/10.1016/j.scitotenv.2015.11.054

Agegnehu, G., Bass, A. M., Nelson, P. N., Muirhead, B., Wright, G., Bird, M. I. (2015). Biochar and biochar-compost as soil amendments: effects on peanut yield, soil properties and greenhouse gas emissions in tropical North Queensland, Australia. *Agric. Ecosyst. Environ.*, *213*, 72–85. https://doi.org/10.1016/j.agee.2015.07.027

Agegnehu, G., Nelson, P. N., Bird, M. I. (2016). The effects of biochar, compost and their mixture and nitrogen fertilizer on yield and nitrogen use efficiency of barley grown on a Nitisol in the highlands of Ethiopia. *Sci. Total Environ.*, *569*, 869–879. https://doi.org/10.1016/j.scitotenv.2016.05.033

Agegnehu, G., Srivastava, A. K., Bird, M. I. (2017). The role of biochar and biochar-compost in improving soil quality and crop performance: A review. *Appl. Soil Ecol.*, *119*, 156–170. https://doi.org/https://doi.org/10.1016/j.apsoil.2017.06.008

Agyarko-Mintah, E., Cowie, A., Van Zwieten, L., Singh, B. P., Smillie, R., Harden, S., Fornasier, F. (2017). Biochar lowers ammonia emission and improves nitrogen retention in poultry litter composting. *Waste Manag.*, *61*, 129–137. https://doi.org/10.1016/j.wasman.2016.12.009

Ahn, H. K., Richard, T. L., Choi, H. L. (2007). Mass and thermal balance during composting of a poultry manure-Wood shavings mixture at different aeration rates. *Process Biochem.*, *42*(2), 215–223. https://doi.org/10.1016/j.procbio.2006.08.005

Akdeniz, N. (2019). A systematic review of biochar use in animal waste composting. *Waste Manag.*, *88*, 291–300. https://doi.org/10.1016/j.wasman.2019.03.054

Akdeniz, Neslihan. (2019). A systematic review of biochar use in animal waste composting. *Waste Manag.*, *88*, 291–300. https://doi.org/10.1016/j.wasman.2019.03.054

Akdeniz, Neslihan, Janni, K. A. (2012). Full-scale biofilter reduction efficiencies assessed using portable 24-hour sampling units. *J. Air Waste Manage. Assoc.*, *62*(2), 170–182.

Akdeniz, Neslihan, Janni, K. A., Salnikov, I. A. (2011). Biofilter performance of pine nuggets and lava rock as media. *Bioresour. Technol.*, *102*(8), 4974–4980.

Akratos, C. S., Tekerlekopoulou, A. G., Vasiliadou, I. A., Vayenas, D. V. (2017). Cocomposting of olive mill waste for the production of soil amendments. In *Olive Mill Waste* (pp. 161–182). Elsevier.

Amalina, F., Razak, A. S. A., Krishnan, S., Zularisam, A. W., Nasrullah, M. (2022). A comprehensive assessment of the method for producing biochar, its characterization, stability, and potential applications in regenerative economic sustainability – A review. *Clean. Mater.*, *3*(December 2021), 100045. https://doi.org/10.1016/j.clema.2022.100045

Anusha, S., Samarasekara, L., Coorey, R. V. (2011). Thermal Capacity as a Function of Moisture Content of Sri Lankan Wood Species: Wheatstone bridge method. *Proc. Tech. Sess.*, *27*(December 2014), 9–16. Retrieved from https://www.researchgate.net/publication/266413397_Thermal_capacity_as_a_function_of_moisture_content_of_Sri_Lankan_wood_species_Wheatstone_bridge_method

Arvanitoyannis, I. S., Ladas, D. (2008). Meat waste treatment methods and potential uses. *Int. J. Food Sci. Technol.*, *43*(3), 543–559.

Awasthi, M. K., Awasthi, S. K., Wang, Q., Wang, Z., Lahori, A. H., Ren, X., … Zhang, Z. (2018). Influence of biochar on volatile fatty acids accumulation and microbial community succession during biosolids composting. *Bioresour. Technol.*, *251*, 158–164. https://doi.org/https://doi.org/10.1016/j.biortech.2017.12.037

Awasthi, M. K., Duan, Y., Awasthi, S. K., Liu, T., Zhang, Z. (2019). Effect of biochar and bacterial inoculum additions on cow dung composting. *Bioresour. Technol.*, *297*(November 2019), 122407. https://doi.org/10.1016/j.biortech.2019.122407

Awasthi, M. K., Wang, Q., Chen, H., Wang, M., Ren, X., Zhao, J., … Zhang, Z. (2017).

Evaluation of biochar amended biosolids co-composting to improve the nutrient transformation and its correlation as a function for the production of nutrient-rich compost. *Bioresour. Technol.*, *237*, 156–166. https://doi.org/10.1016/j.biortech.2017.01.044

Bailey, J. E., Ollis, D. F. (1986). Metabolic stoichiometry and energetics. *Biochem. Eng. Fundam.*, 228–306.

Baltrėnas, P., Baltrėnaitė, E., Kleiza, J., Švedienė, J. (2016). A biochar-based medium in the biofiltration system: Removal efficiency, microorganism propagation, and the medium penetration modeling. *J. Air Waste Manage. Assoc.*, *66*(7), 673–686.

Barrington, S., Choinière, D., Trigui, M., Knight, W. (2002). Effect of carbon source on compost nitrogen and carbon losses. *Bioresour. Technol.*, *83*(3), 189–194.

Bass, A. M., Bird, M. I., Kay, G., Muirhead, B. (2016). Soil properties, greenhouse gas emissions and crop yield under compost, biochar and co-composted biochar in two tropical agronomic systems. *Sci. Total Environ.*, *550*, 459–470. https://doi.org/10.1016/j.scitotenv.2016.01.143

Basso, A. S., Miguez, F. E., Laird, D. A., Horton, R., Westgate, M. (2013). Assessing potential of biochar for increasing water-holding capacity of sandy soils. *GCB Bioenergy*, *5*(2), 132–143. https://doi.org/10.1111/gcbb.12026

Bedada, W., Karltun, E., Lemenih, M., Tolera, M. (2014). Long-term addition of compost and NP fertilizer increases crop yield and improves soil quality in experiments on smallholder farms. *Agric. Ecosyst. Environ.*, *195*, 193–201. https://doi.org/10.1016/j.agee.2014.06.017

Bengtsson, G., Bengtson, P., Månsson, K. F. (2003). Gross nitrogen mineralization-, immobilization-, and nitrification rates as a function of soil C/N ratio and microbial activity. *Soil Biol. Biochem.*, *35*(1), 143–154.

Bernal, M. P., Alburquerque, J. A., Moral, R. (2009). Composting of animal manures and chemical criteria for compost maturity assessment. A review. *Bioresour. Technol.*, *100*(22), 5444–5453.

Biederman, L. A., W., S. H. (2013). Biochar and its effects on plant productivity and nutrient cycling: A meta-analysis. *GCB Bioenergy*, *5*(2), 202–214.

https://doi.org/10.1111/gcbb.12037

Brewer, C. E., Schmidt-rohr, K., Satrio, J. A., Brown, R. C. (2015). Degradation of lignin in ionic liquid with HCl as catalyst. *Environ. Prog. Sustain. Energy*, *35*(3), 809–814. https://doi.org/10.1002/ep

Brust, G. E. (2019). Management strategies for organic vegetable fertility. In *Safety and practice for organic food* (pp. 193–212). Elsevier.

Buchholz, S. C. K. (1993). Nitrogen in the Environment: Nitrogen's Most Common Forms. Retrieved from https://extension.missouri.edu/publications/wq253

Butnan, S., Deenik, J. L., Toomsan, B., Antal, M. J., Vityakon, P. (2015). Biochar characteristics and application rates affecting corn growth and properties of soils contrasting in texture and mineralogy. *Geoderma*, *237*, 105–116.

Cai, H., Chen, T., Liu, H., Gao, D., Zheng, G., Zhang, J. (2010). The effect of salinity and porosity of sewage sludge compost on the growth of vegetable seedlings. *Sci. Hortic. (Amsterdam).*, *124*(3), 381–386.

Castán, E., Satti, P., González-Polo, M., Iglesias, M. C., Mazzarino, M. J. (2016). Managing the value of composts as organic amendments and fertilizers in sandy soils. *Agric. Ecosyst. Environ.*, *224*, 29–38.

Cerozi, B. da S., Fitzsimmons, K. (2016). The effect of pH on phosphorus availability and speciation in an aquaponics nutrient solution. *Bioresour. Technol.*, *219*, 778–781. https://doi.org/10.1016/j.biortech.2016.08.079

Chaganti, V. N., Crohn, D. M. (2015). Evaluating the relative contribution of physiochemical and biological factors in ameliorating a saline-sodic soil amended with composts and biochar and leached with reclaimed water. *Geoderma*, *259*, 45–55. https://doi.org/10.1016/j.geoderma.2015.05.005

Chen, W., Liao, X., Wu, Y., Liang, J. B., Mi, J., Huang, J., … Wang, Y. (2017a). Effects of different types of biochar on methane and ammonia mitigation during layer manure composting. *Waste Manag.*, *61*, 506–515. https://doi.org/10.1016/j.wasman.2017.01.014

Chen, W., Liao, X., Wu, Y. Y., Liang, J. B., Mi, J., Huang, J., … Wang, Y. (2017b). Effects of different types of biochar on methane and ammonia mitigation during layer manure composting. *Waste Manag., 61*, 506–515. https://doi.org/10.1016/j.wasman.2017.01.014

Chen, X. li, Yang, Q. chang. (2018). Effects of intermittent light exposure with red and blue light emitting diodes on growth and carbohydrate accumulation of lettuce. *Sci. Hortic. (Amsterdam)., 234*(February), 220–226. https://doi.org/10.1016/j.scienta.2018.02.055

Cheng, C.-H., Lehmann, J., Thies, J. E., Burton, S. D., Engelhard, M. H. (2006). Oxidation of black carbon by biotic and abiotic processes. *Org. Geochem.*, *37*(11), 1477–1488.

Cheng, C. H., Lehmann, J., Engelhard, M. H. (2008). Natural oxidation of black carbon in soils: Changes in molecular form and surface charge along a climosequence. *Geochim. Cosmochim. Acta, 72*(6), 1598–1610. https://doi.org/10.1016/j.gca.2008.01.010

Chowdhury, M. A., de Neergaard, A., Jensen, L. S. (2014). Potential of aeration flow rate and bio-char addition to reduce greenhouse gas and ammonia emissions during manure composting. *Chemosphere, 97*, 16–25. https://doi.org/10.1016/j.chemosphere.2013.10.030

Clough, T., Condron, L., Kammann, C., Müller, C. (2013). A review of biochar and soil nitrogen dynamics. *Agronomy, 3*(2), 275–293.

Colla, G., Kim, H. J., Kyriacou, M. C., Rouphael, Y. (2018). Nitrate in fruits and vegetables. *Sci. Hortic. (Amsterdam)., 237*(October 2017), 221–238. https://doi.org/10.1016/j.scienta.2018.04.016

Cooper, J., Greenberg, I., Ludwig, B., Hippich, L., Fischer, D., Glaser, B., Kaiser, M. (2020). Effect of biochar and compost on soil properties and organic matter in aggregate size fractions under field conditions. *Agric. Ecosyst. Environ., 295*(February), 106882. https://doi.org/10.1016/j.agee.2020.106882

Costa, T., Akdeniz, N. (2019). A review of the animal disease outbreaks and biosecure animal mortality composting systems. *Waste Manag., 90*, 121–131.

Costa, T., Akdeniz, N., Gates, R. S., Lowe, J., Zhang, Y. (2021). Testing the plastic-wrapped composting system to dispose of swine mortalities during an animal disease outbreak. *J. Environ. Qual., 50*(4), 899–910. https://doi.org/10.1002/jeq2.20235

Czekała, W., Malińska, K., Cáceres, R., Janczak, D., Dach, J., Lewicki, A. (2016). Co-composting of poultry manure mixtures amended with biochar - The effect of biochar on temperature and C-CO2 emission. *Bioresour. Technol.*, *200*, 921–927. https://doi.org/10.1016/j.biortech.2015.11.019

Datta, A. K. (2002). *Biological and bioenvironmental heat and mass transfer*. CRC Press.

de Guardia, A., Petiot, C., Benoist, J. C., Druilhe, C. (2012). Characterization and modelling of the heat transfers in a pilot-scale reactor during composting under forced aeration. *Waste Manag.*, *32*(6), 1091–1105. https://doi.org/10.1016/j.wasman.2011.12.028

De Guardia, A., Petiot, C., Benoist, J. C., Druilhe, C. (2012). Characterization and modelling of the heat transfers in a pilot-scale reactor during composting under forced aeration. *Waste Manag.*, *32*(6), 1091–1105.

DeLuca, T. H., Gundale, M. J., MacKenzie, M. D., Jones, D. L. (2015). Biochar effects on soil nutrient transformations. *Biochar Environ. Manag. Sci. Technol. Implement.*, *2*, 421–454.

Devereux, R. C., Sturrock, C. J., Mooney, S. J. (2012). The effects of biochar on soil physical properties and winter wheat growth. *Earth Environ. Sci. Trans. R. Soc. Edinburgh*, *103*(1), 13–18. https://doi.org/10.1017/S1755691012000011

Dias, B. O., Silva, C. A., Higashikawa, F. S. F. S. F. S., Roig, A. A. A., Sánchez-Monedero, M. A., Sanchez-Monedero, M. A., Sánchez-Monedero, M. A. (2010). Use of biochar as bulking agent for the composting of poultry manure: effect on organic matter degradation and humification. *Bioresour. Technol.*, *101*(4), 1239–1246. https://doi.org/10.1016/j.biortech.2009.09.024

Dias, B. O., Silva, C. A., Higashikawa, F. S., Roig, A., Sánchez-Monedero, M. A. (2010). Use of biochar as bulking agent for the composting of poultry manure: effect on organic matter degradation and humification. *Bioresour. Technol.*, *101*, 1239–1246.

Domingues, R. R., Trugilho, P. F., Silva, C. A., Melo, I. C. N. A. de, Melo, L. C. A., Magriotis, Z. M., Sanchez-Monedero, M. A. (2017). Properties of biochar derived from wood and high-nutrient biomasses with the aim of agronomic and environmental benefits. *PLoS One*, *12*(5), e0176884.

Du, J., Zhang, Y., Hu, B., Qv, M., Ma, C., Wei, M., Zhang, H. (2019). Insight into the potentiality of big biochar particle as an amendment in aerobic composting of sewage sludge. *Bioresour. Technol.*, *288*(March), 121469. https://doi.org/10.1016/j.biortech.2019.121469

Du, J., Zhang, Y., Qu, M., Yin, Y., Fan, K., Hu, B., … Ma, C. (2019). Effects of biochar on the microbial activity and community structure during sewage sludge composting. *Bioresour. Technol.*, *272*, 171–179. https://doi.org/https://doi.org/10.1016/j.biortech.2018.10.020

Duan, Y., Awasthi, S. K., Liu, T., Verma, S., Wang, Q., Chen, H., … Awasthi, M. K. (2019). Positive impact of biochar alone and combined with bacterial consortium amendment on improvement of bacterial community during cow manure composting. *Bioresour. Technol.*, *280*(February), 79–87. https://doi.org/10.1016/j.biortech.2019.02.026

EFSA. (n.d.). African swine fever. Retrieved from https://www.efsa.europa.eu/en/topics/topic/african-swine-fever

El-Naggar, A., Soo, S., Rinklebe, J., Farooq, M., Song, H. (2019). Geoderma Biochar application to low fertility soils : A review of current status , and future prospects. *Geoderma*, *337*(September 2018), 536–554. https://doi.org/10.1016/j.geoderma.2018.09.034

Elkhalifa, S., Al-Ansari, T., Mackey, H. R., McKay, G. (2019). Food waste to biochars through pyrolysis: A review. *Resour. Conserv. Recycl.*, *144*, 310–320.

Elving, J., Emmoth, E., Albihn, A., Vinnerås, B., Ottoson, J. (2012). Composting for avian influenza virus elimination. *Appl. Environ. Microbiol.*, *78*(9), 3280–3285.

EPA 200.7. (1994). Method 200.7: Determination of Metals and Trace Elements in Water and Wastes by Inductively Coupled Plasma-Atomic Emission Spectrometry.

EPA method# 5220D. (1980). Chemical oxygen demand standard method. *Fed. Regist.*, *45*(78), 26811–26812.

EPA method #1684. (2001). Total, Fixed, and Volatile Solids in Water, Solids, and Biosolids.

Fabbri, D., Torri, C., Spokas, K. A. (2012). Analytical pyrolysis of synthetic chars derived from biomass with potential agronomic application (biochar). Relationships with impacts on

microbial carbon dioxide production. *J. Anal. Appl. Pyrolysis*, *93*, 77–84.

Ferri, R., Donna, F., Smith, D. R., Guazzetti, S., Zacco, A., Rizzo, L., … Lucchini, R. G. (2012). Heavy metals in soil and salad in the proximity of historical ferroalloy emission. *J. Environ. Prot. (Irvine,. Calif).*, *3*(5), 374.

Fischer, D., Glaser, B. (2012). Synergisms between compost and biochar for sustainable soil amelioration. In Kumar, S and Bharti, A (Ed.), *Management of organic waste* (pp. 167–198). JANEZA TRDINE9, RIJEKA, 51000, CROATIA: InTech.

Flory, G. A. (2022). Preparing the U.S. for an Outbreak of African Swine Fever.

Flory, G., Peer, R. (2017). Mesophillic Static Pile Composting Of Animal Carcasses. *Biocycle*, *58*(3), 65.

Galinato, S. P., Yoder, J. K., Granatstein, D. (2011). The economic value of biochar in crop production and carbon sequestration. *Energy Policy*, *39*(10), 6344–6350. https://doi.org/10.1016/j.enpol.2011.07.035

Gao, S., DeLuca, T. H., Cleveland, C. C. (2019). Biochar additions alter phosphorus and nitrogen availability in agricultural ecosystems: A meta-analysis. *Sci. Total Environ.*, *654*, 463–472. https://doi.org/10.1016/j.scitotenv.2018.11.124

Gavili, E., Moosavi, A. A., Moradi, F. (2018). Assessing cattle manure biochar potential for ameliorating physical soil features and spinach responses under drought stress conditions. *Arch. Agron. Soil Sci.*, *64*(12), 1714–1727.

Giagnoni, L., Martellini, T., Scodellini, R., Cincinelli, A., Renella, G. (2020). Co-composting: An Opportunity to Produce Compost with Designated Tailor-Made Properties. In *Organic Waste Composting through Nexus Thinking* (pp. 185–211). Springer, Cham.

Glanville, T. D., Ahn, H., Akdeniz, N., Crawford, B. P., Koziel, J. A. (2016). Performance of a plastic-wrapped composting system for biosecure emergency disposal of disease-related swine mortalities. *Waste Manag.*, *48*. https://doi.org/10.1016/j.wasman.2015.11.006

Glaser, B., Haumaier, L., Guggenberger, G., Zech, W. (2001). The'Terra Preta'phenomenon: a model for sustainable agriculture in the humid tropics. *Naturwissenschaften*, *88*, 37–41.

Glaser, B., Wiedner, K., Seelig, S., Schmidt, H.-P., Gerber, H. (2015). Biochar organic fertilizers from natural resources as substitute for mineral fertilizers. *Agron. Sustain. Dev.*, *35*, 667–678.

Glisczynski, F. von, Pude, R., Amelung, W., Sandhage-Hofmann, A. (2016). Biochar-compost substrates in short-rotation coppice: Effects on soil and trees in a three-year field experiment. *J. Plant Nutr. Soil Sci.*, *179*(4), 574–583.

Godlewska, P., Schmidt, H. P., Ok, Y. S., Oleszczuk, P. (2017). Biochar for composting improvement and contaminants reduction. A review. *Bioresour. Technol.*, *246*(July), 193–202. https://doi.org/https://doi.org/10.1016/j.biortech.2017.07.095

Guan, J., Chan, M., Grenier, C., Wilkie, D. C., Brooks, B. W., Spencer, J. L. (2009). Survival of avian influenza and Newcastle disease viruses in compost and at ambient temperatures based on virus isolation and real-time reverse transcriptase PCR. *Avian Dis.*, *53*(1), 26–33.

Gul, S., Whalen, J. K., Thomas, B. W., Sachdeva, V., Deng, H. (2015). Physico-chemical properties and microbial responses in biochar-amended soils: Mechanisms and future directions. *Agric. Ecosyst. Environ.*, *206*, 46–59. https://doi.org/10.1016/j.agee.2015.03.015

Guo, X. xia, Liu, H. tao, Zhang, J. (2020). The role of biochar in organic waste composting and soil improvement: A review. *Waste Manag.*, *102*, 884–899. https://doi.org/10.1016/j.wasman.2019.12.003

Hachicha, S., Sellami, F., Cegarra, J., Hachicha, R., Drira, N., Medhioub, K., Ammar, E. (2009). Biological activity during co-composting of sludge issued from the OMW evaporation ponds with poultry manure—Physico-chemical characterization of the processed organic matter. *J. Hazard. Mater.*, *162*(1), 402–409.

Hagemann, N., Joseph, S., Schmidt, H.-P., Kammann, C. I., Harter, J., Borch, T., … Elliott, K. W. (2017). Organic coating on biochar explains its nutrient retention and stimulation of soil fertility. *Nat. Commun.*, *8*, 1089.

Hagemann, N., Joseph, S., Schmidt, H.-P. P., Kammann, C. I., Harter, J., Borch, T., … Kappler, A. (2017). Organic coating on biochar explains its nutrient retention and stimulation of soil fertility. *Nat. Commun.*, *8*(1), 1089. https://doi.org/10.1038/s41467-017-01123-0

Hale, S., Hanley, K., Lehmann, J., Zimmerman, A., Cornelissen, G. (2011). Effects of Chemical, Biological, and Physical Aging As Well As Soil Addition on the Sorption of Pyrene to Activated Carbon and Biochar. *Environ. Sci. Technol.*, *45*(24), 10445–10453. https://doi.org/10.1021/es202970x

Haug, R. (2018). *The practical handbook of compost engineering*. Routledge.

Haug, R. T. (1993). *The Practical Handbook of Compost Engineering*. Lewis Publishers.

Heber, A. J., Bogan, W. W., Ni, J. Q., Lim, T. T., Ramirez-Dorronsoro, J. C., Cortus, E. L., … Zhang, R. (2008). The National Air Emissions Monitoring Study: Overview of barn sources. *Livest. Environ. VIII - Proc. 8th Int. Symp.*, (701), 199–206. https://doi.org/10.13031/2013.25499

Heber, Albert J., Ni, J. Q., Lim, T. T., Tao, P. C., Schmidt, A. M., Koziel, J. A., … Zhang, Y. (2006). Quality assured measurements of animal building emissions: Gas concentrations. *J. Air Waste Manag. Assoc.*, *56*(10), 1472–1483. https://doi.org/10.1080/10473289.2006.10465680

Heinonen-Tanski, H., Mohaibes, M., Karinen, P., Koivunen, J. (2006). Methods to reduce pathogen microorganisms in manure. *Livest. Sci.*, *102*(3), 248–255. https://doi.org/https://doi.org/10.1016/j.livsci.2006.03.024

Hu, W., Zheng, G., Fang, D., Cui, C., Liang, J., Zhou, L. (2015). Bioleached sludge composting drastically reducing ammonia volatilization as well as decreasing bulking agent dosage and improving compost quality: A case study. *Waste Manag.*, *44*, 55–62. https://doi.org/10.1016/j.wasman.2015.07.023

Ibrahim, A., Usman, A. R. A., Al-Wabel, M. I., Nadeem, M., Ok, Y. S., Al-Omran, A. (2017). Effects of conocarpus biochar on hydraulic properties of calcareous sandy soil: influence of particle size and application depth. *Arch. Agron. Soil Sci.*, *63*(2), 185–197. https://doi.org/https://doi.org/10.1080/03650340.2016.1193785

IL Dept. of Agriculture. (1990). Illinois Dead Animal Disposal Act.

Imbeah, M. (1998). Composting piggery waste: a review. *Bioresour. Technol.*, *63*(3), 197–203.

Ishizuka, J. (1992). Trends in biological nitrogen fixation research and application. *Biol. Nitrogen Fixat. Sustain. Agric.*, *49*, 197–209.

Janczak, D., Malinska, K., Czekala, W., Caceres, R., Lewicki, A., Dach, J. (2017). Biochar to reduce ammonia emissions in gaseous and liquid phase during composting of poultry manure with wheat straw. *Waste Manag.*, *66*, 36–45. https://doi.org/10.1016/j.wasman.2017.04.033

Janczak, D., Malińska, K., Czekała, W., Cáceres, R., Lewicki, A., Dach, J. (2017). Biochar to reduce ammonia emissions in gaseous and liquid phase during composting of poultry manure with wheat straw. *Waste Manag.*, *66*, 36–45. https://doi.org/https://doi.org/10.1016/j.wasman.2017.04.033

Jeffery, S., Abalos, D., Spokas, K. A., Verheijen, F. G. A. (2015). Biochar effects on crop yield. In Johannes Lehmann & S. Joseph (Eds.), *Biochar for environmental management: science technology and implementation* (2nd ed., p. 928). Routledge, New York.

Jeffery, S., Verheijen, F. G. A. A., van der Velde, M., Bastos, A. C. (2011). A quantitative review of the effects of biochar application to soils on crop productivity using meta-analysis. *Agric. Ecosyst. Environ.*, *144*(1), 175–187. https://doi.org/10.1016/j.agee.2011.08.015

Ji, M., Wang, X., Usman, M., Liu, F., Dan, Y., Zhou, L., … Sang, W. (2022). Effects of different feedstocks-based biochar on soil remediation: A review. *Environ. Pollut.*, *294*(April 2021), 118655. https://doi.org/10.1016/j.envpol.2021.118655

Jia, X., Wang, M., Yuan, W., Shah, S., Shi, W., Meng, X., … Yang, B. (2016). N2O Emission and Nitrogen Transformation in Chicken Manure and Biochar Co-Composting. *Trans. ASABE*, *59*(5), 1277–1283. https://doi.org/10.13031/trans.59.11685

Jian, S., Li, J., Chen, J., Wang, G., Mayes, M. A., Dzantor, K. E., … Luo, Y. (2016). Soil extracellular enzyme activities, soil carbon and nitrogen storage under nitrogen fertilization: A meta-analysis. *Soil Biol. Biochem.*, *101*, 32–43.

Jindo, K., Mizumoto, H., Sawada, Y., Sanchez-Monedero, M. A., Sonoki, T. (2014). Physical and chemical characterization of biochars derived from different agricultural residues.

Biogeosciences, *11*(23), 6613–6621. https://doi.org/10.5194/bg-11-6613-2014

Jindo, Keiji, Sánchez-Monedero, M. A., Hernández, T., García, C., Furukawa, T., Matsumoto, K., … Bastida, F. (2012). Biochar influences the microbial community structure during manure composting with agricultural wastes. *Sci. Total Environ.*, *416*, 476–481.

Jindo, Keiji, Sonoki, T., Matsumoto, K., Canellas, L., Roig, A. A., Sanchez-Monedero, M. A. (2016). Influence of biochar addition on the humic substances of composting manures. *Waste Manag.*, *49*, 545–552. https://doi.org/10.1016/j.wasman.2016.01.007

Jirka, A. M., Carter, M. J. (1975). Micro Semi-Automated Analysis of Surface and Waste Waters for Chemical Oxygen Demand. *Anal. Chem.*, *47*(8), 1397–1402. https://doi.org/10.1021/ac60358a004

Joern, B. C., Brichford, S. L. (1993). Calculating manure and manure nutrient application rate. *AY*.

Johnson, C., Albrecht, G., Ketterings, Q., Beckman, J., Stockin, K. (2005). Fact sheet 2-nitrogen basics.

Jones, S., Bardos, R. P., Kidd, P. S., Mench, M., de Leij, F., Hutchings, T., … Menger, P. (2016). Biochar and compost amendments enhance copper immobilisation and support plant growth in contaminated soils. *J. Environ. Manage.*, *171*, 101–112. https://doi.org/10.1016/j.jenvman.2016.01.024

Joseph, S. D. D., Camps-Arbestain, M., Lin, Y., Munroe, P., Chia, C. H. H., Hook, J., … Amonette, J. E. (2010). An investigation into the reactions of biochar in soil. *Soil Res.*, *48*(7), 501–515. https://doi.org/10.1071/SR10009

Kammann, C. I., Schmidt, H.-P., Messerschmidt, N., Linsel, S., Steffens, D., Müller, C., … Joseph, S. (2015). Plant growth improvement mediated by nitrate capture in co-composted biochar. *Sci. Rep.*, *5*, 11080.

Kätterer, T., Roobroeck, D., Andrén, O., Kimutai, G., Karltun, E., Kirchmann, H., … de Nowina, K. R. (2019). Biochar addition persistently increased soil fertility and yields in maize-soybean rotations over 10 years in sub-humid regions of Kenya. *F. Crop. Res.*, *235*, 18–26.

Kaudal, B. B., Weatherley, A. J. (2018). Agronomic effectiveness of urban biochar aged through co-composting with food waste. *Waste Manag.*, *77*, 87–97. https://doi.org/10.1016/j.wasman.2018.04.042

Kavitha, B., Reddy, P. V. L., Kim, B., Lee, S. S., Pandey, S. K., Kim, K. H. (2018). Benefits and limitations of biochar amendment in agricultural soils: A review. *J. Environ. Manage.*, *227*(August), 146–154. https://doi.org/10.1016/j.jenvman.2018.08.082

Khan, M. A. I., Ueno, K., Horimoto, S., Komai, F., Someya, T., Inoue, K., … Ono, Y. (2009). CIELAB color variables as indicators of compost stability. *Waste Manag.*, *29*(12), 2969–2975. https://doi.org/10.1016/j.wasman.2009.06.021

Khan, N., Clark, I., Sánchez-Monedero, M. A., Shea, S., Meier, S., Qi, F., … Bolan, N. (2016). Physical and chemical properties of biochars co-composted with biowastes and incubated with a chicken litter compost. *Chemosphere*, *142*, 14–23. https://doi.org/10.1016/j.chemosphere.2015.05.065

Khanmohammadi, Z., Afyuni, M., Mosaddeghi, M. R. (2015). Effect of pyrolysis temperature on chemical and physical properties of sewage sludge biochar. *Waste Manag. Res.*, *33*(3), 275–283. https://doi.org/10.1177/0734242X14565210

Laird, D., Fleming, P., Wang, B., Horton, R., Karlen, D. (2010). Biochar impact on nutrient leaching from a Midwestern agricultural soil. *Geoderma*, *158*(3–4), 436–442. https://doi.org/10.1016/j.geoderma.2010.05.012

Lasaridi, K., Protopapa, I., Kotsou, M., Pilidis, G., Manios, T., Kyriacou, A. (2006). Quality assessment of composts in the Greek market: The need for standards and quality assurance. *J. Environ. Manage.*, *80*(1), 58–65. https://doi.org/10.1016/j.jenvman.2005.08.011

Lashari, M. S., Liu, Y., Li, L., Pan, W., Fu, J., Pan, G., … Yu, X. (2013). Effects of amendment of biochar-manure compost in conjunction with pyroligneous solution on soil quality and wheat yield of a salt-stressed cropland from Central China Great Plain. *F. Crop. Res.*, *144*(3), 113–118. https://doi.org/10.1016/j.fcr.2012.11.015

Lashari, M. S., Ye, Y., Ji, H., Li, L., Kibue, G. W., Lu, H., … Pan, G. (2015). Biochar–manure compost in conjunction with pyroligneous solution alleviated salt stress and improved leaf

bioactivity of maize in a saline soil from central China: a 2-year field experiment. *J. Sci. Food Agric.*, *95*(6), 1321–1327. https://doi.org/10.1002/jsfa.6825

Lee, C.-H., Wang, C.-C., Lin, H.-H., Lee, S. S., Tsang, D. C. W., Jien, S.-H., Ok, Y. S. (2018). In-situ biochar application conserves nutrients while simultaneously mitigating runoff and erosion of an Fe-oxide-enriched tropical soil. *Sci. Total Environ.*, *619*, 665–671. https://doi.org/10.1016/j.scitotenv.2017.11.023

Lehmann, J., Joseph, S. (2015). Biochar for environmental management: an introduction. In J. Lehmann & S. Joseph (Eds.), *Biochar for environmental management: science technology and implementation* (2nd ed., p. 928). Routledge, New York.

Lehmann, Johannes, da Silva, J. P., Steiner, C., Nehls, T., Zech, W., Glaser, B. (2003). Nutrient availability and leaching in an archaeological Anthrosol and a Ferralsol of the Central Amazon basin: fertilizer, manure and charcoal amendments. *Plant Soil*, *249*, 343–357.

Lehmann, Johannes, Joseph, S. (2015). Biochar for environmental management: an introduction. In Johannes Lehmann & S. Joseph (Eds.) (p. 928). Routledge, New York.

Lehmann, Johannes, Rillig, M. C., Thies, J., Masiello, C. A., Hockaday, W. C., Crowley, D. (2011a). Biochar effects on soil biota–a review. *Soil Biol. Biochem.*, *43*(9), 1812–1836.

Lehmann, Johannes, Rillig, M. C., Thies, J., Masiello, C. A., Hockaday, W. C., Crowley, D. (2011b). Biochar effects on soil biota - A review. *Soil Biol. Biochem.*, *43*(9), 1812–1836. https://doi.org/10.1016/j.soilbio.2011.04.022

Leng, L., Xiong, Q., Yang, L., Li, H., Zhou, Y., Zhang, W., … Huang, H. (2021). An overview on engineering the surface area and porosity of biochar. *Sci. Total Environ.*, *763*, 144204. https://doi.org/10.1016/j.scitotenv.2020.144204

Li-Xian, Y., Guo-Liang, L., Shi-Hua, T., Gavin, S., Zhao-Huan, H. (2007). Salinity of animal manure and potential risk of secondary soil salinization through successive manure application. *Sci. Total Environ.*, *383*(1), 106–114. https://doi.org/https://doi.org/10.1016/j.scitotenv.2007.05.027

Li, M., Liu, M., Li, Z. pei, Jiang, C. yu, Wu, M. (2016). Soil N transformation and microbial community structure as affected by adding biochar to a paddy soil of subtropical China. *J.*

Integr. Agric., *15*(1), 209–219. https://doi.org/10.1016/S2095-3119(15)61136-4

Li, R., Wang, Q., Zhang, Z., Zhang, G., Li, Z., Wang, L., Zheng, J. (2015). Nutrient transformation during aerobic composting of pig manure with biochar prepared at different temperatures. *Environ. Technol.*, *36*(7), 815–826. https://doi.org/10.1080/09593330.2014.963692

Liu, H. H., Fu, Y., Yu, J., Liu, H. H. (2016). Accumulation and primary metabolism of nitrate in lettuce (Lactuca sativa L. var. Youmaicai) grown under three different light sources. *Commun. Soil Sci. Plant Anal.*, *47*(17), 1994–2002.

Liu, H., Wang, L., Lei, M. (2019). Positive impact of biochar amendment on thermal balance during swine manure composting at relatively low ambient temperature. *Bioresour. Technol.*, *273*, 25–33. https://doi.org/https://doi.org/10.1016/j.biortech.2018.10.033

Liu, N., Zhou, J., Han, L., Ma, S., Sun, X., Huang, G. (2017). Role and multi-scale characterization of bamboo biochar during poultry manure aerobic composting. *Bioresour. Technol.*, *241*, 190–199. https://doi.org/10.1016/j.biortech.2017.03.144

Liu, X., Zhang, A., Ji, C., Joseph, S., Bian, R., Li, L., … Paz-Ferreiro, J. (2013). Biochar's effect on crop productivity and the dependence on experimental conditions-a meta-analysis of literature data. *Plant Soil*, *373*(1–2), 583–594. https://doi.org/10.1007/s11104-013-1806-x

Lopez-Cano, I., Roig, A. A. A., Luz Cayuela, M., Antonio Alburquerque, J., Angel Sanchez-Monedero, M., López-Cano, I., … Angel Sanchez-Monedero, M. (2016). Biochar improves N cycling during composting of olive mill wastes and sheep manure. *Waste Manag.*, *49*, 553–559. https://doi.org/10.1016/j.wasman.2015.12.031

Lou, Z., Sun, Y., Bian, S., Ali Baig, S., Hu, B., Xu, X., … Xu, X. (2017). Nutrient conservation during spent mushroom compost application using spent mushroom substrate derived biochar. *Chemosphere*, *169*, 23–31. https://doi.org/10.1016/j.chemosphere.2016.11.044

Luo, X., Liu, G., Xia, Y., Chen, L., Jiang, Z., Zheng, H., Wang, Z. (2017). Use of biochar-compost to improve properties and productivity of the degraded coastal soil in the Yellow River Delta, China. *J. Soils Sediments*, *17*(3), 780–789. https://doi.org/10.1007/s11368-016-1361-1

MAFES (The Maine Agricultural and Forest Experiment Station). (2016). Compost Report Interpretation Guide.

Malińska, K., Zabochnicka-Świątek, M., Dach, J. (2014). Effects of biochar amendment on ammonia emission during composting of sewage sludge. *Ecol. Eng., 71*, 474–478. https://doi.org/10.1016/j.ecoleng.2014.07.012

Martins, O., Dewes, T. (1992). Loss of nitrogenous compounds during composting of animal wastes. *Bioresour. Technol., 42*, 103–111.

Masiello, C. A., Dugan, B., Brewer, C. E., Spokas, K. A., Novak, J. M., Liu, Z., Sorrenti, G. (2015). Biochar effects on soil hydrology. In J. Lehmann & S. Joseph (Eds.), *Biochar for environmental management: science technology and implementation* (2nd ed., p. 928). Routledge, New York.

Mason, I. G., Milke, M. W. (2005). Physical modelling of the composting environment: A review. Part 1: Reactor systems. *Waste Manag., 25*(5), 481–500. https://doi.org/10.1016/j.wasman.2005.01.015

Medina, V. F., Martinez-Guerra, E., Cosper, S. C. (2019). Military Solid and Hazardous Wastes: The Army Corps of Engineers Disaster Debris Management Mission. In *Waste* (pp. 553–565). Elsevier.

Meeker, E. W., Wagner, E. C. (1933). Titration of ammonia in presence of boric acid. Macro- and micro- Kjeldahl procedures. *Ind. Eng. Chem. Anal. Ed., 5*(6), 396–398.

Mekuria, W., Noble, A., Sengtaheuanghoung, O., Hoanh, C. T., Bossio, D., Sipaseuth, N., … Langan, S. (2014). Organic and clay-based soil amendments increase maize yield, total nutrient uptake, and soil properties in Lao PDR. *Agroecol. Sustain. Food Syst., 38*, 936–961.

Mia, S., van Groenigen, J. W., van de Voorde, T. F. J., Oram, N. J., Bezemer, T. M., Mommer, L., Jeffery, S. (2014). Biochar application rate affects biological nitrogen fixation in red clover conditional on potassium availability. *Agric. Ecosyst. Environ., 191*, 83–91. https://doi.org/10.1016/j.agee.2014.03.011

Midwest Laboratories Inc. (2019). Compost results interpretations.

Montes-Morán, M. A., Suárez, D., Menéndez, J. A., Fuente, E. (2004). On the nature of basic sites on carbon surfaces: An overview. *Carbon N. Y.*, *42*(7), 1219–1224. https://doi.org/10.1016/j.carbon.2004.01.023

Mukherjee, A., Lal, R. (2013). Biochar Impacts on Soil Physical Properties and Greenhouse Gas Emissions. *Agronomy*, *3*(2), 313–339. https://doi.org/10.3390/agronomy3020313

Mukome, F. N. D., Parikh, S. J. (2016). Chemical, physical, and surface characterization of biochar. In Y. S. Ok, S. M. Uchimiya, S. X. Chang, & N. Bolan (Eds.), *Biochar: production, characterization and applications* (p. 407).

Nakasaki, K., Yaguchi, H., Sasaki, Y., Kubota, H. (1992). Effects of CN ratio on thermophilic composting of garbage. *J. Ferment. Bioeng.*, *73*(1), 43–45.

NEMI-SM 2510B. (1997). Standard Methods: 2510B: Conductivity.

NEMI-SM 4500 H+B. (2011). Standard Methods: 4500-H+B: pH in Water by Potentiometry.

NEMI-SM 4500 NH3 C. (1997). Standard Methods: 4500-NH3 C: Ammonia by Titration.

Nguyen, T. T. N., Xu, C.-Y., Tahmasbian, I., Che, R., Xu, Z., Zhou, X., … Bai, S. H. (2017). Effects of biochar on soil available inorganic nitrogen: a review and meta-analysis. *Geoderma*, *288*, 79–96.

NRAES. (1999). *Field guide to on-farm composting*. (M. Dougherty, Ed.). Ithaca, NY: Natural Resource, Agriculture and Engineering Service.

NRCS - USDA. (2014). *Inherent Factors Affecting Soil EC*. Retrieved from https://www.nrcs.usda.gov/Internet/FSE_DOCUMENTS/nrcs142p2_052803.pdf

NRCS - USDA. (2015). Emergency animal mortality management.

Ogawa, M., Okimori, Y. (2010). Pioneering works in biochar research, Japan. *Soil Res.*, *48*(6–7), 489–500. https://doi.org/10.1071/SR10006

Oldfield, T. L., Sikirica, N., Mondini, C., López, G., Kuikman, P. J., Holden, N. M. (2018). Biochar, compost and biochar-compost blend as options to recover nutrients and sequester carbon. *J. Environ. Manage.*, *218*, 465–476. https://doi.org/10.1016/j.jenvman.2018.04.061

Oleszczuk, P., Rycaj, M., Lehmann, J., Cornelissen, G. (2012). Ecotoxicology and Environmental Safety Influence of activated carbon and biochar on phytotoxicity of air-dried sewage sludges to Lepidium sativum. *Ecotoxicol. Environ. Saf.*, *80*, 321–326. https://doi.org/10.1016/j.ecoenv.2012.03.015

Onwosi, C. O., Igbokwe, V. C., Odimba, J. N., Eke, I. E., Nwankwoala, M. O., Iroh, I. N., Ezeogu, L. I. (2017). Composting technology in waste stabilization : On the methods , challenges and future prospects. *J. Environ. Manage.*, *190*, 140–157. https://doi.org/10.1016/j.jenvman.2016.12.051

Ortas, I. (2016). The role of mycorrhizae and biochar in plant growth and soil quality. In V. J. Bruckman, E. A. Varol, B. B. Uzun, & J. Liu (Eds.), *Biochar application as a soil amendment* (pp. 336–350). Cambridge University Press.

Özçimen, D., Ersoy-Meriçboyu, A. (2010). Characterization of biochar and bio-oil samples obtained from carbonization of various biomass materials. *Renew. Energy*, *35*(6), 1319–1324. https://doi.org/10.1016/j.renene.2009.11.042

PAI-DK01. (1994). *Nitrogen, Total Kjeldahl, Method PAI-DK01 (Block Digestion, Steam Distillation, Titrimetric Detection)*. College Station, TX 77842.

Pariyar, P., Kumari, K., Jain, M. K., Jadhao, P. S. (2020). Evaluation of change in biochar properties derived from different feedstock and pyrolysis temperature for environmental and agricultural application. *Sci. Total Environ.*, *713*, 136433.

Peralta-Videa, J. R., Lopez, M. L., Narayan, M., Saupe, G., Gardea-Torresdey, J. (2009). The biochemistry of environmental heavy metal uptake by plants: Implications for the food chain. *Int. J. Biochem. Cell Biol.*, *41*(8–9), 1665–1677. https://doi.org/10.1016/j.biocel.2009.03.005

Prasad, M., Tzortzakis, N., McDaniel, N. (2018). Chemical characterization of biochar and assessment of the nutrient dynamics by means of preliminary plant growth tests. *J. Environ. Manage.*, *216*, 89–95. https://doi.org/https://doi.org/10.1016/j.jenvman.2017.04.020

Prost, K., Borchard, N., Siemens, J., Kautz, T., Séquaris, J.-M., Möller, A., Amelung, W. (2013). Biochar Affected by Composting with Farmyard Manure. *J. Environ. Qual.*, *42*(1), 164.

https://doi.org/10.1080/0305569032000159804

Qayyum, M. F., Liaquat, F., Rehman, R. A., Gul, M., ul Hye, M. Z., Rizwan, M., … ur Rehaman, M. Z. (2017). Effects of co-composting of farm manure and biochar on plant growth and carbon mineralization in an alkaline soil. *Environ. Sci. Pollut. Res.*, *24*(33), 26060–26068. https://doi.org/10.1007/s11356-017-0227-4

Qiao-Hong, Z. H. U., Xin-Hua, P., HUANG, T.-Q., Zu-Bin, X. I. E., Holden, N. M. (2014). Effect of biochar addition on maize growth and nitrogen use efficiency in acidic red soils. *Pedosphere*, *24*(6), 699–708.

Qin, J., Qian, S., Chen, Q., Chen, L., Yan, L., Shen, G. (2019). Cow manure-derived biochar: its catalytic properties and influential factors. *J. Hazard. Mater.*, *371*, 381–388.

Qiu, X., Zhou, G., Zhang, J., Wang, W. (2019). Microbial community responses to biochar addition when a green waste and manure mix are composted: A molecular ecological network analysis. *Bioresour. Technol.*, *273*, 666–671. https://doi.org/https://doi.org/10.1016/j.biortech.2018.12.001

Quilliam, R. S., Deluca, T. H., Jones, D. L. (2013). Biochar application reduces nodulation but increases nitrogenase activity in clover. *Plant Soil*, *366*(1), 83–92.

Rakshit, A. (2018). *Soil Amendments for Sustainability: Challenges and Perspectives*. https://doi.org/10.1201/9781351027021

Ravindran, B., Nguyen, D. D., Chaudhary, D. K., Chang, S. W., Kim, J., Lee, S. R., … Lee, J. (2019). Influence of biochar on physico-chemical and microbial community during swine manure composting process. *J. Environ. Manage.*, *232*, 592–599. https://doi.org/https://doi.org/10.1016/j.jenvman.2018.11.119

Reddy, N., Crohn, D. M. (2012). Compost induced soil salinity: a new prediction method and its effect on plant growth. *Compost Sci. Util.*, *20*(3), 133–140.

Rondon, M. A. M. A., Lehmann, J., Ramirez, J., Hurtado, M., Ramírez, J., Hurtado, M. (2007). Biological nitrogen fixation by common beans (Phaseolus vulgaris L.) increases with bio-char additions. *Biol. Fertil. Soils*, *43*(6), 699–708.

Roy, D., Azaïs, A., Benkaraache, S., Drogui, P., Tyagi, R. D. (2018). Composting leachate: characterization, treatment, and future perspectives. *Rev. Environ. Sci. Bio/Technology*, *17*(2), 323–349.

Saifullah, Dahlawi, S., Naeem, A., Rengel, Z., Naidu, R. (2018). Biochar application for the remediation of salt-affected soils: Challenges and opportunities. *Sci. Total Environ.*, *625*, 320–335. https://doi.org/10.1016/j.scitotenv.2017.12.257

Salehi, A., Tasdighi, H., Gholamhoseini, M. (2016). Evaluation of proline, chlorophyll, soluble sugar content and uptake of nutrients in the German chamomile (Matricaria chamomilla L.) under drought stress and organic fertilizer treatments. *Asian Pac. J. Trop. Biomed.*, *6*(10), 886–891.

Sánchez-García, M., Alburquerque, J. A., Sánchez-Monedero, M. A., Roig, A., Cayuela, M. L. (2015). Biochar accelerates organic matter degradation and enhances N mineralisation during composting of poultry manure without a relevant impact on gas emissions. *Bioresour. Technol.*, *192*, 272–279. https://doi.org/https://doi.org/10.1016/j.biortech.2015.05.003

Sanchez-Monedero, M. A., Cayuela, M. L., Roig, A., Jindo, K., Mondini, C., Bolan, N. (2017). Role of biochar as an additive in organic waste composting. *Bioresour. Technol.*, *247*(September 2017), 1155–1164. https://doi.org/10.1016/j.biortech.2017.09.193

Sánchez-Monedero, M. A., Sánchez-García, M., Alburquerque, J. A., Cayuela, M. L. (2019). Biochar reduces volatile organic compounds generated during chicken manure composting. *Bioresour. Technol.*, *288*(May), 121584. https://doi.org/10.1016/j.biortech.2019.121584

Schmidt, H.-P. P., Kammann, C., Niggli, C., Evangelou, M. W. H. H., Mackie, K. A., Abiven, S. (2014). Biochar and biochar-compost as soil amendments to a vineyard soil: Influences on plant growth, nutrient uptake, plant health and grape quality. *Agric. Ecosyst. Environ.*, *191*, 117–123. https://doi.org/10.1016/j.agee.2014.04.001

Schulz, H., Dunst, G., Glaser, B. (2013). Positive effects of composted biochar on plant growth and soil fertility. *Agron. Sustain. Dev.*, *33*(4), 817–827. https://doi.org/10.1007/s13593-013-0150-0

Schulz, H., Glaser, B. (2012). Effects of biochar compared to organic and inorganic fertilizers on soil quality and plant growth in a greenhouse experiment. *J. Plant Nutr. Soil Sci.*, *175*(3), 410–422. https://doi.org/10.1002/jpln.201100143

Shaaban, M., Van Zwieten, L., Bashir, S., Younas, A., Núñez-Delgado, A., Chhajro, M. A., … Hu, R. (2018). A concise review of biochar application to agricultural soils to improve soil conditions and fight pollution. *J. Environ. Manage.*, *228*(September), 429–440. https://doi.org/10.1016/j.jenvman.2018.09.006

Shan, G., Li, W., Gao, Y., Tan, W., Xi, B. (2021). Additives for reducing nitrogen loss during composting: A review. *J. Clean. Prod.*, *307*(December 2020), 127308. https://doi.org/10.1016/j.jclepro.2021.127308

Sigmund, G., Hüffer, T., Hofmann, T., Kah, M. (2017). Biochar total surface area and total pore volume determined by N2 and CO2 physisorption are strongly influenced by degassing temperature. *Sci. Total Environ.*, *580*, 770–775. https://doi.org/10.1016/j.scitotenv.2016.12.023

Singh, B., Dolk, M. M., Shen, Q., Camps-Arbestain, M. (2017). Biochar pH, electrical conductivity and liming potential. *Biochar A Guid. to Anal. Methods*, *23*.

Siripon, K., Tansakul, A., Mittal, G. S. (2007). Heat transfer modeling of chicken cooking in hot water. *Food Res. Int.*, *40*(7), 923–930.

Sommers, L. E. (1977). Chemical composition of sewage sludges and analysis of their potential use as fertilizers 1. *J. Environ. Qual.*, *6*(2), 225–232.

Spokas, K. A., Cantrell, K. B., Novak, J. M., Archer, D. W., Ippolito, J. A., Collins, H. P., … Kurt A. Spokas, Keri B. Cantrell, Jeffrey M. Novak, David W. Archer, James A. Ippolito, Harold P. Collins, Akwasi A. Boateng, Isabel M. Lima, Marshall C. Lamb, Andrew J. McAloon, R. D. L. and K. A. N. (2012). Biochar: A Synthesis of Its Agronomic Impact beyond Carbon Sequestration. *J. Environ. Qual.*, *41*, 973–989. https://doi.org/10.2134/jeq2011.0069

Steiner, C., Das, K. C., Melear, N., Lakly, D. (2010a). Reducing nitrogen loss during poultry litter composting ising biochar. *J. Environ. Qual.*, *39*(4), 1236.

https://doi.org/10.2134/jeq2009.0337

Steiner, C., Das, K. C., Melear, N., Lakly, D. (2010b). Reducing nitrogen loss during poultry litter composting using biochar. *J. Environ. Qual.*, *39*(4), 1236–1242. https://doi.org/10.2134/jeq2009.0337

Steiner, C., Glaser, B., Teixeira, W. G., Lehmann, J., Blum, W. E. H., Zech, W. (2008). Nitrogen retention and plant uptake on a highly weathered central Amazonian Ferralsol amended with compost and charcoal. *J. Plant Nutr. Soil Sci.*, *171*(6), 893–899. https://doi.org/10.1002/jpln.200625199

Steiner, C., Sánchez-Monedero, M. A., Kammann, C., Sanchez, M. A., Kammann, C. (2015). Biochar as an additive to compost and growing media. In Johannes Lehmann & S. Joseph (Eds.), *Biochar for Environmentall Management* (2nd ed, p. 928). Routledge, New York.

Steiner, C., Sanchez, M. A., Kammann, C. (2015). Biochar as an additive to compost and growing media. In Johannes Lehmann & S. Joseph (Eds.), *Biochar for environmental management: science technology and implementation* (2nd ed., p. 928). Routledge, New York.

Sun, D., Lan, Y., Xu, E. G., Meng, J., Chen, W. (2016). Biochar as a novel niche for culturing microbial communities in composting. *Waste Manag.*, *54*, 93–100. https://doi.org/https://doi.org/10.1016/j.wasman.2016.05.004

Tagoe, S. O., Horiuchi, T., Matsui, T. (2008). Effects of carbonized and dried chicken manures on the growth, yield, and N content of soybean. *Plant Soil*, *306*(1), 211–220.

Thies, J. E., Rillig, M. C., Graber, E. R. (2015). Biochar effects on the abundance, activity and diversity of the soil biota. In J. Lehmann & S. Joseph (Eds.), *Biochar for environmental management: science technology and implementation* (2nd ed., p. 928). Routledge, New York.

Thompson, W. H., Leege, P. B., Millner, P. D., Watson, M. E. (2002). Test methods for the examination of composting and compost. *U.S. Compost. Counc. U.S. Dept. Agric.*

TMECC, U. S. (2002). Test methods for the examination of composting and compost. *Wayne Thompson (Ed)*. US Government printing office.

USDA-APHIS. (2014). Layers 2013 Part I: Reference of health and management practices on table-egg farms in the United States.

USDA-APHIS. (2017). Composting Livestock 2017 Livestock Mortality Composting Protocol.

USDA-APHIS. (2021). African Swine Fever (ASF).

USDA-APHIS. (2022). USDA Confirms Highly Pathogenic Avian Influenza in a Commercial Turkey Flock in Dubois County, Indiana.

USDA. (2021). African Swine Fever (ASF). Retrieved from https://www.aphis.usda.gov/aphis/ourfocus/animalhealth/animal-disease-information/swine-disease-information/african-swine-fever/african-swine-fever

USEPA. (2003). *Environmental Regulations and Technology Control of Pathogens and Vector Attraction in Sewage Sludge Control of Pathogens and Vector Attraction*. Cincinnati, OH.

Usowicz, B., Lipiec, J., Łukowski, M., Marczewski, W., Usowicz, J. (2016). The effect of biochar application on thermal properties and albedo of loess soil under grassland and fallow. *Soil Tillage Res., 164*, 45–51. https://doi.org/10.1016/j.still.2016.03.009

van Ginkel, J. T. (1996). *Physical and biochemical processes in composting material*. Wageningen University and Research.

Vandecasteele, B., Sinicco, T., D'Hose, T., Nest, T. Vanden, Mondini, C. (2016). Biochar amendment before or after composting affects compost quality and N losses, but not P plant uptake. *J. Environ. Manage., 168*, 200–209.

von Glisczynski, F., Sandhage-Hofmann, A., Amelung, W., Pude, R. (2016). Biochar-compost substrates do not promote growth and fruit quality of a replanted German apple orchard with fertile Haplic Luvisol soils. *Sci. Hortic. (Amsterdam)., 213*, 110–114. https://doi.org/10.1016/j.scienta.2016.10.023

Wang, B., Gao, B., Zimmerman, A. R., Zheng, Y., Lyu, H. (2018). Novel biochar-impregnated calcium alginate beads with improved water holding and nutrient retention properties. *J. Environ. Manage., 209*, 105–111. https://doi.org/10.1016/j.jenvman.2017.12.041

Wang, B., Lian, G., Lee, X., Gao, B., Li, L., Liu, T., … Zheng, Y. (2020). Phosphogypsum as a

novel modifier for distillers grains biochar removal of phosphate from water. *Chemosphere*, *238*, 124684. https://doi.org/10.1016/j.chemosphere.2019.124684

Wang, H., Zheng, H., Jiang, Z., Dai, Y., Liu, G., Chen, L., … Wang, Z. (2017). Efficacies of biochar and biochar-based amendment on vegetable yield and nitrogen utilization in four consecutive planting seasons. *Sci. Total Environ.*, *593*, 124–133. https://doi.org/10.1016/j.scitotenv.2017.03.096

Wang, K., Mao, H., Wang, Z., Tian, Y. (2018). Succession of organics metabolic function of bacterial community in swine manure composting. *J. Hazard. Mater.*, *360*, 471–480.

Wang, Q., Awasthi, M. K., Ren, X., Zhao, J., Li, R., Wang, Z., … Zhang, Z. (2017). Comparison of biochar, zeolite and their mixture amendment for aiding organic matter transformation and nitrogen conservation during pig manure composting. *Bioresour. Technol.*, *245*, 300–308. https://doi.org/https://doi.org/10.1016/j.biortech.2017.08.158

Wang, X., Zhao, Y., Wang, H., Zhao, X., Cui, H., Wei, Z. (2017). Reducing nitrogen loss and phytotoxicity during beer vinasse composting with biochar addition. *Waste Manag.*, *61*, 150–156. https://doi.org/10.1016/j.wasman.2016.12.024

Wang, Yongjiang, Niu, W., Ai, P. (2016). Assessing thermal conductivity of composting reactor with attention on varying thermal resistance between compost and the inner surface. *Waste Manag.*, *58*, 144–151. https://doi.org/10.1016/j.wasman.2016.09.018

Wang, Yu, Hu, Y., Zhao, X., Wang, S., Xing, G. (2013). Comparisons of biochar properties from wood material and crop residues at different temperatures and residence times. *Energy & Fuels*, *27*(10), 5890–5899.

Wang, Yuchuan, Akdeniz, N., Yi, S. (2021). Biochar-amended poultry mortality composting to increase compost temperatures, reduce ammonia emissions, and decrease leachate's chemical oxygen demand. *Agric. Ecosyst. Environ.*, *315*(March), 107451. https://doi.org/10.1016/j.agee.2021.107451

Wang, Yuchuan, Villamil, M. B., Davidson, P. C., Akdeniz, N. (2019). A quantitative understanding of the role of co-composted biochar in plant growth using meta-analysis. *Sci. Total Environ.*, *685*, 741–752. https://doi.org/10.1016/j.scitotenv.2019.06.244

Waqas, M., Nizami, A. S., Aburiazaiza, A. S., Barakat, M. A., Ismail, I. M. I. I., Rashid, M. I. (2017). Optimization of food waste compost with the use of biochar. *J. Environ. Manage.*, *216*, 70–81. https://doi.org/10.1016/j.jenvman.2017.06.015

Waqas, M., Nizami, A. S., Aburiazaiza, A. S., Barakat, M. A., Ismail, I. M. I., Rashid, M. I. (2018). Optimization of food waste compost with the use of biochar. *J. Environ. Manage.*, *216*(SI), 70–81. https://doi.org/10.1016/j.jenvman.2017.06.015

Warnock, D. D., Lehmann, J., Kuyper, T. W., Rilling, M. C. (2007). Mycorrhizal responses to biochar in soil-concepts and mechanisms. *Plant Soil*, *300*, 9–20.

Weber, K., Quicker, P. (2018). Properties of biochar. *Fuel*, *217*, 240–261.

Wei, L., Shutao, W., Jin, Z., Tong, X. (2014). Biochar influences the microbial community structure during tomato stalk composting with chicken manure. *Bioresour. Technol.*, *154*, 148–154.

Weppen, P. (2001). Process calorimetry on composting of municipal organic wastes. *Biomass and Bioenergy*, *21*(4), 289–299. https://doi.org/10.1016/S0961-9534(01)00033-2

Xiao, L., Yuan, G., Feng, L., Bi, D., Wei, J. (2020). Soil properties and the growth of wheat (Triticum aestivum L.) and maize (Zea mays L.) in response to reed (phragmites communis) biochar use in a salt-affected soil in the Yellow River Delta. *Agric. Ecosyst. Environ.*, *303*(3), 107124. https://doi.org/10.1016/j.agee.2020.107124

Xiao, R., Awasthi, M. K., Li, R., Park, J., Pensky, S. M., Wang, Q., … Zhang, Z. (2017). Recent developments in biochar utilization as an additive in organic solid waste composting: A review. *Bioresour. Technol.*, *246*, 203–213. https://doi.org/https://doi.org/10.1016/j.biortech.2017.07.090

Xu, G., Sun, J. N., Shao, H. B., Chang, S. X. (2014). Biochar had effects on phosphorus sorption and desorption in three soils with differing acidity. *Ecol. Eng.*, *62*, 54–60. https://doi.org/10.1016/j.ecoleng.2013.10.027

Xu, J., Adair, C. W., Deshusses, M. A. (2016). Performance evaluation of a full-scale innovative swine waste-to-energy system. *Bioresour. Technol.*, *216*, 494–502. https://doi.org/10.1016/j.biortech.2016.05.089

Yan, N., Marschner, P., Cao, W., Zuo, C., Qin, W. (2015). Influence of salinity and water content on soil microorganisms. *Int. Soil Water Conserv. Res.*, *3*(4), 316–323.

Yang, Y., Kumar Awasthi, M., Du, W., Ren, X., Lei, T., Lv, J. (2019). Compost supplementation with nitrogen loss and greenhouse gas emissions during pig manure composting. *Bioresour. Technol.*, *297*(November 2019), 122435. https://doi.org/10.1016/j.biortech.2019.122435

Ye, M., Sun, M., Chen, X., Feng, Y., Wan, J., Liu, K., … Schwab, A. P. (2017). Feasibility of sulfate-calcined eggshells for removing pathogenic bacteria and antibiotic resistance genes from landfill leachates. *Waste Manag.*, *63*, 275–283.

Yu, Haowei, Zou, W., Chen, J., Chen, H., Yu, Z., Huang, J., … Gao, B. (2019). Biochar amendment improves crop production in problem soils: A review. *J. Environ. Manage.*, *232*(October 2018), 8–21. https://doi.org/10.1016/J.JENVMAN.2018.10.117

Yu, Huiyong, Xie, B., Khan, R., Shen, G. (2019). The changes in carbon, nitrogen components and humic substances during organic-inorganic aerobic co-composting. *Bioresour. Technol.*, *271*, 228–235. https://doi.org/https://doi.org/10.1016/j.biortech.2018.09.088

Yuan, J., Chadwick, D., Zhang, D., Li, G., Chen, S., Luo, W., … Peng, S. (2016). Effects of aeration rate on maturity and gaseous emissions during sewage sludge composting. *Waste Manag.*, *56*, 403–410.

Yuan, Y., Chen, H., Yuan, W., Williams, D., Walker, J. T., Shi, W. (2017). Is biochar-manure co-compost a better solution for soil health improvement and N2O emissions mitigation? *Soil Biol. Biochem.*, *113*, 14–25. https://doi.org/10.1016/j.soilbio.2017.05.025

Zhang, J., Chen, G., Sun, H., Zhou, S., Zou, G. (2016). Straw biochar hastens organic matter degradation and produces nutrient-rich compost. *Bioresour. Technol.*, *200*, 876–883. https://doi.org/10.1016/j.ijscr.2016.06.047

Zhang, L., Sun, X. (2014). Changes in physical, chemical, and microbiological properties during the two-stage co-composting of green waste with spent mushroom compost and biochar. *Bioresour. Technol.*, *171*, 274–284. https://doi.org/10.1016/j.biortech.2014.08.079

Zhang, P., Li, Y., Cao, Y., Han, L. (2019). Characteristics of tetracycline adsorption by cow manure biochar prepared at different pyrolysis temperatures. *Bioresour. Technol.*, *285*,

121348.

Zheng, B. X., Ding, K., Yang, X. R., Wadaan, M. A. M., Hozzein, W. N., Peñuelas, J., Zhu, Y. G. (2019). Straw biochar increases the abundance of inorganic phosphate solubilizing bacterial community for better rape (Brassica napus) growth and phosphate uptake. *Sci. Total Environ.*, *647*, 1113–1120. https://doi.org/10.1016/j.scitotenv.2018.07.454

Zhou, H., Yang, W. T., Zhou, X., Liu, L., Gu, J. F., Wang, W. L., … Liao, B. H. (2016). Accumulation of heavy metals in vegetable species planted in contaminated soils and the health risk assessment. *Int. J. Environ. Res. Public Health*, *13*(3). https://doi.org/10.3390/ijerph13030289

Zhu, X., Chen, B., Zhu, L., Xing, B. (2017). Effects and mechanisms of biochar-microbe interactions in soil improvement and pollution remediation: A review. *Environ. Pollut.*, *227*, 98–115. https://doi.org/10.1016/j.envpol.2017.04.032